

# AI-Face: A Million-Scale Demographically Annotated AI-Generated Face Dataset and Fairness Benchmark

Li Lin<sup>1</sup>, Santosh<sup>1</sup>, Xin Wang<sup>2</sup>, Shu Hu<sup>1\*</sup>

<sup>1</sup>Purdue University <sup>2</sup>University at Albany, SUNY

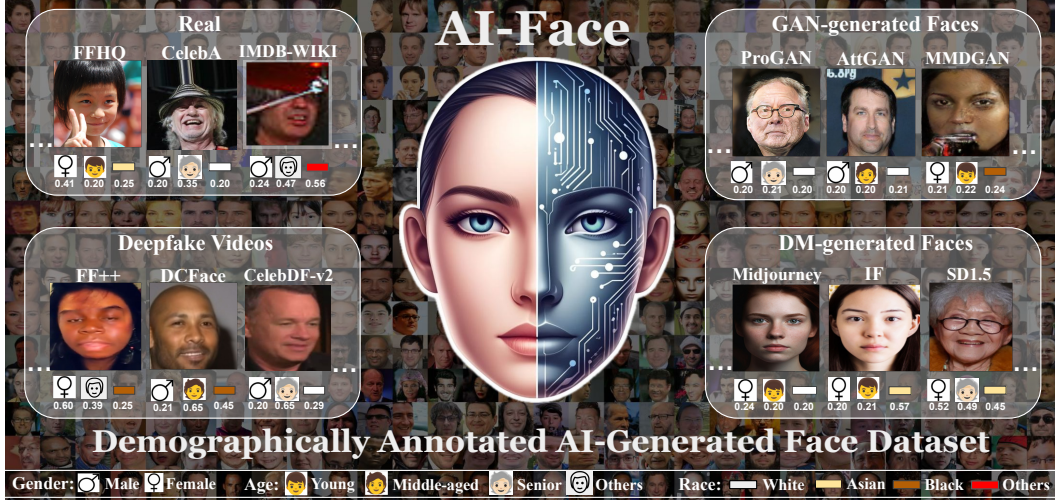


Figure 1: Overview of AI-Face dataset. Each face has three demographic annotations with uncertainty scores.

## Abstract

AI-generated faces have enriched human life, such as entertainment, education, and art. However, they also pose misuse risks. Therefore, detecting AI-generated faces becomes crucial, yet current detectors show biased performance across different demographic groups. Mitigating biases can be done by designing algorithmic fairness methods, which usually require demographically annotated face datasets for model training. However, no existing dataset comprehensively encompasses both demographic attributes and diverse generative methods, which hinders the development of fair detectors for AI-generated faces. In this work, we introduce the **AI-Face** dataset, the *first* million-scale demographically annotated AI-generated face image dataset, including real faces, faces from deepfake videos, and faces generated by Generative Adversarial Networks and Diffusion Models. Based on this dataset, we conduct the *first* comprehensive fairness benchmark to assess various AI face detectors and provide valuable insights and findings to promote the future fair design of AI face detectors. Our AI-Face dataset and benchmark code are publicly available at <https://github.com/Purdue-M2/AI-Face-FairnessBench>.

## 1 Introduction

AI-generated faces are created using sophisticated AI technologies that are visually difficult to discern from real ones [1]. They can be summarized into three categories: deepfake videos [2] created by typically using Variational Autoencoders (VAEs) [3, 4], faces generated from Generative Adversarial Networks (GANs) [5–8], and Diffusion Models (DMs) [9]. These technologies have significantly

\*Corresponding author: Shu Hu ([hu968@purdue.edu](mailto:hu968@purdue.edu))

advanced the realism and controllability of synthetic facial representations. Generated faces can enrich media and increase creativity [10]. However, they also carry significant risks of misuse. For example, during the 2024 United States presidential election, fake face images of Donald Trump surrounded by groups of black people smiling and laughing to encourage African Americans to vote Republican are spreading online [11]. This could distort public opinion and erode people’s trust in media [12, 13], necessitating the detection of AI-generated faces for their ethical use.

However, one major issue existing in current AI face detectors [14–17] is biased detection (*i.e.*, unfair detection performance among demographic groups [18–21]). Mitigating biases can be done by designing algorithmic fairness methods, but they usually require demographically annotated face datasets for model training. For example, works like [20, 21] have made efforts to enhance fairness in the detection based on A-FF++ [19] and A-DFD [19]. However, both datasets are limited to containing only faces from deepfake videos, which could cause the trained models not to be applicable for fairly detecting faces generated by GANs and DMs. Although a few datasets (*e.g.*, GenData [22]) cover GAN and DM faces, their demographic annotations are not comprehensive. Most importantly, no existing dataset is diverse enough in generation methods to develop AI face detectors that can cope with rapidly evolved generative models. *These limitations of existing datasets hamper the development of fair technologies for detecting AI-generated faces.*

Moreover, benchmarking fairness provides a direct method to uncover prevalent and unique fairness issues in recent AI-generated face detection. However, there is a lack of a comprehensive benchmark to estimate the fairness of existing AI face detectors. Existing benchmarks [23–26] primarily assess utility, neglecting systematic fairness evaluation. One study [18] does evaluate fairness in detection models, but their examination is only based on deepfake video datasets using a few outdated detectors. Detectors’ fairness performance on GAN faces and DM faces has not been extensively explored. *The absence of a comprehensive fairness benchmark impedes a thorough understanding of the fairness behaviors of recent AI face detectors and obscures the research path for detector fairness guarantees.*

In this work, we build the **first** million-scale demographically annotated AI-generated face image dataset: **AI-Face** (see Fig. 1). The face images are collected from various public datasets, including the real faces that are usually used to train AI face generators, faces from deepfake videos, and faces generated by GANs and DMs. Each face is demographically annotated with an uncertainty score on each predicted demographic attribute by our designed Contrastive Language-Image Pretraining (CLIP) [27]-based lightweight annotator. To improve the quality of annotations, we recruit three humans to correct annotations with high uncertainty scores manually. Next, we conduct the **first** comprehensive fairness benchmark on our dataset to estimate the fairness performance of 12 representative detectors coming from four model types. Our benchmark exposes common and unique fairness challenges in recent AI face detectors, providing essential insights that can guide and enhance the future design of fair AI face detectors. Our contributions are as follows:

- We build the first comprehensive million-scale demographically annotated AI-generated face Dataset by leveraging our developed lightweight annotator with human correction.
- We conduct the first comprehensive fairness benchmark of AI-generated face detectors, providing an extensive fairness assessment of current representative detectors.
- Based on our experiments and observations, we summarize the unsolved questions and offer valuable insights within this research domain, setting the stage for future investigations.

## 2 Background and Motivation

**AI-generated Faces and Biased Detection.** AI-generated face images, created by advanced AI technologies, are visually difficult to discern from real ones, see Fig. 1. They can be summarized into three categories: 1) *Deepfake Videos*. Initiated in 2017 [13], these use face-swapping techniques with a variational autoencoder to replace a face in a target video with one from a source [3, 4]. Note that our paper focuses solely on images extracted from videos. 2) *GAN-generated Faces*. Post-2017, Generative Adversarial Networks (GANs) [28] like StyleGANs [6–8] have significantly improved generated face realism. 3) *DM-generated Faces*. Diffusion models (DMs), emerging in 2021, generate detailed faces from textual descriptions and offer greater controllability. Tools like MidJourney [29] and DALLE2 [30] facilitate customized face generation. While these AI-generated faces can enhance visual media and creativity [10], they also pose risks, such as being misused in social media profiles [31, 32]. Therefore, numerous studies focus on detecting AI-generated

Dataset	Face Images		Generation Category			#Generation Methods	Source of Real Images	Demographic Annotation		
	#Real	#Fake	Deepfake Videos	GAN	DM			Gender	Race	Age
A-FF++ [19]	29.8K	149.1K	✓			5	YouTube	✓	✓	✓
	10.8K	89.6K	✓			5	Self-Recording	✓	✓	✓
	54.5K	52.6K	✓	✓		8	Self-Recording	✓	✓	✓
	26.3K	166.5K	✓			1	Self-Recording	✓	✓	✓
	870.3K	321.5K	✓			1	Self-Recording	✓	✓	✓
	2.9M	14.7M	✓			1	Self-Recording	✓	✓	✓
	1K	50.4K	✓	✓		3	YouTube	✓		✓
	392.3K	653.4K	✓	✓		3	YouTube	✓		✓
	-	20K	✓	✓		3	CelebA [36]	✓		
	Ours	866K	1.2M	✓	✓	✓	FFHQ [6], CASIA-WebFace [37], CelebA [36] IMDB-WIKI [38], real from FF++ [2], DFDC [39], DFD [40], Celeb-DF-v2 [41]	✓	✓	✓

Table 1: Quantitative comparison of existing AI-generated face datasets and ours.

faces [14–17], but current detectors often show performance disparities among demographic groups like race and gender [18–21]. This bias can lead to unfair targeting or exclusion, undermining trust in detection models. Recent efforts [20, 21] aim to enhance fairness in deepfake detection but mainly address deepfake videos, overlooking biases in detecting GAN and DM-generated faces.

**The Related Existing Datasets.** Current AI-generated facial datasets with demographic annotations are limited in size, generation categories, methods, and annotations, as illustrated in Table 1. For instance, A-FF++, A-DFD, A-DFDC, and A-Celeb-DF-v2 [19] are deepfake video datasets with fewer than one million images. Datasets like DF-1.0 [33] and DF-Platter [35] lack comprehensive demographic annotations. Additionally, existing datasets offer limited generation methods. These limitations hinder the development of fairer AI face detectors, motivating us to build a million-scale demographically annotated AI-Face dataset.

#### Benchmark for Detecting AI-generated Faces

Benchmarks are essential for evaluating AI-generated face detectors under standardized conditions. Existing benchmarks, as shown in Table 2, mainly focus on detectors’ utility, often overlooking fairness [23–26]. Only Loc et al. [18] examined detector fairness. However, their study focused only on deepfake video datasets, not on GAN- and DM-generated faces.

This motivates us to conduct a comprehensive benchmark to evaluate AI face detectors’ fairness.

Existing Benchmarks	Category			Scope of Benchmark	
	Deepfake Videos	GAN	DM	Utility	Fairness
DeepfakeBench [25]	✓	✓		✓	
Lin et al. [24]	✓	✓		✓	
Le et al. [26]	✓	✓		✓	
CDBB [23]		✓		✓	
Loc et al. [18]	✓			✓	✓
Ours	✓	✓	✓	✓	✓

Table 2: Comparison with existing AI-generated face detection benchmarks.

### 3 The Demographically Annotated AI-Face Dataset

To address the prohibitive time consuming of manual annotation, we introduce two phases to build our dataset: *Annotator Development* and *Demographically Annotation Generation*, as shown in Fig. 2.

#### 3.1 Phase 1: Annotator Development

**Problem Definition.** There are existing online software (*e.g.*, Face++ [42]) and open-source tools (*e.g.*, InsightFace [43]) for face attribute prediction. However, they fall short of our task due to two reasons: 1) They are mostly designed for face recognition and trained on datasets of real face images but lack generalization capability for annotating AI-generated face images. 2) They do not provide uncertainty scores for their predictions that can be used to identify mispredicted samples for further annotation correction. Given a training dataset  $\mathbb{D} = \{(X_i, G_i, A_i, R_i)\}_{i=1}^n$  with size  $n$ , where  $X_i, G_i \in \{\text{Female, Male}\}$ ,  $A_i \in \{\text{Young, Middle-aged, Senior, Others}\}$ , and  $R_i \in \{\text{Asian, White, Black, Others}\}$  represent the  $i$ -th face image, and its gender, age, and race labels/attributes, respectively. Our goal is to design a lightweight, generalizable annotator based on  $\mathbb{D}$  to predict facial demographic attributes with uncertainty scores for each face image in our dataset.

**Annotator.** Architecture: We utilize CLIP [27] for its strong zero-shot and few-shot learning capabilities. Leveraging CLIP’s pre-training on diverse datasets, we create a lightweight annotator for facial images. Our annotator employs a frozen pre-trained CLIP ViT L/14 [44] as a feature extractor  $\mathbf{E}$  followed by a trainable 3-layer Multilayer Perceptron (MLP) as a multi-task (*i.e.*, gender, age, and race prediction) classifier parameterized by  $\theta$ . Loss: For each image  $X_i$ , its feature  $f_i$  is obtained through  $f_i = \mathbf{E}(X_i)$  and then is fed into the MLP multi-task classifier with conventional

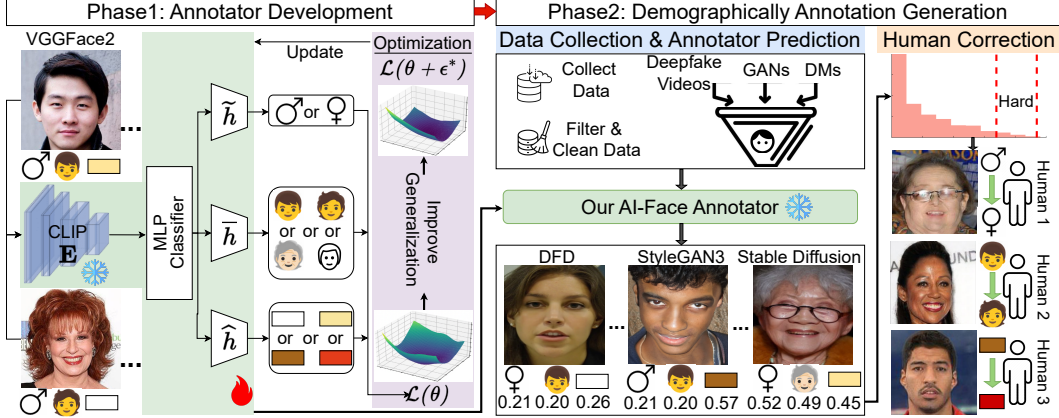


Figure 2: *Generation pipeline of our Demographically Annotated AI-Face Dataset*. First, we develop a lightweight facial attribute annotator trained on the VGGFace2 dataset. Second, we collect and filter face images from Deepfake Videos, GAN-generated faces, and DM-generated faces found in public datasets. Our AI-Face annotator then predicts facial attributes with uncertainty scores for each image. Third, samples with high uncertainty are manually reviewed and corrected by three humans to improve annotation quality.

classification losses for face attribute prediction. The learning objective is formulated as:  $\mathcal{L}(\theta) = C(\tilde{h}(f_i), G_i) + C(\bar{h}(f_i), A_i) + C(\hat{h}(f_i), R_i)$ , where  $C(\cdot, \cdot)$  represents the (binary) cross-entropy (CE) loss.  $\tilde{h}$ ,  $\bar{h}$ , and  $\hat{h}$  represent the classification heads for gender, age, and race, respectively. **Optimization:** Traditional optimization methods like stochastic gradient descent can lead to poor model generalization due to sharp loss landscapes with multiple local and global minima. To address this, we use Sharpness-Aware Minimization (SAM) [45] to enhance our annotator’s generalization by flattening the loss landscape. Specifically, flattening is attained by determining the optimal  $\epsilon^*$  for perturbing model parameters  $\theta$  to maximize the loss, formulated as:  $\epsilon^* = \arg \max_{\|\epsilon\|_2 \leq \gamma} \mathcal{L}(\theta + \epsilon) \approx \arg \max_{\|\epsilon\|_2 \leq \gamma} \epsilon^\top \nabla_\theta \mathcal{L} = \gamma \text{sign}(\nabla_\theta \mathcal{L})$ , where  $\gamma$  controls the perturbation magnitude. This is approximated using a first-order Taylor expansion, assuming  $\epsilon$  is small. The final equation is obtained by solving a dual norm problem, where  $\text{sign}$  represents a sign function and  $\nabla_\theta \mathcal{L}$  being the gradient of  $\mathcal{L}$  with respect to  $\theta$ . As a result, the model parameters are updated by solving:  $\min_\theta \mathcal{L}(\theta + \epsilon^*)$ .

**Uncertainty Estimation.** Although the high prediction performance of our annotator can be obtained, the labels may still be mispredicted due to the ambiguity of the face images (see an example in Fig. 3). Therefore, it is crucial to provide an uncertainty score for each prediction from the annotator. To this end, inspired by [46], we incorporate dropout techniques at each layer of MLP for uncertainty estimation in testing. This involves performing  $k$  stochastic forward passes for a given test image  $X$ , each with a unique dropout pattern. So, we can obtain  $k$  distinct softmax outputs for each demographic attribute  $a$ , denoted as  $\{x^{1,(a)}, \dots, x^{k,(a)}\}$ . Then, the uncertainty score for  $a$  on image  $X$  (denoted as  $V(X^{(a)})$ ) is calculated as  $V(X^{(a)}) = 1 - \left\{ \frac{1-\rho}{k} \sum_{i=1}^k x^{i,(a)} - \frac{\rho}{k^2} \sum_{i=1}^k \sum_{j=1}^k |x^{i,(a)} - x^{j,(a)}| \right\}$ , where  $\rho \in [0, 1]$  is a user-defined parameter to counterweight the measure of centrality (*i.e.*, the first term in  $\{\}$  indicates the likelihood of the prediction being correct) and dispersion (*i.e.*, the second term in  $\{\}$  reflects the consensus among the stochastic outputs).

**Evaluation.** To demonstrate our annotator’s effectiveness, we will answer the following questions: **Q1:** How are the general performance and generalization capability of our annotator compared with the baselines? **Q2:** How does sample difficulty affect the annotator’s performance? In leveraging the good generalization capabilities of CLIP, our annotator is trained on the VGGFace2 [47] dataset, which contains 9.1K individuals with 3.3M images. More importantly, [48] provides comprehensive demographic annotations for this dataset. We compare our annotator with the current state-of-the-art face attribute prediction tools Face++ [42] and InsightFace [43]. Since they do not offer predictions for the race attribute, our evaluation is confined to gender and age. The mean and standard deviation are reported based on 5 random runs. More details are in Appendix A.1.1.

For Q1, **Setting:** We perform *intra-domain* (train on VGGFace2, test on its official test set) and *cross-domain* (train on VGGFace2, test on four AI-generated face datasets) evaluations. Specifically,

Type	Dataset	Attribute	Level											
			All			Easy			Medium			Hard		
			InsightFace [43]	Face++ [42]	Ours	InsightFace [43]	Face++ [42]	Ours	InsightFace [43]	Face++ [42]	Ours	InsightFace [43]	Face++ [42]	Ours
Intra-Domain	VGGFace2 [47]	Gender	76.7289 (0.4985)	78.0764 (0.4266)	<b>83.8978</b> <b>(0.3697)</b>	97.0133 (0.1293)	97.0863 (0.3414)	<b>99.7333</b> <b>(0.1265)</b>	74.2400 (0.8182)	75.356 (0.5938)	<b>87.5333</b> <b>(0.5007)</b>	58.9333 (0.5481)	61.787 (0.3445)	<b>64.4267</b> <b>(0.4818)</b>
		Age	54.4311 (0.7443)	58.4889 (0.7341)	<b>77.4044</b> <b>(0.6714)</b>	68.000 (0.5530)	73.0067 (0.6534)	<b>98.4133</b> <b>(0.1543)</b>	49.8000 (0.6613)	53.2467 (0.8465)	<b>78.9733</b> <b>(1.0771)</b>	45.4933 (1.0186)	49.2134 (0.7025)	<b>54.8267</b> <b>(0.7827)</b>
Cross-Domain	A-FF++ [19]	Gender	84.9733 (0.4651)	89.1714 (0.1974)	<b>91.3000</b> <b>(0.2058)</b>	96.8267 (0.3832)	98.0528 (0.1483)	<b>98.9333</b> <b>(0.0943)</b>	88.0933 (0.4668)	94.3074 (0.2586)	<b>98.8667</b> <b>(0.1033)</b>	70.0000 (0.5452)	75.1539 (0.1854)	<b>76.1000</b> <b>(0.4197)</b>
		Age	59.4867 (0.9291)	64.1893 (0.7609)	<b>75.5393</b> <b>(0.5130)</b>	71.254 (0.5973)	80.5980 (0.4140)	<b>93.1980</b> <b>(0.3110)</b>	58.1720 (0.4489)	63.8340 (0.6733)	<b>81.1960</b> <b>(0.4702)</b>	49.0340 (1.7410)	48.1360 (1.1954)	<b>52.2240</b> <b>(0.7577)</b>
	A-DFDC [19]	Gender	70.1111 (0.5037)	76.0917 (0.6290)	<b>78.2922</b> <b>(0.5178)</b>	85.8533 (0.5239)	92.1414 (0.5447)	<b>96.2933</b> <b>(0.5927)</b>	68.4666 (0.5667)	73.5088 (0.4910)	<b>76.2005</b> <b>(0.5028)</b>	56.0133 (0.5014)	<b>62.6249</b> <b>(0.8513)</b>	62.3334 (0.4580)
	A-DFD [19]	Age	66.6967 (0.8015)	69.5907 (0.5687)	<b>77.1800</b> <b>(0.6300)</b>	72.1580 (0.6785)	84.5000 (0.4908)	<b>95.3820</b> <b>(0.3247)</b>	64.398 (0.9182)	64.238 (0.5423)	<b>73.1620</b> <b>(0.8592)</b>	<b>63.5340</b> <b>(0.8078)</b>	60.034 (0.6730)	62.9960 (0.7061)
A-Celeb-DF-v2 [19]	Gender	66.7156 (0.7681)	70.7983 (1.2229)	<b>74.9822</b> <b>(0.6029)</b>	85.5467 (0.6791)	88.9791 (0.8297)	<b>94.0400</b> <b>(0.2999)</b>	60.5467 (0.9017)	64.2144 (1.3436)	<b>70.0267</b> <b>(0.9471)</b>	54.0533 (0.7235)	59.2015 (1.4953)	<b>60.8800</b> <b>(0.5616)</b>	
	A-Celeb-DF-v2 [19]	Gender	91.9244 (0.3003)	90.8100 (0.4487)	<b>95.1489</b> <b>(0.4088)</b>	98.9733 (0.1769)	98.1867 (0.2286)	<b>99.9867</b> <b>(0.0267)</b>	94.0000 (0.3239)	94.4933 (0.5052)	<b>99.7600</b> <b>(0.0998)</b>	82.8000 (0.4000)	79.7500 (0.6124)	<b>85.7000</b> <b>(1.1000)</b>

Table 3: Comparing our annotator against Face++ [42] and InsightFace [43] under intra-domain and cross-domain evaluations (Accuracy (%)) on different levels of sample difficulty. The prediction mean and standard deviation (in parentheses) are reported. The best results are shown in **Bold**. More results are in Appendix A.1.3.

A-FF++, A-DFDC, A-DFD, and A-Celeb-DF-v2 are selected from [19] for cross-domain evaluation. Since A-DFD and A-Celeb-DF-v2 have limited age and race annotations, our evaluation of these two is confined to gender. These datasets are chosen because they closely match our objective and are not used to train Face++ and InsightFace. Results: The ‘All’ results in Table 3 demonstrate our annotator’s superiority in general performance and generalization capability against Face++ and InsightFace. Under intra-domain evaluation, it surpasses the second-best method, Face++, by 5.8% on gender and 18.9% on age. In cross-domain evaluation, our annotator maintains high accuracy on all datasets, reflecting good generalization. Remarkably, on the A-FF++ dataset, our annotator outperforms Face++ by a substantial margin of up to 11.4% and InsightFace by 16.1% on age.

For Q2, Setting: We also design a stratified evaluation method by separating each test dataset into three subsets—*Easy*, *Medium*, and *Hard* based on the estimated uncertainty scores. Specifically, for each demographic attribute  $a$ , we define two thresholds  $t_1^a$  and  $t_2^a$ , where  $t_1^a < t_2^a$  (more details are in Appendix A.1.2). Then, we have  $Easy = \{X \mid V(X^{(a)}) < t_1^a\}$ ,  $Medium = \{X \mid t_1^a \leq V(X^{(a)}) \leq t_2^a\}$ , and  $Hard = \{X \mid V(X^{(a)}) > t_2^a\}$ . Next, we sample 1,500 images from each subset. This stratification is crucial for a thorough examination of the model’s performance across a broad spectrum of data challenges. To avoid attribute-specific biases, each subset is balanced with respect to attribute. Results: Table 3 illustrates that while all methods show decreased accuracy as the sample difficulty level increases, our annotator demonstrates greater resilience. For example, under intra-domain evaluation, our annotator’s gender performance drops by 10.2% from easy to medium difficulty, compared to Face++’s 21.7% drop. In cross-domain scenario, our annotator experiences a 14.3% reduction on gender in A-Celeb-DF-v2 [19], versus InsightFace’s 16.2% from easy to hard.

### 3.2 Phase 2: Demographically Annotation Generation

**Data Collection.** We build our AI-Face dataset by collecting and integrating public AI-generated face images sourced from academic publications, GitHub repositories, and commercial tools. More details are in Appendix A.2.1. Specifically, the fake face images in our dataset originate from **4 Deepfake Video datasets** (i.e., A-FF++ [19], A-DFDC [19], A-DFD [19], and A-Celeb-DF-v2 [19]), generated by **10 GAN** models (i.e., AttGAN [49], MMDGAN [50], StarGAN [49], StyleGANs [49, 51, 52], MSGGAN [50], ProGAN [53], STGAN [50], and VQGAN [54]), and **8 DM** models (i.e., DALLE2 [55], IF [55], Midjourney [55], DCFace [56], Latent Diffusion [57], Palette [58], Stable Diffusion v1.5 [59], Stable Diffusion Inpainting [59]). This constitutes a total of 1,245,660 fake face images in our dataset. These fake images are correspondingly generated from **8 real** source datasets (i.e., FFHQ [6], CASIA-WebFace [37], IMDB-WIKI [38], CelebA [36], and real images from FF++ [2], DFDC [39], DFD [40], and Celeb-DF-v2 [41]). This constitutes a total of 866,096 real face images in our dataset. In general, our dataset contains 30 subsets and 37 generation methods (i.e., 5 in A-FF++, 5 in A-DFD, 8 in A-DFDC, 1 in A-Celeb-DF-v2, 10 GANs, and 8 DMs). We use RetinaFace [60] for detecting and cropping faces to ensure each image only contains one face.

**Annotator Prediction.** For our collected images, annotation generation is iterative, integrating uncertainty scores into each prediction by our annotator in Phase 1, as shown in Fig. 2.

**Human Correction.** As described in ‘Uncertainty Estimation’ in Section 3.1, the annotator may mispredict ambiguous face images, necessitating human review and correction. To this

Type	Datasets	Gender			Age			Race		
		ACC(%)	Precision(%)	Recall(%)	ACC(%)	Precision(%)	Recall(%)	ACC(%)	Precision(%)	Recall(%)
For Q1	A-FF++ [19]	8.0163	17.3354	5.8314	19.9002	30.6658	29.6071	28.7865	35.7122	<b>41.1687</b>
	Ours-FF++ (w/o Correction)	<b>91.9837</b>	<b>82.6646</b>	<b>94.1684</b>	<b>21.1830</b>	<b>32.1232</b>	<b>45.7231</b>	<b>45.9775</b>	<b>50.3803</b>	40.1949
	A-DFDC [19]	20.2252	27.5332	21.6538	16.7493	29.0640	29.5519	18.1115	15.1092	22.0637
For Q2	Ours (w/o Correction)	83.4167	83.4167	83.4242	43.8333	43.8333	54.1792	67.4167	65.0718	59.2350
	Ours	<b>84.8333</b>	<b>84.8738</b>	<b>84.8599</b>	<b>44.7500</b>	<b>44.0937</b>	<b>54.6033</b>	<b>68.8333</b>	<b>66.6440</b>	<b>61.3225</b>
	For Q3	Ours	98.6667	98.6688	98.6667	56.2500	50.1748	53.0514	86.2500	75.5216

Table 4: Evaluation results of our dataset annotation quality for questions Q1, Q2, and Q3. ‘Ours-FF++ (w/o Correction),’ ‘Ours-DFDC (w/o Correction),’ and ‘Ours (w/o Correction)’ represent our predicted annotations on A-FF++, A-DFDC, and our entire dataset without human correction, respectively. ACC represents Accuracy.

end, we propose two annotation correction strategies: 1) For subsets that have the same images and demographic attribute classes as those in existing datasets, such as A-FF++ [19] and A-DFDC [19], we filter out images that may need human correction based on annotation inconsistency. 2) For the rest of the subsets, we identify the most ambiguous images that need human correction based on uncertainty scores. Specifically, for demographic attribute  $a_j$  on subset  $j$ , we define a specific threshold  $t^{a_j}$  (more details are in Appendix A.2.2). If  $V(X^{(a_j)}) > t^{a_j}$ , the annotation for attribute  $a_j$  of the image  $X$  will undergo a verification process, potentially requiring human re-annotation (see Fig. 3). In practice, we recruit three humans to correct the filtered images, consolidating their evaluations with a majority vote to finalize annotations.

**Evaluation.** To estimate our dataset’s quality, we will answer the following questions: **Q1:** Can we directly incorporate the existing annotations into our dataset? **Q2:** How is the effectiveness of human correction? **Q3:** How is the overall annotations’ quality of our dataset?

For Q1, **Setting:** We compare our dataset’s annotation quality before human correction on A-FF++ (*i.e.*, Ours-FF++ (w/o Correction)) and A-DFDC (*i.e.*, Ours-DFDC (w/o Correction)) against their existing annotation from [19]. We regard human re-labeled annotations as the ground truth. **Results:** The results in Table 4 ‘For Q1’ show superior annotation accuracy of our datasets. For example, Ours-FF++ (w/o Correction) surpasses A-FF++ by 83.97% in gender accuracy, and Ours-DFDC (w/o Correction) exceeds A-DFDC by 59.55%. The large performance indicates that identified images by annotation inconsistency are mislabeled in A-FF++ [19] and A-DFDC [19], and thus cannot be directly merged into our dataset. Some examples are shown in Appendix A.2.3.

For Q2, **Setting:** We consider two dataset versions: 1) Ours (w/o Correction), where annotations are not corrected by humans. 2) Ours, where annotations are corrected by humans. With the help of the uncertainty score, we sample 1,200 attribute-balanced images (400 easy, 400 medium, and 400 hard) from the whole dataset to ensure a fair evaluation. Three humans re-annotated these images to establish ground truth. **Results:** Table 4 ‘For Q2’ shows that human corrections improve performance across all attributes, increasing accuracy by 1.42% for gender, 0.92% for age, and 1.42% for race, validating the effectiveness of our correction strategy. More results see Appendix A.2.4.

For Q3, **Setting:** We randomly sample 1,200 images from the whole dataset. Three humans also re-annotated these images to create ground truth. **Results:** As shown in Table 4 ‘For Q3’, Ours reflects the approximate overall annotation quality of our dataset. Notably, the annotations of gender and race attributes show high correctness (*e.g.*, 98.6667% ACC on gender and 86.2500% ACC on race). However, the age annotation shows a lower accuracy since it is challenging to differentiate.

## 4 Fairness Benchmark Experiments

In this section, we estimate the existing AI-generated image detectors’ fairness performance alongside their utility on our AI-Face Dataset (80%/20% for Train/Test). Our goal is to show the significance of our dataset and expose the fairness issues of recent detectors in combating AI-generated faces.

**Detection Methods.** Our benchmark has implemented 12 detectors, as detailed in Appendix B.1. The methodologies cover a spectrum that is specifically tailored to detect AI-generated faces from

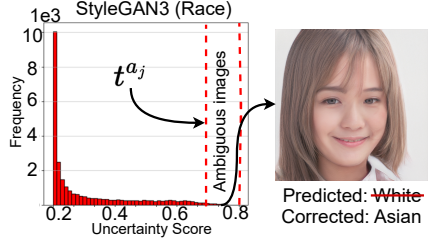


Figure 3: Uncertainty-based strategy for identifying ambiguous faces for human correction.

Measure	Attribute	Metric	Model Type												
			Naive			Frequency			Spatial			Fairness-enhanced			
			Xception [61]	EfficientB4 [62]	ViT-B/16 [63]	F3Net [64]	SPSL [65]	SRM [66]	UCF [16]	UnivFD [67]	CORE [68]	DAW-FDD [20]	DAG-FDD [20]	PG-FDD [21]	
Fairness↓	Gender	$F_{MEO}(\%)$	0.387	1.176	0.187	0.279	0.454	0.533	0.305	0.458	1.635	0.404	0.272	0.236	
		$F_{DP}(\%)$	2.843	2.052	2.489	2.941	2.998	2.433	2.890	2.456	1.977	2.979	2.799	2.614	
		$F_{OAE}(\%)$	0.271	0.595	0.422	0.086	0.188	0.268	0.169	0.557	0.977	0.123	0.192	0.134	
	Race	$F_{MEO}(\%)$	4.386	8.307	13.078	3.094	4.736	5.470	3.188	14.663	16.001	3.461	3.344	1.956	
		$F_{OAE}(\%)$	3.509	5.659	5.351	2.217	2.201	4.044	1.847	6.505	5.105	1.365	1.847	1.132	
		$F_{EO}(\%)$	0.439	1.229	0.235	0.552	0.577	0.536	0.346	0.490	1.846	0.699	0.407	0.237	
	Age	$F_{MEO}(\%)$	1.695	3.028	8.931	1.319	1.025	1.090	0.854	5.818	6.964	2.838	0.809	0.781	
		$F_{DP}(\%)$	6.242	6.724	6.264	6.357	6.340	5.905	6.257	6.260	5.030	6.249	6.140	6.098	
		$F_{OAE}(\%)$	1.028	1.619	3.948	1.017	0.710	0.934	0.635	4.966	3.652	2.610	0.606	0.506	
	Intersection	$F_{EO}(\%)$	4.116	6.080	12.888	3.694	2.827	3.116	2.479	15.252	8.382	7.361	2.171	1.587	
		$F_{MEO}(\%)$	7.113	9.999	14.667	4.739	7.320	9.731	4.606	17.606	19.303	5.316	4.708	2.604	
		$F_{OAE}(\%)$	6.174	9.181	7.711	3.692	3.744	6.498	3.061	11.802	6.035	2.641	3.174	1.830	
	Individual	$F_{EO}(\%)$	24.520	42.330	49.075	16.699	16.257	25.983	13.932	68.449	47.016	14.539	14.118	8.618	
		$F_{IND}(\%)$	112.067	585.935	0.125	46.083	22.982	1.383	3.246	8.606	0.598	28.437	13.706	0.477	
		$\text{Avg-}F_R$	6.824	9.529	7.706	5.941	6.647	5.471	4.353	9.941	9.235	6.118	3.765	2.059	
	Utility↑	$\text{Avg-}F_{MR}$			8.020		6.020		7.843			3.981			
		ACC(%)	97.639	95.404	93.719	98.229	98.274	97.978	98.635	90.229	96.087	97.316	98.543	99.079	
		AUC(%)	99.768	99.117	98.914	99.826	99.767	99.885	96.030	98.846	99.703	99.871	99.937		
		AP(%)	99.846	99.359	99.240	99.885	99.853	99.829	99.917	96.973	98.987	99.802	99.916	99.956	
		EER(%)	2.388	4.794	5.829	1.741	1.610	2.134	1.365	10.680	4.656	2.701	1.365	1.212	
		Training Time / Epoch	1h35min	3h07min	3h26min	1h41min	1h37min	4h05min	5h10min	5h07min	1h36min	1h45min	1h38min	7h43min	

Table 5: Overall performance. Top 3 values on each metric are highlighted in green, blue, and yellow.

Deepfake Videos, GANs, and DMs. They can be classified into four types: *Naive detectors*: refer to backbone models that can be directly utilized as the detector for binary classification, including CNN-based (*i.e.*, Xception [61] and EfficientB4 [62]) and transformer-based (*i.e.*, ViT-B/16 [63]). *Frequency-based*: explore the frequency domain for forgery detection (*i.e.*, F3Net [64], SPSL [65], and SRM [66]). *Spatial-based*: focus on mining spatial characteristics (*e.g.*, texture) within images for detection (*i.e.*, UCF [16], UnivFD [67], and CORE [68]). *Fairness-enhanced*: focus on improving fairness in AI-generated face detection by designing specific algorithms (*i.e.*, DAW-FDD [20], DAG-FDD [20], and PG-FDD [21]). Implementation and training details refer to Appendix B.2.

**Evaluation Metrics.** To provide a comprehensive benchmarking, we consider 5 fairness metrics commonly used in fairness community [69–73] and 4 widely used utility metrics. For *fairness* metrics, we consider Demographic Parity ( $F_{DP}$ ) [69, 70], Max Equalized Odds ( $F_{MEO}$ ) [72], Equal Odds ( $F_{EO}$ ) [71], and Overall Accuracy Equality ( $F_{OAE}$ ) [72] for evaluating group (*e.g.*, gender) and intersectional (*e.g.*, individuals of a specific race and simultaneously a specific gender) fairness. We also use individual fairness ( $F_{IND}$ ) [73, 74] (*i.e.*, similar individuals should have similar predicted outcomes) for estimation. Fairness metrics definition can be found in Appendix B.3. To compare detectors’ performance clearly and fairly, we define the Average Fairness Rank ( $\text{Avg-}F_R$ ), which ranks each detector on each fairness metric and averages these ranks. We also define  $\text{Avg-}F_{MR}$  for the average rank across methods within a model type. For *utility* metrics, we employ Accuracy (ACC), the Area Under the ROC Curve (AUC), Average Precision (AP), and Equal Error Rate (EER).

**Results.** Overall Performance. Table 5 reports the overall performance on our AI-Face test set. Our observations are: 1) Most detectors do not have fairness except for Fairness-enhanced detectors, which demonstrate relatively lower performance disparities. 2) The top 3 performing methods are PG-FDD [21], DAG-FDD [20], and UCF [16] according to  $\text{Avg-}F_R$ . 3) According to  $\text{Avg-}F_{MR}$ , Fairness-enhanced detectors demonstrate superior performance. Frequency detectors surpass both Spatial and Naive detectors. A possible reason is that frequency features are more focused on the forgery trace while weakening the demographic features. This highlights a potential avenue for future research to enhance detector fairness by integrating frequency features with fairness-enhanced algorithms. 4) 9 out of 12 detectors have an AUC higher than 99%, demonstrating our AI-Face dataset is significant for training AI-face detectors in resulting high utility. 5) PG-FDD demonstrates superior performance but has a long training time, which can be explored and addressed in the future.

**Performance on Different Subsets.** Fig. 4 demonstrates the intersectional  $F_{EO}$  and AUC performance of detectors on each test subset (*e.g.*, subsets originate from different generative methods). We observe that the fairness performance varies a lot among different generative methods in every detector. The largest bias on most detectors comes from detecting face images generated by STGAN [75] and Commercial Tools (CT), including DALLE2 [55], IF [55], and Midjourney [55]. Moreover, the stable utility demonstrates our dataset’s expansiveness and diversity, enabling effective training to detect AI-generated faces from various generative methods. Full evaluation results are in Appendix B.4.

**Performance on Different Subgroups.** We conduct an analysis of all detectors on intersectional subgroups: Male-White (M-W), Male-Black (M-B), Male-Asian (M-A), Male-Others (M-A), Female-White (F-W), Female-Black (F-B), Female-Asian (F-A), Female-Others (F-O). As shown in Fig. 5, it

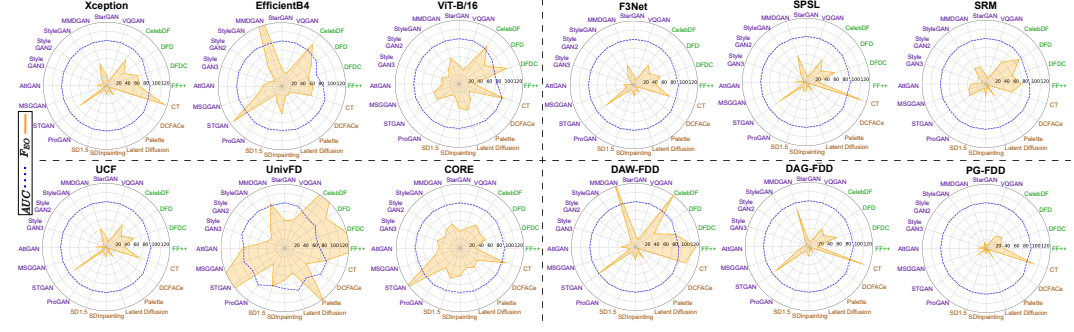


Figure 4: Visualization of the intersectional  $FEO$  (%) and  $AUC$  (%) of detectors on different subsets. The smaller  $FEO$  polygon area represents better fairness. The larger  $AUC$  area means better utility.

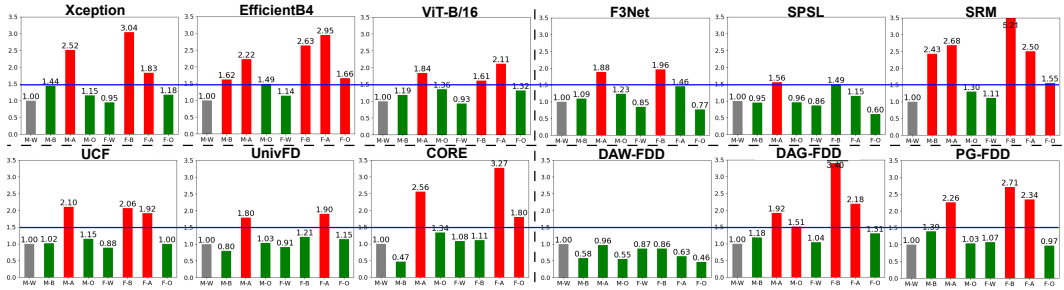


Figure 5: Ratios of FPR for each subgroup to reference subgroup Male-White (M-W). The blue line indicates the 50% margin above. Red and green bars indicate the above and below of the margin, respectively.

plots the ratios of FPR for each subgroup to a reference group (M-W). 1) It is clear that facial images of M-A, F-B, and F-A are more likely to be mistakenly detected as fake than facial images of M-W. 2) However, the FPR of M-W is higher than others in DAW-FDD. This highlights a challenge in algorithmic fairness methods: improving performance for minority groups can inadvertently raise the error rate for the majority group (e.g., M-W). See demographic distribution in Appendix A.2.1.

**Fairness Robustness Evaluation.** Images spread on public platforms usually undergo post-processing. Therefore, it is important to estimate the capability of detectors to preserve fairness robustness while handling distorted images. We apply 6 post-processing methods: Random Crop (RC) [76], Rotation (RT) [25], Brightness Contrast (BC) [25], Hue Saturation Value (HSV) [25], Gaussian Blur (GB) [25], and JPEG Compression (JC) [77] to the test images (see Appendix B.5 for more details). Fig. 6 shows each detector’s intersectional  $FEO$  and AUC performance changes after using post-processing. Our observations are: 1) These impairments tend to wash out forensic traces, to the point that detectors have significant performance degradation. 2) Recent Fairness-enhanced detectors struggle to maintain fairness when images undergo post-processing. 3) Transform-based models (i.e., ViT-B/16 [63] and UnivFD [67]) demonstrate stronger robustness compared with CNN-based models. 4) JPEG Compression and Gaussian Blur cause notably greater performance degradation compared to others. See Appendix B.6 for more robustness analysis with respect to different degrees of post-processing.

**Fairness Generalization Evaluation.** To evaluate detectors’ fairness generalization capability, we train them on AI-Face and test them on A-DF-1.0, DF-Platter, and GenData, none of which are part of AI-Face. Results on gender attribute in Table 6 show that: 1) According to  $Avg-F_R$ , the top three methods excelling in fairness preservation are PG-FDD, Xception, and CORE. PG-FDD, specifically designed for fairness generalization, leads to overall performance. However, it does not excel in terms of performance changes compared with intra-domain test results from Table 5, indicating room for improvement in its generalization capabilities. 2) CORE is notable for demonstrating negative fairness performance changes on A-DF-1.0 and GenData, suggesting techniques within CORE that could be potentially explored to enhance fairness generalization. More results are in Appendix B.7.

**Effect of Increasing Training Set Size.** We randomly sample 20%, 40%, 60%, and 80% of each training subset from AI-Face to assess the impact of training size

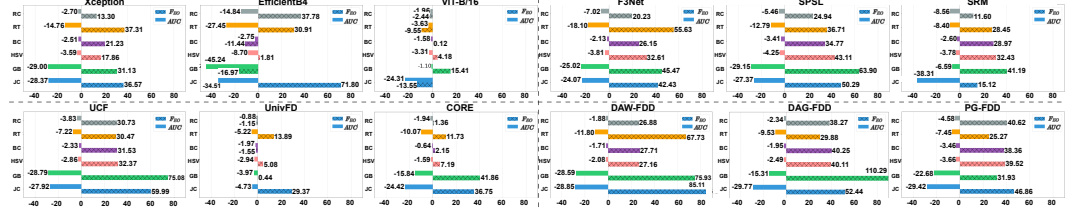


Figure 6: Visualization of performance changes after post-processing. Shorter bar represents better robustness.

Model Type	Detector	Dataset								Avg- $F_R$	
		A-DF-I.0 [19]		DF-Platter [35]		GenData [22]					
		Fairness(%)	Utility(%)	Fairness(%)	Utility(%)	Fairness(%)	Utility(%)				
		$F_{EO}$	AUC	$F_{EO}$	AUC	$F_{EO}$	AUC	$F_{EO}$	AUC		
Naive	Xception [61]	4.237(±3.956)	9.198(±8.759)	82.479(±17.289)	2.308(±2.037)	8.691(±8.252)	75.933(±23.835)	0.438(±0.167)	1.724(±1.385)	94.315(±5.453) <b>5.167</b>	
	EfficientB4 [62]	3.689(±3.094)	17.017(±15.788)	61.436(±37.681)	4.459(±3.864)	10.191(±8.962)	63.871(±35.246)	<b>0.001</b> (±0.594)	3.621(±2.392)	87.522(±1.595) <b>8.000</b>	
	ViT-B/16 [63]	4.45(±4.028)	9.154(±8.919)	70.896(±28.018)	2.531(±2.109)	5.557(±5.32)	68.935(±29.979)	1.249(±0.827)	2.874(±2.639)	89.109(±9.805) <b>6.667</b>	
Frequency	F3Net [64]	1.749(±1.663)	19.484(±18.932)	<b>86.265(±13.561)</b>	2.995(±2.909)	5.445(±4.893)	82.421(±17.405)	0.155(±0.069)	2.927(±2.375)	93.882(±5.944) <b>6.000</b>	
	SPSL [65]	8.497(±8.309)	2.430(±1.853)	75.177(±24.609)	3.323(±3.135)	8.966(±8.389)	82.024(±17.762)	0.138(±0.050)	2.321(±1.744)	94.320(±5.466) <b>6.167</b>	
	SRM [66]	3.708(±3.440)	<b>1.169(±0.633)</b>	65.779(±33.988)	4.976(±4.708)	33.702(±33.166)	72.777(±26.990)	1.545(±1.277)	2.378(±1.842)	94.130(±5.637) <b>8.000</b>	
Spatial	UCF [16]	2.930(±2.761)	9.924(±9.578)	83.260(±16.625)	3.536(±3.367)	9.395(±9.049)	83.92(±15.965)	1.346(±1.177)	1.377(±1.031)	94.948(±4.937) <b>6.500</b>	
	UniFD [67]	14.149(±13.592)	1.833(±1.343)	65.810(±30.220)	7.686(±7.129)	11.701(±11.211)	69.483(±26.547)	0.903(±0.346)	2.227(±1.737)	85.965(±10.065) <b>8.167</b>	
	CORE [68]	<b>0.308(±0.669)</b>	11.854(±10.000)	79.222(±19.624)	3.966(±2.989)	<b>5.267(±3.421)</b>	81.264(±17.582)	<b>0.056(±0.972)</b>	2.943(±1.097)	94.329(±4.517) <b>5.667</b>	
Fairness-enhanced	DAW-FDD [20]	5.040(±4.917)	4.993(±4.294)	80.308(±19.395)	2.577(±2.454)	7.253(±6.554)	78.562(±21.141)	0.205(±0.082)	2.708(±2.009)	93.876(±5.827) <b>6.000</b>	
	DAG-FDD [20]	4.279(±4.087)	13.565(±13.158)	85.859(±14.012)	3.885(±3.693)	7.350(±6.943)	83.153(±16.718)	1.062(±0.870)	1.688(±1.281)	94.326(±5.545) <b>7.167</b>	
	PG-FDD [21]	4.263(±4.129)	11.077(±10.840)	81.174(±18.763)	<b>1.984(±1.850)</b>	<b>4.715(±4.478)</b>	<b>84.572(±15.365)</b>	1.205(±1.071)	<b>1.159(±0.922)</b>	<b>94.962(±4.975)</b> <b>4.500</b>	

Table 6: Fairness generalization results based on the gender attribute. The smallest performance changes (in parentheses) and the best performance are in **bold** and in **red**, respectively.

on performance. Key observations from Fig. 7: 1) The performance of Uni-vFD changes slightest and cannot be improved with the increasing of data size. 2) Overall, detectors' performance improves with larger training set size, though few show fluctuations (e.g., ViT-B/16 and CORE). 3) A larger training set may improve utility but not always fairness. For example, Xception and SRM show increased utility when training size grows from 60% to 80%, but fairness worsens. Similar trends are observed in DAG-FDD and SPSL when the training set size increases from 40% to 60%. See Appendix B.8 for full results.

2) Overall, detectors' performance improves with larger training set size, though few show fluctuations (e.g., ViT-B/16 and CORE). 3) A larger training set may improve utility but not always fairness. For example, Xception and SRM show increased utility when training size grows from 60% to 80%, but fairness worsens. Similar trends are observed in DAG-FDD and SPSL when the training set size increases from 40% to 60%. See Appendix B.8 for full results.

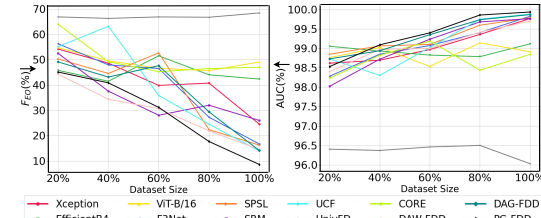


Figure 7: Impact of training set size on detectors' intersectional  $F_{EO}$ (%) and AUC (%).

**Discussion.** According to the above experiments, we summarize the unsolved fairness problems in recent detectors: 1) Detectors' fairness is unstable when detecting face images generated by different generative methods, indicating a future direction for enhancing fairness stability since new generative models continue to emerge. 2) Even though fairness-enhanced detectors exhibit small overall fairness metrics, they still show biased detection towards minority groups. Future studies should be more cautious when designing fair detectors to ensure balanced performance across all demographic groups. 3) There is currently no reliable detector, as all detectors experience severe large performance degradation under image post-processing and cross-domain evaluation. Future studies should aim to develop a unified framework that ensures fairness, robustness, and generalization, as these three characteristics are essential for creating a reliable detector.

## 5 Conclusion

This work presents the **first** demographically annotated million-scale AI-Face dataset, serving as a pivotal foundation for addressing the urgent need for developing fair AI face detectors. Based on our AI-Face dataset, we conduct the **first** comprehensive fairness benchmark, shedding light on the fairness performance and challenges of current representative AI face detectors. Our findings can inspire and guide researchers in refining current models and exploring new methods to mitigate bias.

**Limitation and Future Work:** One limitation is that age annotations in our AI-Face dataset have relatively lower accuracy as the age attribute is often too ambiguous to predict. We will improve our annotator's accuracy in predicting age attributes in the future. Additionally, we plan to extend our fairness benchmark to evaluate large language models like LLaMA2 [78] and GPT4 [79] for detecting AI faces. **Social Impact:** Malicious users could misuse AI-generated face images from our dataset to create fake social media profiles and spread misinformation. To mitigate this risk, only users who submit a signed end-user license agreement (EULA) will be granted access to our dataset.

## Acknowledgment

This work is supported by the U.S. National Science Foundation (NSF) under grant IIS-2348419 and the National Artificial Intelligence Research Resource (NAIRR) Pilot and TACC Lonestar6. The views, opinions and/or findings expressed are those of the author and should not be interpreted as representing the official views or policies of NSF and NAIRR Pilot.

## References

- [1] Li Lin, Neeraj Gupta, Yue Zhang, Hainan Ren, Chun-Hao Liu, Feng Ding, Xin Wang, Xin Li, Luisa Verdoliva, and Shu Hu. Detecting multimedia generated by large ai models: A survey. *arXiv preprint arXiv:2402.00045*, 2024.
- [2] Andreas Rossler, Davide Cozzolino, Luisa Verdoliva, Christian Riess, Justus Thies, and Matthias Nießner. Faceforensics++: Learning to detect manipulated facial images. In *Proceedings of the IEEE/CVF international conference on computer vision*, pages 1–11, 2019.
- [3] Deepfakes github. <https://github.com/deepfakes/faceswap>. Accessed: 2024-04-17.
- [4] Fakeapp. <https://www.fakeapp.com/>. Accessed: 2024-04-17.
- [5] Andrew Brock, Jeff Donahue, and Karen Simonyan. Large scale gan training for high fidelity natural image synthesis. In *7th International Conference on Learning Representations, ICLR 2019*, 2019.
- [6] Tero Karras, Samuli Laine, and Timo Aila. A style-based generator architecture for generative adversarial networks. In *Proceedings of the IEEE/CVF conference on computer vision and pattern recognition*, pages 4401–4410, 2019.
- [7] Tero Karras, Samuli Laine, Miika Aittala, Janne Hellsten, Jaakko Lehtinen, and Timo Aila. Analyzing and improving the image quality of stylegan. In *Proceedings of the IEEE/CVF conference on computer vision and pattern recognition*, pages 8110–8119, 2020.
- [8] Tero Karras, Miika Aittala, Samuli Laine, Erik Härkönen, Janne Hellsten, Jaakko Lehtinen, and Timo Aila. Alias-free generative adversarial networks. *Advances in neural information processing systems*, 34:852–863, 2021.
- [9] Robin Rombach, Andreas Blattmann, Dominik Lorenz, Patrick Esser, and Björn Ommer. High-resolution image synthesis with latent diffusion models. In *Proceedings of the IEEE/CVF conference on computer vision and pattern recognition*, pages 10684–10695, 2022.
- [10] Daniel J Tojin T. Eapen. How generative ai can augment human creativity. <https://hbr.org/2023/07/how-generative-ai-can-augment-human-creativity>, 2023. Accessed: 2024-04-21.
- [11] BBC News. Trump supporters target black voters with faked ai images. <https://www.bbc.com/news/world-us-canada-68440150>, 2024. Accessed: 2023-05-09.
- [12] Henrik Skaug Sætra. Generative ai: Here to stay, but for good? *Technology in Society*, 75:102372, 2023.
- [13] Mika Westerlund. The emergence of deepfake technology: A review. *Technology innovation management review*, 9(11), 2019.
- [14] Wenbo Pu, Jing Hu, Xin Wang, Yuezun Li, Shu Hu, Bin Zhu, Rui Song, Qi Song, Xi Wu, and Siwei Lyu. Learning a deep dual-level network for robust deepfake detection. *Pattern Recognition*, 130:108832, 2022.
- [15] Hui Guo, Shu Hu, Xin Wang, Ming-Ching Chang, and Siwei Lyu. Robust attentive deep neural network for detecting gan-generated faces. *IEEE Access*, 10:32574–32583, 2022.
- [16] Zhiyuan Yan, Yong Zhang, Yanbo Fan, and Baoyuan Wu. Ucf: Uncovering common features for generalizable deepfake detection. In *Proceedings of the IEEE/CVF International Conference on Computer Vision*, pages 22412–22423, 2023.

[17] Lorenzo Papa, Lorenzo Faiella, Luca Corvitto, Luca Maiano, and Irene Amerini. On the use of stable diffusion for creating realistic faces: from generation to detection. In *2023 11th International Workshop on Biometrics and Forensics (IWBF)*, pages 1–6. IEEE, 2023.

[18] Loc Trinh and Yan Liu. An examination of fairness of ai models for deepfake detection. *IJCAI*, 2021.

[19] Ying Xu, Philipp Terhöst, Marius Pedersen, and Kiran Raja. Analyzing fairness in deepfake detection with massively annotated databases. *IEEE Transactions on Technology and Society*, 2024.

[20] Yan Ju, Shu Hu, Shan Jia, George H Chen, and Siwei Lyu. Improving fairness in deepfake detection. In *Proceedings of the IEEE/CVF Winter Conference on Applications of Computer Vision*, pages 4655–4665, 2024.

[21] Li Lin, Xianan He, Yan Ju, Xin Wang, Feng Ding, and Shu Hu. Preserving fairness generalization in deepfake detection. *CVPR*, 2024.

[22] Christopher Teo, Milad Abdollahzadeh, and Ngai-Man Man Cheung. On measuring fairness in generative models. *Advances in Neural Information Processing Systems*, 36, 2024.

[23] Chuqiao Li, Zhiwu Huang, Danda Pani Paudel, Yabin Wang, Mohamad Shahbazi, Xiaopeng Hong, and Luc Van Gool. A continual deepfake detection benchmark: Dataset, methods, and essentials. In *Proceedings of the IEEE/CVF Winter Conference on Applications of Computer Vision*, pages 1339–1349, 2023.

[24] Jingyi Deng, Chenhao Lin, Pengbin Hu, Chao Shen, Qian Wang, Qi Li, and Qiming Li. Towards benchmarking and evaluating deepfake detection. *IEEE Transactions on Dependable and Secure Computing*, 2024.

[25] Zhiyuan Yan, Yong Zhang, Xinhang Yuan, Siwei Lyu, and Baoyuan Wu. Deepfakebench: A comprehensive benchmark of deepfake detection. In *NeurIPS*, 2023.

[26] Binh M Le, Jiwon Kim, Shahroz Tariq, Kristen Moore, Alsharif Abuadbba, and Simon S Woo. Sok: Facial deepfake detectors. *arXiv*, 2024.

[27] Alec Radford, Jong Wook Kim, Chris Hallacy, Aditya Ramesh, Gabriel Goh, Sandhini Agarwal, Girish Sastry, Amanda Askell, Pamela Mishkin, Jack Clark, et al. Learning transferable visual models from natural language supervision. In *International conference on machine learning*, pages 8748–8763. PMLR, 2021.

[28] Ian Goodfellow, Jean Pouget-Abadie, Mehdi Mirza, Bing Xu, David Warde-Farley, Sherjil Ozair, Aaron Courville, and Yoshua Bengio. Generative adversarial nets. *Advances in neural information processing systems*, 27, 2014.

[29] Midjourney. <https://mid-journey.ai/>. Accessed: 2024-04-17.

[30] Aditya Ramesh et al. Hierarchical text-conditional image generation with clip latents. *arXiv*, 1(2):3, 2022.

[31] Donie O’Sullivan. A high school student created a fake 2020 us candidate. twitter verified it. <https://cnn.it/3HpHfzz>, 2020. Accessed: 2024-04-21.

[32] Shannon Bond. That smiling linkedin profile face might be a computer-generated fake. <https://www.npr.org/2022/03/27/1088140809/fake-linkedin-profiles>, 2022. Accessed: 2024-04-21.

[33] Liming Jiang, Ren Li, Wayne Wu, Chen Qian, and Chen Change Loy. Deeperforensics-1.0: A large-scale dataset for real-world face forgery detection. In *Proceedings of the IEEE/CVF conference on computer vision and pattern recognition*, pages 2889–2898, 2020.

[34] Kartik Narayan, Harsh Agarwal, Kartik Thakral, Surbhi Mittal, Mayank Vatsa, and Richa Singh. Deepfy: On deepfake phylogeny. In *2022 IEEE International Joint Conference on Biometrics (IJCB)*, pages 1–10. IEEE, 2022.

[35] Kartik Narayan, Harsh Agarwal, Kartik Thakral, Surbhi Mittal, Mayank Vatsa, and Richa Singh. Df-platter: multi-face heterogeneous deepfake dataset. In *Proceedings of the IEEE/CVF Conference on Computer Vision and Pattern Recognition*, pages 9739–9748, 2023.

[36] Ziwei Liu, Ping Luo, Xiaogang Wang, and Xiaoou Tang. Deep learning face attributes in the wild. In *Proceedings of International Conference on Computer Vision (ICCV)*, December 2015.

[37] Dong Yi, Zhen Lei, Shengcai Liao, and Stan Z Li. Learning face representation from scratch. *arXiv*, 2014.

[38] Rasmus Rothe, Radu Timofte, and Luc Van Gool. Dex: Deep expectation of apparent age from a single image. In *Proceedings of the IEEE international conference on computer vision workshops*, pages 10–15, 2015.

[39] Brian Dolhansky, Joanna Bitton, Ben Pflaum, Jikuo Lu, Russ Howes, Menglin Wang, and Cristian Canton Ferrer. The deepfake detection challenge (dfdc) dataset. *arXiv preprint arXiv:2006.07397*, 2020.

[40] Google Research. Contributing data to deepfake detection research, 2019. Accessed: 2024-04-12.

[41] Yuezun Li, Xin Yang, Pu Sun, Honggang Qi, and Siwei Lyu. Celeb-df: A large-scale challenging dataset for deepfake forensics. In *Proceedings of the IEEE/CVF conference on computer vision and pattern recognition*, pages 3207–3216, 2020.

[42] Megvii Technology Limited. Face++ Face Detection. <https://www.faceplusplus.com/face-detection/>. Accessed: 2024-03.

[43] InsightFace Project Contributors. InsightFace: State-of-the-Art Face Analysis Toolbox. <https://insightface.ai/>. Accessed: 2024-03.

[44] Gabriel Ilharco, Mitchell Wortsman, Ross Wightman, Cade Gordon, Nicholas Carlini, Rohan Taori, Achal Dave, Vaishaal Shankar, Hongseok Namkoong, John Miller, Hannaneh Hajishirzi, Ali Farhadi, and Ludwig Schmidt. Open clip. [https://github.com/mlfoundations/open\\_clip](https://github.com/mlfoundations/open_clip), 2021.

[45] Pierre Foret, Ariel Kleiner, Hossein Mobahi, and Behnam Neyshabur. Sharpness-aware minimization for efficiently improving generalization. In *International Conference on Learning Representations*, 2020.

[46] Philipp Terhörst, Marco Huber, Jan Niklas Kolf, Ines Zelch, Naser Damer, Florian Kirchbuchner, and Arjan Kuijper. Reliable age and gender estimation from face images: Stating the confidence of model predictions. In *2019 IEEE 10th International Conference on Biometrics Theory, Applications and Systems (BTAS)*, pages 1–8. IEEE, 2019.

[47] Qiong Cao, Li Shen, Weidi Xie, Omkar M Parkhi, and Andrew Zisserman. Vggface2: A dataset for recognising faces across pose and age. In *2018 13th IEEE international conference on automatic face & gesture recognition (FG 2018)*, pages 67–74. IEEE, 2018.

[48] Philipp Terhörst, Daniel Fährmann, Jan Niklas Kolf, Naser Damer, Florian Kirchbuchner, and Arjan Kuijper. Maad-face: A massively annotated attribute dataset for face images. *IEEE Transactions on Information Forensics and Security*, 16:3942–3957, 2021.

[49] Oliver Giudice, Luca Guarnera, and Sebastiano Battiato. Fighting deepfakes by detecting gan dct anomalies. *Journal of Imaging*, 7(8):128, 2021.

[50] Vishal Asnani, Xi Yin, Tal Hassner, and Xiaoming Liu. Reverse engineering of generative models: Inferring model hyperparameters from generated images. *IEEE Transactions on Pattern Analysis and Machine Intelligence*, 2023.

[51] David Beniaguev. Synthetic faces high quality (sfhq) dataset, 2022.

[52] Zeyu Lu, Di Huang, Lei Bai, Jingjing Qu, Chengyue Wu, Xihui Liu, and Wanli Ouyang. Seeing is not always believing: Benchmarking human and model perception of ai-generated images. *Advances in Neural Information Processing Systems*, 36, 2024.

[53] L Minh Dang, Syed Ibrahim Hassan, Suhyeon Im, Jaecheol Lee, Sujin Lee, and Hyeonjoon Moon. Deep learning based computer generated face identification using convolutional neural network. *Applied Sciences*, 8(12):2610, 2018.

[54] Patrick Esser, Robin Rombach, and Bjorn Ommer. Taming transformers for high-resolution image synthesis. In *Proceedings of the IEEE/CVF conference on computer vision and pattern recognition*, pages 12873–12883, 2021.

[55] Zhendong Wang, Jianmin Bao, Wengang Zhou, Weilun Wang, Hezhen Hu, Hong Chen, and Houqiang Li. Dire for diffusion-generated image detection. *arXiv preprint arXiv:2303.09295*, 2023.

[56] Minchul Kim, Feng Liu, Anil Jain, and Xiaoming Liu. Dcface: Synthetic face generation with dual condition diffusion model. In *Proceedings of the IEEE/CVF Conference on Computer Vision and Pattern Recognition*, pages 12715–12725, 2023.

[57] Riccardo Corvi, Davide Cozzolino, Giada Zingarini, Giovanni Poggi, Koki Nagano, and Luisa Verdoliva. On the detection of synthetic images generated by diffusion models. In *ICASSP 2023-2023 IEEE International Conference on Acoustics, Speech and Signal Processing (ICASSP)*, pages 1–5. IEEE, 2023.

[58] Md Awsafur Rahman, Bishmoy Paul, Najibul Haque Sarker, Zaber Ibn Abdul Hakim, and Shaikh Anowarul Fattah. Artifact: A large-scale dataset with artificial and factual images for generalizable and robust synthetic image detection. *arXiv e-prints*, pages arXiv–2302, 2023.

[59] Haixu Song, Shiyu Huang, Yinpeng Dong, and Wei-Wei Tu. Robustness and generalizability of deepfake detection: A study with diffusion models. *arXiv preprint arXiv:2309.02218*, 2023.

[60] Jiankang Deng, Jia Guo, Evangelos Ververas, Irene Kotsia, and Stefanos Zafeiriou. Retinaface: Single-shot multi-level face localisation in the wild. In *Proceedings of the IEEE/CVF conference on computer vision and pattern recognition*, pages 5203–5212, 2020.

[61] François Chollet. Xception: Deep learning with depthwise separable convolutions. In *Proceedings of the IEEE conference on computer vision and pattern recognition*, pages 1251–1258, 2017.

[62] Mingxing Tan and Quoc Le. Efficientnet: Rethinking model scaling for convolutional neural networks. In *International conference on machine learning*, pages 6105–6114. PMLR, 2019.

[63] Alexey Dosovitskiy, Lucas Beyer, Alexander Kolesnikov, Dirk Weissenborn, Xiaohua Zhai, Thomas Unterthiner, Mostafa Dehghani, Matthias Minderer, Georg Heigold, Sylvain Gelly, et al. An image is worth 16x16 words: Transformers for image recognition at scale. In *9th International Conference on Learning Representations*, 2021.

[64] Yuyang Qian, Guojun Yin, Lu Sheng, Zixuan Chen, and Jing Shao. Thinking in frequency: Face forgery detection by mining frequency-aware clues. In *European conference on computer vision*, pages 86–103. Springer, 2020.

[65] Honggu Liu, Xiaodan Li, Wenbo Zhou, Yuefeng Chen, Yuan He, Hui Xue, Weiming Zhang, and Nenghai Yu. Spatial-phase shallow learning: rethinking face forgery detection in frequency domain. In *Proceedings of the IEEE/CVF conference on computer vision and pattern recognition*, pages 772–781, 2021.

[66] Yuchen Luo, Yong Zhang, Junchi Yan, and Wei Liu. Generalizing face forgery detection with high-frequency features. In *Proceedings of the IEEE/CVF conference on computer vision and pattern recognition*, pages 16317–16326, 2021.

[67] Utkarsh Ojha, Yuheng Li, and Yong Jae Lee. Towards universal fake image detectors that generalize across generative models. In *Proceedings of the IEEE/CVF Conference on Computer Vision and Pattern Recognition*, pages 24480–24489, 2023.

[68] Yunsheng Ni, Depu Meng, Changqian Yu, Chengbin Quan, Dongchun Ren, and Youjian Zhao. Core: Consistent representation learning for face forgery detection. In *Proceedings of the IEEE/CVF Conference on Computer Vision and Pattern Recognition*, pages 12–21, 2022.

[69] Xiaotian Han, Jianfeng Chi, Yu Chen, Qifan Wang, Han Zhao, Na Zou, and Xia Hu. Ffb: A fair fairness benchmark for in-processing group fairness methods. In *ICLR*, 2024.

[70] Ninareh Mehrabi, Fred Morstatter, Nripsuta Saxena, Kristina Lerman, and Aram Galstyan. A survey on bias and fairness in machine learning. *ACM computing surveys (CSUR)*, 54(6):1–35, 2021.

[71] Jialu Wang, Xin Eric Wang, and Yang Liu. Understanding instance-level impact of fairness constraints. In *International Conference on Machine Learning*, pages 23114–23130. PMLR, 2022.

[72] Hao Wang, Luxi He, Rui Gao, and Flavio P Calmon. Aleatoric and epistemic discrimination in classification. *ICML*, 2023.

[73] Cynthia Dwork, Moritz Hardt, Toniann Pitassi, Omer Reingold, and Richard Zemel. Fairness through awareness. In *Proceedings of the 3rd innovations in theoretical computer science conference*, pages 214–226, 2012.

[74] Shu Hu and George H Chen. Fairness in survival analysis with distributionally robust optimization. *arXiv*, 2023.

[75] Ming Liu, Yukang Ding, Min Xia, Xiao Liu, Errui Ding, Wangmeng Zuo, and Shilei Wen. Stgan: A unified selective transfer network for arbitrary image attribute editing. In *Proceedings of the IEEE/CVF conference on computer vision and pattern recognition*, pages 3673–3682, 2019.

[76] Federico Cocchi, Lorenzo Baraldi, Samuele Poppi, Marcella Cornia, Lorenzo Baraldi, and Rita Cucchiara. Unveiling the impact of image transformations on deepfake detection: An experimental analysis. In *International Conference on Image Analysis and Processing*, pages 345–356. Springer, 2023.

[77] Davide Cozzolino, Giovanni Poggi, Riccardo Corvi, Matthias Nießner, and Luisa Verdoliva. Raising the bar of ai-generated image detection with clip. *arXiv preprint arXiv:2312.00195*, 2023.

[78] Hugo Touvron, Louis Martin, Kevin Stone, Peter Albert, Amjad Almahairi, Yasmine Babaei, Nikolay Bashlykov, Soumya Batra, Prajwal Bhargava, Shruti Bhosale, et al. Llama 2: Open foundation and fine-tuned chat models. *arXiv preprint arXiv:2307.09288*, 2023.

[79] Josh Achiam, Steven Adler, Sandhini Agarwal, Lama Ahmad, Ilge Akkaya, Florencia Leoni Aleman, Diogo Almeida, Janko Altenschmidt, Sam Altman, Shyamal Anadkat, et al. Gpt-4 technical report. *arXiv preprint arXiv:2303.08774*, 2023.

[80] Ying Xu et al. A comprehensive analysis of ai biases in deepfake detection with massively annotated databases. *arXiv*, 2022.

[81] Eran Eider, Roei Enbar, and Tal Hassner. Age and gender estimation of unfiltered faces. *IEEE Transactions on information forensics and security*, 9(12):2170–2179, 2014.

[82] Robert Williamson and Aditya Menon. Fairness risk measures. In *International conference on machine learning*, pages 6786–6797. PMLR, 2019.

[83] Daniel Levy, Yair Carmon, John C Duchi, and Aaron Sidford. Large-scale methods for distributionally robust optimization. *Advances in Neural Information Processing Systems*, 33:8847–8860, 2020.

[84] R Tyrrell Rockafellar, Stanislav Uryasev, et al. Optimization of conditional value-at-risk. *Journal of risk*, 2:21–42, 2000.

[85] Tatsunori Hashimoto, Megha Srivastava, Hongseok Namkoong, and Percy Liang. Fairness without demographics in repeated loss minimization. In *International Conference on Machine Learning*, pages 1929–1938. PMLR, 2018.

[86] John C Duchi and Hongseok Namkoong. Learning models with uniform performance via distributionally robust optimization. *The Annals of Statistics*, 49(3):1378–1406, 2021.

[87] Timnit Gebru, Jamie Morgenstern, Briana Vecchione, Jennifer Wortman Vaughan, Hanna Wallach, Hal Daumé Iii, and Kate Crawford. Datasheets for datasets. *Communications of the ACM*, 64(12):86–92, 2021.

# Appendix

## A The Details of Demographically Annotated AI-Face Dataset

### A.1 Phase1: Annotator Development

#### A.1.1 Annotator Implementation Details

For developing the annotator, all experiments are based on the PyTorch with a single NVIDIA RTX A6000 GPU. For training, we fix the batch size 64, epochs 32, and use Adam optimizer with an initial learning rate  $\beta = 1e - 3$ . Additionally, we employ a Cosine Annealing Learning Rate Scheduler to modulate the learning rate adaptively across the training duration. The hyperparameter  $\gamma$  in SAM optimization is set as 0.05. For uncertainty estimation,  $k$  and  $\rho$  in uncertainty score  $V(X^{(a)})$  are set as 100 and 0.2, respectively.

#### A.1.2 Details of Threshold Settings for Sample Difficulty Level

For Q2, Setting: According to the distribution as shown in Appendix A.2.2, for VGGFace2 [47], A-DFDC [80], and A-DFD [80] test set, the threshold  $t_1^{Gender}$  and  $t_2^{Gender}$  are set as 0.25 and 0.4, respectively. And  $t_1^{Age}$  and  $t_2^{Age}$  are set as 0.3 and 0.5, respectively. The threshold for gender attribute is more strict than age because gender attribute prediction is a relatively easier task than age, as well as reflecting from the distribution. For A-FF++ [80] and A-Celeb-DF-v2 [80], we adjust the threshold  $t_1^{Gender}$  to 0.21 and  $t_2^{Gender}$  to 0.25 in order to get sufficient 1,500 images in each sample difficulty level subset, especially for ‘Hard’ level.

#### A.1.3 Additional Annotator Evaluation Results

From Table 7 to Table 11 are comparison results of our annotator against baselines InsightFace [43] and Face++[42] on detailed attributes. The findings and results align with the results in Table 3 of the submitted manuscript. For cross-domain evaluation, we additionally choose Adience [81] dataset, where images are manually annotated, consisting of over 26.5k real images of over 2.2k different individuals in unconstrained environments, to further validate the effectiveness and good generalization capability of our annotator. Results in table 12 demonstrate our annotator outperforms InsightFace [43] and Face++[42] again. Overall, one intra-domain dataset (VGGFace2) and five cross-domain datasets (A-FF++, A-DFDC, A-DFD, A-Celeb-DF-v2, and Adience) all validate that our annotator’s superior performance against current state-of-the-art face attribute prediction tools Face++ [42] and InsightFace [43].

Level	Method	VGGFace2 [47]														
		Female			Male			Young			Middle_Aged			Senior		
		precision	recall	F1	precision	recall	F1									
All	Face++ [42]	77.042 (0.363)	83.597 (0.789)	80.060 (0.444)	79.571 (0.780)	72.314 (0.516)	75.584 (0.453)	80.201 (2.448)	34.649 (1.182)	46.991 (1.278)	46.049 (0.832)	63.692 (1.588)	53.327 (0.976)	66.266 (1.030)	<b>77.261</b> <b>(1.188)</b>	71.320 (0.955)
	InsightFace [43]	76.560 (0.533)	78.062 (0.737)	77.281 (0.534)	76.946 (0.629)	75.395 (0.555)	76.139 (0.474)	78.730 (2.135)	30.533 (0.961)	42.907 (1.052)	41.660 (1.005)	56.653 (1.429)	47.936 (1.078)	61.426 (0.649)	76.107 (1.212)	67.966 (0.724)
	Ours	<b>81.452</b> (0.413)	<b>89.467</b> (0.331)	<b>85.158</b> (0.323)	<b>87.267</b> (0.393)	<b>82.329</b> (0.572)	<b>82.401</b> (0.438)	<b>95.619</b> (0.565)	<b>80.467</b> (1.343)	<b>86.659</b> (0.629)	<b>91.189</b> (0.565)	<b>75.027</b> (0.880)	<b>81.666</b> (0.629)	<b>88.043</b> (0.585)	76.720 (0.982)	<b>81.747</b> (1.388)
Easy	Face++ [42]	97.482 (0.604)	96.742 (0.549)	97.108 (0.329)	96.697 (0.545)	97.439 (0.642)	97.064 (0.355)	89.360 (0.670)	57.507 (1.825)	69.964 (1.403)	58.673 (0.837)	72.205 (1.397)	64.729 (0.669)	79.536 (1.119)	89.546 (0.600)	84.240 (0.687)
	InsightFace [43]	97.625 (0.403)	96.373 (0.229)	96.994 (0.124)	96.420 (0.206)	97.653 (0.410)	97.073 (0.135)	88.544 (0.917)	50.080 (1.831)	63.957 (1.585)	53.146 (0.621)	65.720 (1.001)	58.762 (0.497)	73.657 (0.808)	88.200 (0.748)	80.271 (0.555)
	Ours	<b>99.575</b> (0.176)	<b>99.893</b> (0.100)	<b>99.734</b> (0.126)	<b>99.893</b> (0.100)	<b>99.573</b> (0.177)	<b>99.733</b> (0.127)	<b>99.720</b> (0.098)	<b>99.760</b> (0.049)	<b>99.740</b> (0.049)	<b>99.279</b> (0.400)	<b>99.000</b> (0.164)	<b>99.139</b> (0.431)	<b>99.551</b> (0.688)	<b>96.480</b> (0.204)	<b>97.988</b>
Medium	Face++ [42]	72.977 (0.292)	81.336 (1.246)	76.927 (0.679)	78.435 (1.101)	69.245 (0.681)	73.549 (0.618)	76.257 (0.732)	24.427 (0.709)	36.996 (1.057)	41.197 (0.961)	61.838 (2.458)	49.446 (1.472)	62.616 (1.171)	73.719 (0.503)	67.710 (0.759)
	InsightFace [43]	73.710 (0.699)	75.360 (1.316)	74.521 (0.907)	74.807 (1.070)	73.120 (0.766)	73.950 (0.755)	74.222 (2.488)	22.080 (0.588)	34.033 (0.928)	37.372 (1.208)	53.480 (2.160)	43.995 (1.535)	58.070 (0.282)	73.840 (1.216)	65.008 (0.497)
	Ours	<b>82.518</b> (0.621)	<b>95.253</b> (0.482)	<b>88.428</b> (0.439)	<b>94.389</b> (0.544)	<b>79.813</b> (0.544)	<b>86.489</b> (0.588)	<b>96.648</b> (0.627)	<b>84.200</b> (1.730)	<b>89.987</b> (0.111)	<b>95.382</b> (0.604)	<b>75.920</b> (1.017)	<b>84.540</b> (0.650)	<b>87.960</b> (0.915)	<b>76.800</b> (1.544)	<b>81.993</b> (1.018)
Hard	Face++ [42]	60.667 (0.194)	72.714 (0.571)	66.146 (0.323)	63.582 (0.694)	50.259 (0.226)	56.140 (0.385)	74.987 (3.942)	22.012 (1.012)	34.013 (1.374)	38.276 (0.697)	<b>57.032</b> (0.910)	45.807 (0.758)	56.647 (0.799)	<b>68.517</b> (2.462)	62.009 (1.420)
	InsightFace [43]	58.345 (0.498)	62.453 (0.667)	60.329 (0.570)	59.611 (0.610)	55.413 (0.489)	57.435 (0.533)	73.425 (2.999)	19.440 (0.463)	30.730 (0.642)	34.462 (1.187)	50.760 (1.127)	41.050 (1.202)	52.550 (0.858)	66.280 (1.671)	58.618 (1.121)
	Ours	<b>62.263</b> (0.443)	<b>73.255</b> (0.410)	<b>67.312</b> (0.403)	<b>67.518</b> (0.534)	<b>55.600</b> (0.680)	<b>60.982</b> (0.604)	<b>90.490</b> (0.971)	<b>57.440</b> (2.218)	<b>70.249</b> (1.726)	<b>78.905</b> (1.564)	50.160 (1.222)	<b>61.315</b> (0.941)	<b>76.617</b> (1.600)	56.880 (1.933)	<b>65.260</b> (1.288)

Table 7: Detailed comparison of our annotator against Face++ [42] and InsightFace [43] on VGGFace2 dataset. ‘All’ denotes the averaged metrics across three levels of sample difficulty: ‘Easy’, ‘Medium,’ and ‘Hard.’ Prediction mean and standard deviation (in parentheses) of each method across 5 random samplings and testings within each level are reported. The best results are shown in Bold.

Level	Method	A-FF++ [80]														
		Female			Male			Young			Middle_Aged			Senior		
		precision	recall	F1	precision	recall	F1	precision	recall	F1	precision	recall	F1	precision	recall	F1
All	Face++ [42]	<b>90.106</b>	88.345	89.129	88.560	<b>90.007</b>	89.201	74.707	72.839	73.547	52.934	<b>81.935</b>	63.981	84.769	37.933	51.193
	InsightFace [43]	<b>(0.282)</b>	(0.400)	(0.220)	(0.323)	<b>(0.295)</b>	(0.188)	(1.264)	(0.581)	(0.656)	(0.790)	<b>(1.288)</b>	(0.852)	(0.922)	(1.705)	(1.884)
	Ours	87.918	81.284	84.344	82.787	88.662	85.533	67.148	83.284	74.317	48.659	74.220	58.725	<b>93.455</b>	20.959	33.854
Easy	Face++ [42]	<b>98.157</b>	97.947	98.052	97.950	<b>98.159</b>	98.054	85.686	93.398	89.372	69.170	89.520	78.036	<b>95.646</b>	58.880	72.888
	InsightFace [43]	97.004	96.640	96.820	96.656	97.013	96.833	76.172	98.120	85.762	61.246	86.840	71.828	98.106	28.800	44.524
	Ours	97.987	<b>99.920</b>	<b>98.944</b>	<b>99.919</b>	97.947	<b>98.923</b>	<b>91.450</b>	<b>100.000</b>	<b>95.530</b>	<b>99.494</b>	<b>94.320</b>	<b>96.838</b>	95.154	<b>85.022</b>	<b>89.802</b>
Medium	Face++ [42]	98.839	89.590	93.985	90.605	<b>98.960</b>	94.597	84.212	80.092	82.098	48.990	<b>86.710</b>	62.604	91.594	25.400	39.746
	InsightFace [43]	(0.312)	(0.691)	(0.146)	(0.131)	<b>(0.308)</b>	(0.151)	(0.625)	(1.072)	(0.676)	(0.878)	(0.431)	(0.651)	<b>(0.371)</b>	(0.546)	(0.427)
	Ours	95.655	79.813	87.017	82.685	96.373	89.005	69.090	85.800	76.542	45.982	73.680	56.622	<b>96.654</b>	15.040	26.022
Hard	Face++ [42]	<b>73.323</b>	77.498	75.352	77.123	<b>72.901</b>	<b>74.952</b>	54.224	45.026	49.172	40.642	<b>69.576</b>	51.302	67.066	29.518	40.946
	InsightFace [43]	<b>(0.231)</b>	(0.374)	(0.220)	(0.284)	<b>(0.292)</b>	<b>(0.184)</b>	(2.425)	(0.291)	(0.960)	(0.901)	<b>(2.847)</b>	(1.385)	(1.727)	(2.881)	(3.122)
	Ours	71.096	67.400	69.194	69.020	72.600	70.762	56.182	<b>65.932</b>	60.648	38.748	62.140	47.724	85.604	19.036	31.016

Table 8: *Detailed comparison of our annotator against Face++ [42] and InsightFace [43] on A-FF++ dataset. ‘All’ denotes the averaged metrics across three levels of sample difficulty: ‘Easy,’ ‘Medium,’ and ‘Hard.’ Prediction mean and standard deviation (in parentheses) of each method across 5 random samplings and testings within each level are reported. The best results are shown in Bold.*

Level	Method	A-DFDC [19]														
		Female			Male			Young			Middle_Aged			Senior		
		precision	recall	F1												
All	Face++ [42]	74.751	83.324	78.453	78.824	68.797	72.922	74.499	81.417	77.479	58.696	74.613	65.608	85.533	52.741	63.542
	InsightFace [43]	(0.675)	(0.948)	(0.603)	(0.933)	(0.929)	(0.732)	(0.567)	(1.186)	(0.772)	(0.688)	(0.420)	(0.496)	(0.792)	(1.559)	(1.469)
	Ours	72.691	64.662	68.376	68.160	<b>75.560</b>	71.623	71.209	<b>86.658</b>	77.985	58.102	76.777	66.086	83.061	36.659	49.620
Easy	Face++ [42]	<b>94.124</b>	89.917	91.965	90.351	94.367	92.309	86.386	96.596	91.316	73.340	85.560	78.974	99.440	71.324	83.066
	InsightFace [43]	(0.977)	(1.010)	(0.564)	(0.835)	(1.025)	(0.553)	(0.691)	(0.715)	(0.489)	(0.853)	(0.933)	(0.622)	(0.255)	(1.015)	(0.768)
	Ours	91.874	78.693	84.753	81.389	93.013	86.801	73.580	95.760	83.216	62.690	77.960	69.494	94.034	42.760	58.776
Medium	Face++ [42]	<b>95.289</b>	<b>97.413</b>	<b>96.337</b>	<b>97.353</b>	<b>95.173</b>	<b>96.248</b>	<b>97.448</b>	<b>99.240</b>	<b>98.334</b>	<b>94.902</b>	<b>96.996</b>	<b>95.938</b>	<b>99.730</b>	<b>89.844</b>	<b>94.528</b>
	InsightFace [43]	(0.191)	(0.136)	(0.566)	(0.622)	(0.848)	(0.619)	(0.633)	(1.103)	(0.752)	(0.670)	(0.540)	(0.280)	(0.168)	(0.433)	(0.303)
	Ours	90.438	81.415	75.529	77.764	65.533	<b>71.124</b>	70.980	64.526	67.584	53.830	69.930	60.828	73.342	58.332	64.972
Hard	Face++ [42]	69.072	<b>95.067</b>	<b>80.011</b>	<b>92.097</b>	57.433	70.746	<b>89.568</b>	67.934	<b>77.250</b>	<b>94.220</b>	69.246	<b>79.824</b>	<b>82.306</b>	<b>82.014</b>	<b>82.158</b>
	InsightFace [43]	(0.350)	(0.680)	(0.444)	(1.027)	(0.512)	(0.593)	(0.325)	(2.048)	(1.451)	(1.257)	(0.431)	(0.524)	(1.062)	(0.908)	(0.891)
	Ours	59.692	<b>78.639</b>	<b>67.866</b>	<b>68.357</b>	46.489	55.334	65.930	83.128	73.536	48.918	68.350	57.022	83.816	28.568	42.588

Table 9: *Detailed comparison of our annotator against Face++ [42] and InsightFace [43] on A-DFDC dataset. ‘All’ denotes the averaged metrics across three levels of sample difficulty: ‘Easy,’ ‘Medium,’ and ‘Hard.’ Prediction mean and standard deviation (in parentheses) of each method across 5 random samplings and testings within each level are reported. The best results are shown in Bold.*

## A.2 Phase2: Demographically Annotation Generation

### A.2.1 Detailed Information of Datasets

Table 13 shows the detailed information of all subsets we collected and incorporated into our AI-Face dataset. It covers fake facial images from deepfake videos, generated from GANs and DMs. The corresponding real sources of most AI-generated face subsets are FFHQ [6] and CelebA [36]. In general, our AI-Face dataset contains 30 subsets (22 fake subsets and 8 real subsets) and 37 generation methods (methods are summed as 5 in A-FF++, 5 in A-DFD, 8 in A-DFDC, 1 in A-Celeb-DF-v2, 10 GANs, and 8 DMs), including a total of 1,245,660 fake face images and 866,096 real face images. Fig. A.1 visualizes face images of each subset. Fig. A.2 further demonstrates the detailed demographic distribution of our AI-Face dataset. The dataset is relatively gender-balanced, and the subjects are majorly young and white individuals.

### A.2.2 Details of Threshold Settings for Human Correction

In this section, we present uncertainty score distributions of each attribute (*i.e.*, Gender, Age, and Race) of each subset in our AI-Face dataset, as shown from Fig. A.4 to Fig. A.31. Overall, our annotator shows higher confidence in predicting gender attributes compared to predicting age, as observed from these uncertainty score distributions. It is clear that different subsets show different

Level	Method	A-DFD[19]					
		Female			Male		
		precision	recall	F1	precision	recall	F1
All	Face++ [42]	<b>74.375</b> ( <b>1.442</b> )	62.743 (1.445)	67.925 (1.256)	68.258 (1.197)	78.854 (1.544)	<b>73.096</b> ( <b>1.228</b> )
	InsightFace [43]	71.967 (1.062)	51.796 (1.161)	59.975 (1.053)	63.600 (0.651)	<b>81.636</b> ( <b>0.863</b> )	71.405 (0.660)
	Ours	72.884 (0.580)	<b>83.547</b> ( <b>0.753</b> )	<b>77.548</b> ( <b>0.538</b> )	<b>78.938</b> ( <b>0.750</b> )	66.418 (0.979)	71.615 (0.783)
Easy	Face++ [42]	<b>95.014</b> ( <b>0.377</b> )	82.284 (1.876)	88.179 (1.011)	84.398 (1.378)	<b>95.677</b> ( <b>0.391</b> )	89.676 (0.686)
	InsightFace [43]	94.405 (0.777)	75.573 (0.956)	83.944 (0.794)	79.639 (0.683)	95.520 (0.634)	86.858 (0.596)
	Ours	94.434 (0.418)	<b>93.600</b> ( <b>0.566</b> )	<b>94.013</b> ( <b>0.307</b> )	<b>93.659</b> ( <b>0.517</b> )	94.480 (0.451)	<b>94.066</b> ( <b>0.295</b> )
Medium	Face++ [42]	<b>65.536</b> ( <b>1.779</b> )	60.151 (1.249)	62.715 (1.202)	63.114 (1.077)	68.283 (2.356)	<b>65.587</b> ( <b>1.566</b> )
	InsightFace [43]	64.397 (1.071)	47.147 (1.433)	54.434 (1.310)	58.323 (0.769)	<b>73.947</b> ( <b>0.646</b> )	65.211 (0.671)
	Ours	65.158 (0.886)	<b>86.133</b> ( <b>0.625</b> )	<b>74.188</b> ( <b>0.666</b> )	<b>79.536</b> ( <b>0.911</b> )	53.920 (1.776)	64.258 (1.472)
Hard	Face++ [42]	<b>62.576</b> ( <b>2.170</b> )	45.793 (1.210)	52.882 (1.556)	57.261 (1.137)	72.603 (1.885)	<b>64.024</b> ( <b>1.433</b> )
	InsightFace [43]	57.100 (1.339)	32.667 (1.096)	41.547 (1.054)	52.838 (0.501)	<b>75.440</b> ( <b>1.310</b> )	62.145 (0.714)
	Ours	59.062 (0.437)	<b>70.907</b> ( <b>1.068</b> )	<b>64.442</b> ( <b>0.641</b> )	<b>63.618</b> ( <b>0.820</b> )	50.853 (0.709)	56.520 (0.582)

Table 10: Detailed comparison of our annotator against Face++ [42] and InsightFace [43] on A-DFD dataset. ‘All’ denotes the averaged metrics across three levels of sample difficulty: ‘Easy,’ ‘Medium,’ and ‘Hard.’ Prediction mean and standard deviation (in parentheses) of each method across 5 random samplings and testings within each level are reported. The best results are shown in Bold.

distributions, so we dynamically adjust the threshold  $t^{a_j}$  for each attribute  $a$  on subset  $j$  defined in ‘Human Correction’ in Section 3.2. First, we fit the distribution with gamma distribution and calculate its mean and standard deviation. Then, the  $t^{a_j}$  is calculated using  $Mean + \lambda Std$ . After getting the threshold, we can get the total image number within each subset that needed human correction. We assume it takes three seconds for a human to correct one annotation for one image, then we can calculate the total time needed for a human to correct these images beyond the threshold. Therefore, The  $\lambda$  is dynamically adjusted based on the distribution and the total time needed for human correction.

### A.2.3 Examples of Mislabeled images in A-FF++ and A-DFDC

In the evaluation results for Q1 in Section 3.2, we have validated that we cannot directly incorporate existing annotations into our AI-Face dataset. Fig. A.3 displays some image examples where annotations in A-FF++ [80] and A-DFDC [80] are inconsistent with the annotations given by our annotator. A-FF and A-DFDC have mislabeled annotations for ambiguous facial images, whereas our annotator can accurately predict them. This visualization of images further validates that existing annotations cannot be directly merged into our dataset.

### A.2.4 Additional Results of Validating the Effectiveness of Human Correction Strategy

Since A-DFD [19] and A-Celeb-DF-v2 [19] provide gender annotation, we can compare our two versions of datasets with it. One is Ours before human correction (*i.e.*, Ours-DFD(w/o Correction) and Ours-A-Celeb-DF-v2(w/o Correction)), another one is Ours after human correction (*i.e.*, Ours-DFD (Correction) and Ours-A-Celeb-DF-v2 (Correction)). As same setting as in evaluation for Q2 Section 3.2, we sample 1,200 attribute-balanced images (400 easy, 400 medium, and 400 hard) based on uncertainty score. Three humans re-annotated these images to establish ground truth. As shown in Table 14, Ours-DFD (Correction) and Ours-A-Celeb-DF-v2 (Correction) outperforms ours without correction version and A-DFD and A-Celeb-DF-v2 (*e.g.*, the accuracy of Ours-DFD (Correction) is 22.866% higher than A-DFD and 13.526% higher than Ours-DFD(w/o Correction)). This suggests that our dataset annotation quality is much better than the existing annotation in A-DFD [19] and A-Celeb-DF-v2 [19]. And our human correction strategy further improves our dataset annotation quality.

Level	Method	A-Celeb-DF-v2 [19]					
		Female			Male		
		precision	recall	F1	precision	recall	F1
All	Face++ [42]	<b>97.624</b> ( <b>0.815</b> )	83.302 (0.727)	89.455 (0.438)	86.517 (0.494)	<b>98.318</b> ( <b>0.640</b> )	91.819 (0.453)
	InsightFace [43]	97.442 (0.537)	85.842 (0.569)	91.041 (0.317)	88.079 (0.388)	98.007 (0.464)	92.635 (0.299)
	Ours	96.381 (0.756)	<b>93.611</b> ( <b>0.564</b> )	<b>94.921</b> ( <b>0.400</b> )	<b>94.147</b> ( <b>0.422</b> )	96.687 (0.782)	<b>95.355</b> ( <b>0.426</b> )
Easy	Face++ [42]	99.889 (0.055)	96.480 (0.418)	98.155 (0.236)	96.598 (0.392)	99.893 (0.053)	98.218 (0.222)
	InsightFace [43]	99.837 (0.054)	98.107 (0.352)	98.964 (0.180)	98.140 (0.340)	99.840 (0.053)	98.983 (0.174)
	Ours	<b>100.000</b> ( <b>0.000</b> )	<b>99.973</b> ( <b>0.053</b> )	<b>99.987</b> ( <b>0.027</b> )	<b>99.973</b> ( <b>0.053</b> )	<b>100.000</b> ( <b>0.000</b> )	<b>99.987</b> ( <b>0.027</b> )
Medium	Face++ [42]	99.732 (0.199)	89.227 (0.952)	94.185 (0.558)	90.260 (0.787)	<b>99.760</b> ( <b>0.177</b> )	94.771 (0.460)
	InsightFace [43]	99.639 (0.226)	88.320 (0.496)	93.638 (0.354)	89.513 (0.412)	99.680 (0.200)	94.323 (0.298)
	Ours	<b>99.760</b> ( <b>0.053</b> )	<b>99.760</b> ( <b>0.177</b> )	<b>99.760</b> ( <b>0.100</b> )	<b>99.760</b> ( <b>0.176</b> )	<b>99.760</b> ( <b>0.053</b> )	<b>99.760</b> ( <b>0.100</b> )
Hard	Face++ [42]	<b>93.251</b> ( <b>2.190</b> )	64.200 (0.812)	76.024 (0.519)	72.694 (0.304)	<b>95.300</b> ( <b>1.691</b> )	82.469 (0.679)
	InsightFace [43]	92.850 (1.331)	71.100 (0.860)	80.521 (0.417)	76.584 (0.412)	94.500 (1.140)	84.600 (0.424)
	Ours	89.384 (2.214)	<b>81.100</b> ( <b>1.463</b> )	<b>85.015</b> ( <b>1.073</b> )	<b>82.707</b> ( <b>1.037</b> )	90.300 (2.294)	<b>86.319</b> ( <b>1.150</b> )

Table 11: *Detailed comparison of our annotator against Face++ [42] and InsightFace [43] on A-Celeb-DF-v2 dataset. ‘All’ denotes the averaged metrics across three levels of sample difficulty: ‘Easy,’ ‘Medium,’ and ‘Hard.’ Prediction mean and standard deviation (in parentheses) of each method across 5 random samplings and testings within each level are reported. The best results are shown in Bold.*

Level	Method	Adience [81]														
		Female			Male			Young			Middle_Aged			Senior		
		precision	recall	F1												
All	Face++ [42]	71.800 (0.900)	87.124 (0.743)	76.457 (0.797)	84.701 (0.863)	71.257 (0.601)	76.322 (0.444)	<b>89.823</b> ( <b>1.024</b> )	68.558 (0.696)	77.632 (1.569)	<b>51.442</b> ( <b>1.397</b> )	<b>70.678</b> ( <b>1.313</b> )	<b>58.668</b> ( <b>3.051</b> )	50.280 (3.228)	<b>76.456</b> ( <b>2.199</b> )	60.540
	InsightFace [43]	67.003 (0.687)	74.180 (1.140)	68.487 (0.650)	73.848 (1.068)	67.877 (0.722)	69.512 (0.585)	86.510 (1.147)	37.559 (1.079)	51.425 (1.225)	37.028 (0.888)	65.519 (1.304)	45.545 (0.884)	26.775 (1.672)	72.412 (2.321)	38.946 (2.045)
	Ours	<b>78.103</b> ( <b>0.732</b> )	<b>94.416</b> ( <b>0.338</b> )	<b>83.852</b> ( <b>0.603</b> )	<b>96.915</b> ( <b>0.382</b> )	<b>82.496</b> ( <b>0.607</b> )	<b>88.602</b> ( <b>0.443</b> )	77.517 (0.500)	<b>81.767</b> ( <b>0.963</b> )	<b>79.579</b> ( <b>0.579</b> )	48.206 (1.794)	37.327 (0.529)	41.843 (1.061)	<b>67.352</b> ( <b>3.613</b> )	69.370 (3.679)	<b>68.241</b> ( <b>3.258</b> )
Easy	Face++ [42]	97.977 (0.251)	93.613 (0.646)	95.658 (0.273)	92.325 (0.660)	97.319 (0.344)	94.754 (0.253)	96.754 (0.746)	81.939 (0.434)	88.730 (0.434)	33.469 (2.274)	68.722 (1.985)	44.960 (2.095)	59.861 (4.706)	88.473 (4.331)	71.165 (2.485)
	InsightFace [43]	96.613 (0.210)	89.815 (1.000)	93.087 (0.537)	88.180 (0.980)	96.009 (0.331)	91.925 (0.540)	<b>97.076</b> ( <b>0.455</b> )	58.063 (0.819)	72.662 (0.717)	19.981 (0.942)	<b>70.808</b> ( <b>2.276</b> )	31.150 (1.185)	26.572 (2.943)	84.972 (2.722)	40.411 (3.521)
	Ours	<b>99.822</b> ( <b>0.104</b> )	<b>99.974</b> ( <b>0.052</b> )	<b>99.898</b> ( <b>0.078</b> )	<b>99.969</b> ( <b>0.063</b> )	<b>99.776</b> ( <b>0.124</b> )	<b>99.872</b> ( <b>0.094</b> )	93.651 (0.599)	<b>97.159</b> ( <b>0.507</b> )	<b>95.372</b> ( <b>0.455</b> )	<b>57.920</b> ( <b>2.428</b> )	37.414 (0.217)	<b>45.375</b> ( <b>1.469</b> )	<b>97.721</b> ( <b>3.063</b> )	<b>96.833</b> ( <b>2.986</b> )	<b>97.221</b> ( <b>2.037</b> )
Medium	Face++ [42]	82.280 (1.064)	87.626 (0.710)	84.863 (0.617)	72.271 (1.249)	63.091 (1.654)	67.350 (0.996)	<b>90.557</b> ( <b>0.379</b> )	64.622 (1.015)	75.413 (1.015)	<b>57.229</b> ( <b>1.350</b> )	<b>71.100</b> ( <b>1.350</b> )	<b>63.397</b> ( <b>1.350</b> )	47.362 (2.070)	<b>75.972</b> ( <b>3.031</b> )	58.295 (1.800)
	InsightFace [43]	78.900 (1.250)	75.366 (0.827)	77.087 (0.818)	55.589 (0.852)	60.493 (1.375)	57.923 (0.637)	83.417 (2.029)	30.372 (1.239)	44.510 (2.587)	40.618 (0.713)	61.066 (0.618)	48.776 (1.616)	26.303 (2.274)	65.071 (1.300)	37.453 (2.744)
	Ours	<b>92.671</b> ( <b>0.607</b> )	<b>99.184</b> ( <b>0.280</b> )	<b>95.816</b> ( <b>0.385</b> )	<b>98.159</b> ( <b>0.599</b> )	<b>84.639</b> ( <b>0.735</b> )	<b>90.897</b> ( <b>0.505</b> )	76.159 (0.372)	<b>80.899</b> ( <b>0.913</b> )	<b>78.455</b> ( <b>0.492</b> )	40.740 (1.307)	34.599 (0.808)	37.409 (0.812)	<b>69.317</b> ( <b>5.848</b> )	69.799 (5.737)	<b>69.532</b> ( <b>5.645</b> )
Hard	Face++ [42]	35.144 (1.384)	80.134 (0.874)	48.851 (1.502)	89.507 (0.591)	53.361 (0.522)	66.860 (0.701)	<b>82.159</b> ( <b>0.682</b> )	59.114 ( <b>0.638</b> )	<b>68.752</b> ( <b>0.697</b> )	<b>63.628</b> ( <b>0.626</b> )	<b>72.212</b> ( <b>0.495</b> )	<b>67.646</b> ( <b>2.376</b> )	43.617 (2.322)	<b>64.923</b> ( <b>2.311</b> )	<b>52.162</b> (2.092)
	InsightFace [43]	25.495 (0.602)	57.358 (1.154)	35.287 (0.596)	77.776 (1.373)	47.129 (0.460)	58.688 (0.572)	79.037 (0.956)	24.242 (0.280)	37.102 (0.372)	50.485 (0.789)	64.681 (0.923)	56.708 (0.848)	27.452 (0.773)	<b>67.194</b> ( <b>1.967</b> )	38.973 (0.999)
	Ours	<b>41.818</b> ( <b>1.484</b> )	<b>84.089</b> ( <b>0.684</b> )	<b>55.842</b> ( <b>1.345</b> )	<b>92.619</b> ( <b>0.486</b> )	<b>63.072</b> ( <b>0.962</b> )	<b>75.038</b> ( <b>0.730</b> )	62.742 (0.530)	<b>67.243</b> ( <b>1.468</b> )	64.907 (0.790)	45.958 (1.648)	39.968 (1.648)	42.745 (0.563)	35.018 (0.902)	41.479 (1.929)	37.972 (2.314)

Table 12: *Detailed comparison of our annotator against Face++ [42] and InsightFace [43] on Adience dataset. ‘All’ denotes the averaged metrics across three levels of sample difficulty: ‘Easy,’ ‘Medium,’ and ‘Hard.’ Prediction mean and standard deviation (in parentheses) of each method across 5 random samplings and testings within each level are reported. The best results are shown in Bold.*

## B Fairness Benchmark

### B.1 Details of Detection Methods

**Xception** [61]: is a deep convolutional neural network (CNN) architecture that relies on depthwise separable convolutions. This approach significantly reduces the number of parameters and computational cost while maintaining high performance. Xception serves as a classic backbone in deepfake detectors.

**EfficientB4** [62]: is part of the EfficientNet family [62], which utilizes a novel model scaling method that uniformly scales all dimensions of depth, width, and resolution using a compound coefficient. EfficientNet also serves as a classic backbone in deepfake detectors.

Methods	#Samples	FFHQ [6]	CASIA-WebFace [37]	IMDB-WIKI [38]	CelebA [36]	A-FF+ (Real) [80]	A-DFDC (Real) [80]	A-DFD (Real) [80]	A-Celeb-DF-v2 (Real) [80]
A-FF++ [2]	105K					✓			
A-DFDC [39]	37K					✓			
A-DFD [40]	31K						✓		
A-Celeb-DF-v2 [41]	155K								✓
AttGAN [49]	6K					✓			
MMDGAN [50]	1K					✓			
StarGAN [49]	5.6K					✓			
StyleGAN [49]	10K	✓							
StyleGAN2 [51]	118K	✓							
StyleGAN3 [52]	26.7K	✓							
MSG-StyleGAN [50]	1K					✓			
ProGAN [53]	100K					✓			
STGAN [50]	1K					✓			
VQGAN [54]	50K	✓							
DALLE2 [55]	204					✓			
IF [55]	505					✓			
Midjourney [55]	100					✓			
DFCFace [56]	529K								
Latent Diffusion [57]	20K	✓							
Palette [58]	6K					✓			
SD v1.5 [59]	18K								
SD Inpainting [59]	20.9K								
<b>Total</b>	<b>1,245,660</b>	<b>70,000</b>	<b>474,876</b>	<b>26,788</b>	<b>202,502</b>	<b>21,593</b>	<b>37,836</b>	<b>8,856</b>	<b>23,645</b>
						<b>866,096</b>			

Table 13: Number of real and fake images from different fake image datasets and their corresponding real image sources.

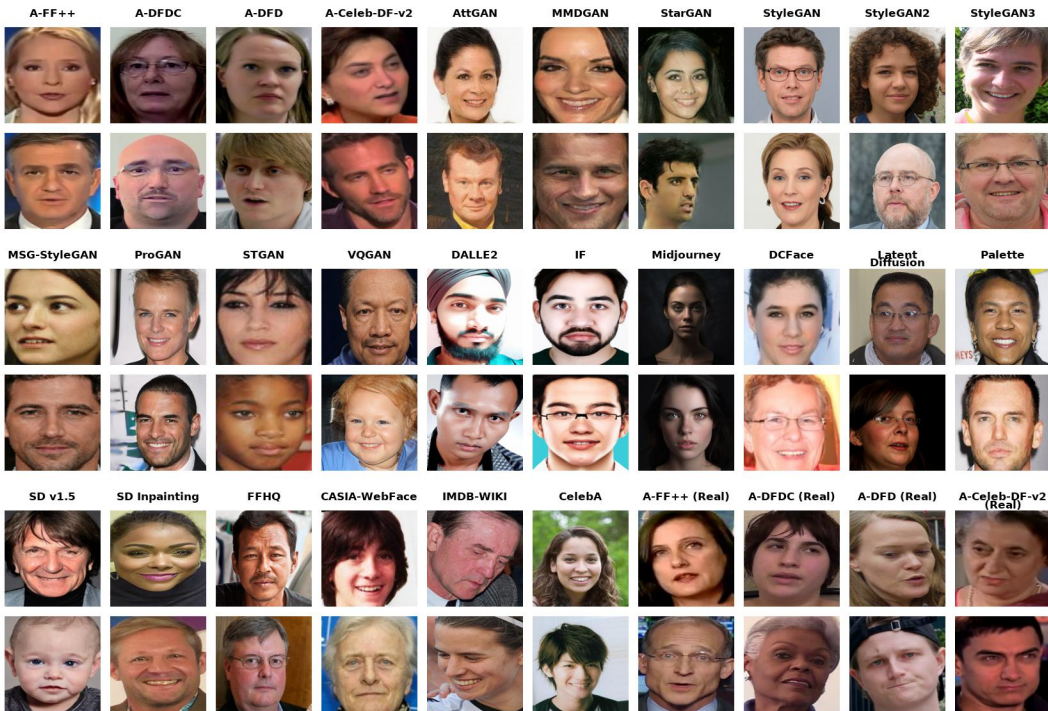


Figure A.1: Visualization of images in AI-Face dataset. SD is short for Stable Diffusion.

**ViT-B/16** [63]: is a model that applies the transformer architecture, the 'B' denotes the base model size, and '16' indicates the patch size. ViT-B/16 splits images into 16 patches, linearly embeds each patch, adds positional embeddings, and feeds the resulting sequence of vectors into a standard transformer encoder.

**F3Net** [64]: utilizes a cross-attention two-stream network to effectively identify frequency-aware clues by integrating two branches: FAD and LFS. The FAD (Frequency-aware Decomposition) module divides the input image into various frequency bands using learnable partitions, representing the image with frequency-aware components to detect forgery patterns through this decomposition. Meanwhile, the LFS (Localized Frequency Statistics) module captures local frequency statistics to highlight statistical differences between authentic and counterfeit faces.

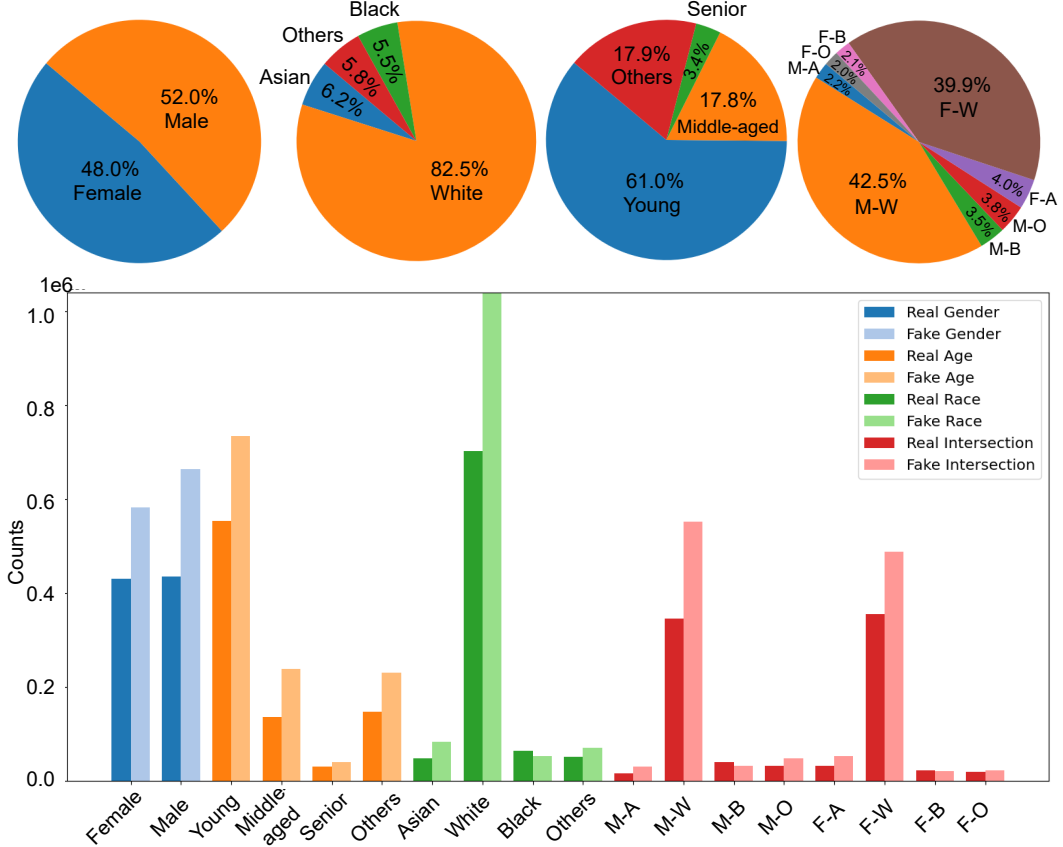


Figure A.2: Detailed demographic distribution of AI-Face dataset.

Gender		ACC	Precision	Recall	F1
A-DFD [19]		70.612	71.347	74.245	69.900
Ours-DFD(w/o Correction)		79.952	79.868	83.979	79.308
Ours-DFD (Correction)		<b>93.478</b>	<b>91.673</b>	<b>95.034</b>	<b>92.898</b>
A-Celeb-DF-v2 [19]		89.697	90.622	90.622	89.697
Ours-A-Celeb-DF-v2(w/o Correction)		91.414	91.404	91.831	91.391
Ours-A-Celeb-DF-v2 (Correction)		<b>93.535</b>	<b>93.655</b>	<b>94.087</b>	<b>93.525</b>

Table 14: Evaluation results to demonstrate the effectiveness of human correction strategy.

**SPSL** [65]: integrates spatial image data with the phase spectrum to detect up-sampling artifacts in face forgeries, enhancing the model’s generalization ability for face forgery detection. The paper provides a theoretical analysis of the effectiveness of using the phase spectrum. Additionally, it highlights that local texture information is more important than high-level semantic information for accurately detecting face forgeries.

**SRM** [66]: extracts high-frequency noise features and combines two different representations from the RGB and frequency domains to enhance the model’s generalization ability for face forgery detection.

**UCF** [16]: presents a multi-task disentanglement framework designed to tackle two key challenges in deepfake detection: overfitting to irrelevant features and overfitting to method-specific textures. By identifying and leveraging common features, this framework aims to improve the model’s generalization ability.

**UnivFD** [67]: uses the frozen CLIP ViT-L/14 [44] as feature extractor and trains the last linear layer to classify fake and real images.



Figure A.3: Examples of face images where annotations in A-FF++ and A-DFDC are inconsistent with Ours-FF++ (w/o Correction) and Ours-DFDC (w/o Correction).

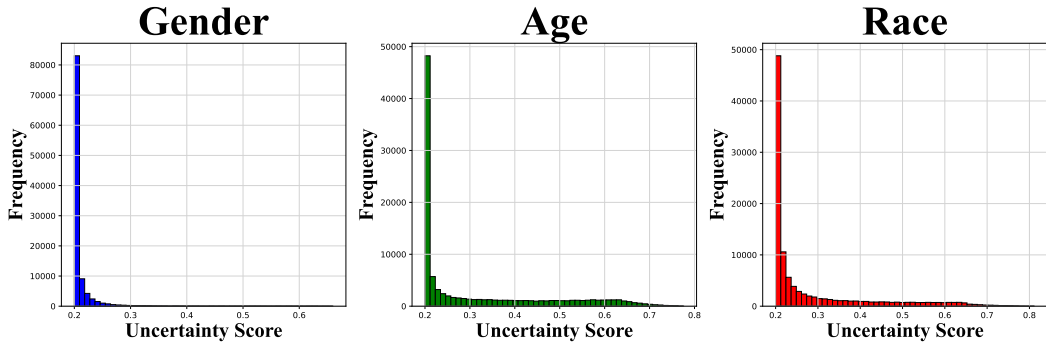


Figure A.4: Uncertainty Score histograms for gender, age and race for A-FF++ [2] dataset.

**CORE** [68]: explicitly enforces the consistency of different representations. It first captures various representations through different augmentations and then regularizes the cosine distance between these representations to enhance their consistency.

**DAW-FDD** [20]: a demographic-aware Fair Deepfake Detection (DAW-FDD) method leverages demographic information and employs an existing fairness risk measure [82]. At a high level, DAW-FDD aims to ensure that the losses achieved by different user-specified groups of interest (e.g., different races or genders) are similar to each other (so that the AI face detector is not more accurate on one group vs another) and, moreover, that the losses across all groups are low. Specifically, DAW-FDD uses a CVaR [83, 84] loss function across groups (to address imbalance in demographic groups) and, per group, DAW-FDD uses another CVaR loss function (to address imbalance in real vs AI-generated training examples).

**DAG-FDD** [20]: a demographic-agnostic Fair Deepfake Detection (DAG-FDD) method, which is based on the distributionally robust optimization (DRO) [85, 86]. To use DAG-FDD, the user does not have to specify which attributes to treat as sensitive such as race and gender, only need to specify a probability threshold for a minority group without explicitly identifying all possible groups.

**PG-FDD** [21]: PG-FDD (Preserving Generalization Fair Deepfake Detection) employs disentanglement learning to extract demographic and domain-agnostic forgery features, promoting fair learning across a flattened loss landscape. Its framework combines disentanglement learning, fairness learning, and optimization modules. The disentanglement module introduces a loss to expose demographic and domain-agnostic features that enhance fairness generalization. The fairness learning module combines these features to promote fair learning, guided by generalization principles. The optimization module flattens the loss landscape, helping the model escape suboptimal solutions and strengthen fairness generalization.

## B.2 Implementation Details

For fairness benchmark, all experiments are based on the PyTorch with a single NVIDIA RTX A6000 GPU. During training, we utilize SGD optimizer with a learning rate of 0.0005, with momentum of 0.9 and weight decay of 0.005. The batch size is set to 128 for most detectors. However, for the SRM [66], UCF [16], and PG-FDD [21], the batch size is adjusted to 32 due to GPU memory. For

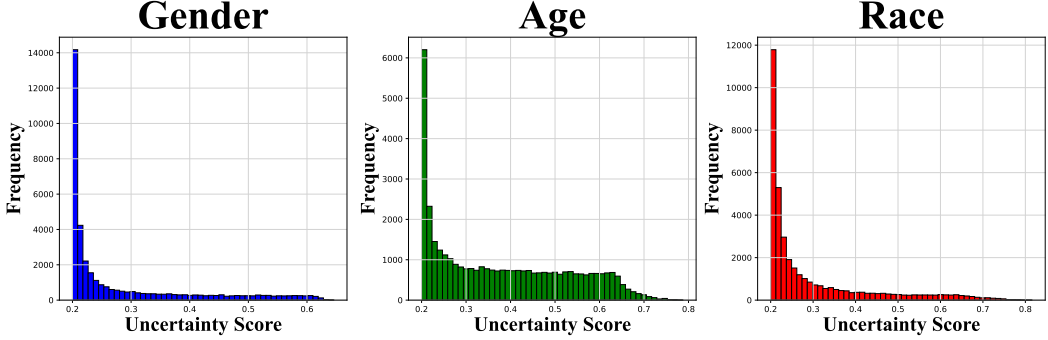


Figure A.5: *Uncertainty Score histograms for gender, age and race for A-DFDC [39] dataset.*

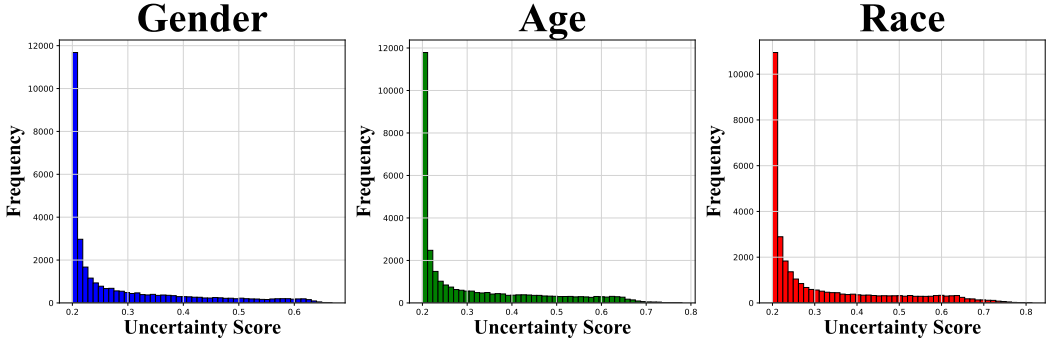


Figure A.6: *Uncertainty Score histograms for gender, age and race for A-DFD [40] dataset.*

hyperparameters defined in these detectors, we use the default values set in their original papers. All detectors are initialized with their official pre-trained weights, and trained for 5 epochs.

### B.3 Fairness Metrics

We assume a test set comprising indices  $\{1, \dots, n\}$ .  $Y_j$  and  $\hat{Y}_j$  respectively represent the true and predicted labels of the sample  $X_j$ . Their values are binary, where 0 means real and 1 means fake. For all fairness metrics, a lower value means better performance.

$$\begin{aligned}
 F_{EO} &:= \sum_{\mathcal{J}_j \in \mathcal{J}} \sum_{q=0}^1 \left| \frac{\sum_{j=1}^n \mathbb{I}_{[\hat{Y}_j=1, D_j=\mathcal{J}_j, Y_j=q]}}{\sum_{j=1}^n \mathbb{I}_{[D_j=\mathcal{J}_j, Y_j=q]}} - \frac{\sum_{j=1}^n \mathbb{I}_{[\hat{Y}_j=1, Y_j=q]}}{\sum_{j=1}^n \mathbb{I}_{[Y_j=q]}} \right|, \\
 F_{OAE} &:= \max_{\mathcal{J}_j \in \mathcal{J}} \left\{ \frac{\sum_{j=1}^n \mathbb{I}_{[\hat{Y}_j=Y_j, D_j=\mathcal{J}_j]}}{\sum_{j=1}^n \mathbb{I}_{[D_j=\mathcal{J}_j]}} - \min_{\mathcal{J}'_j \in \mathcal{J}} \frac{\sum_{j=1}^n \mathbb{I}_{[\hat{Y}_j=Y_j, D_j=\mathcal{J}'_j]}}{\sum_{j=1}^n \mathbb{I}_{[D_j=\mathcal{J}'_j]}} \right\}, \\
 F_{DP} &:= \max_{q \in \{0,1\}} \left\{ \max_{\mathcal{J}_j \in \mathcal{J}} \frac{\sum_{j=1}^n \mathbb{I}_{[\hat{Y}_j=q, D_j=\mathcal{J}_j]}}{\sum_{j=1}^n \mathbb{I}_{[D_j=\mathcal{J}_j]}} - \min_{\mathcal{J}'_j \in \mathcal{J}} \frac{\sum_{j=1}^n \mathbb{I}_{[\hat{Y}_j=q, D_j=\mathcal{J}'_j]}}{\sum_{j=1}^n \mathbb{I}_{[D_j=\mathcal{J}'_j]}} \right\}, \\
 F_{MEO} &:= \max_{q, q' \in \{0,1\}} \left\{ \max_{\mathcal{J}_j \in \mathcal{J}} \frac{\sum_{j=1}^n \mathbb{I}_{[\hat{Y}_j=q, Y_j=q', D_j=\mathcal{J}_j]}}{\sum_{j=1}^n \mathbb{I}_{[D_j=\mathcal{J}_j, Y_j=q]}} - \min_{\mathcal{J}'_j \in \mathcal{J}} \frac{\sum_{j=1}^n \mathbb{I}_{[\hat{Y}_j=q, Y_j=q', D_j=\mathcal{J}'_j]}}{\sum_{j=1}^n \mathbb{I}_{[D_j=\mathcal{J}'_j, Y_j=q]}} \right\}, \\
 F_{IND} &:= \sum_{j=1}^n \sum_{l=j+1}^n \mathbb{I}_{[|f(X_j) - f(X_l)| - \delta \|X_j - X_l\|]}, \\
 \text{Avg-}F_R &:= \frac{1}{|F|} \sum_{f \in F} R_{m,f}, \text{Avg-}F_{MR} := \frac{1}{|M_t|} \sum_{m \in M_t} \text{Avg-}F_R.
 \end{aligned}$$

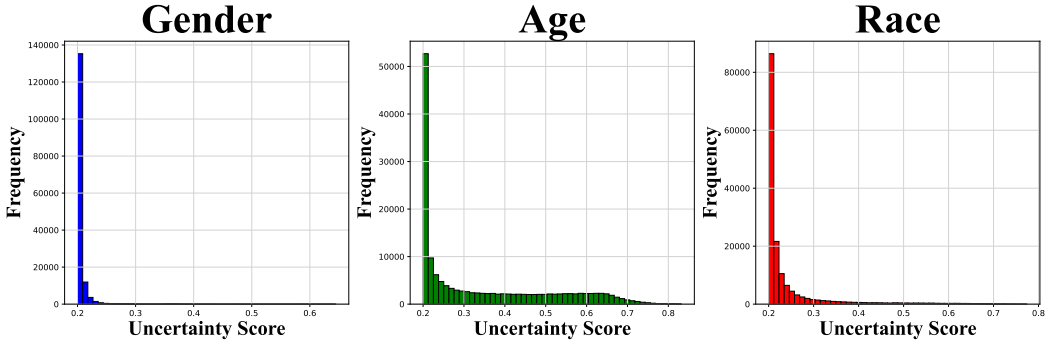


Figure A.7: Uncertainty Score histograms for gender, age and race for A-Celeb-DF-v2 [41] dataset.

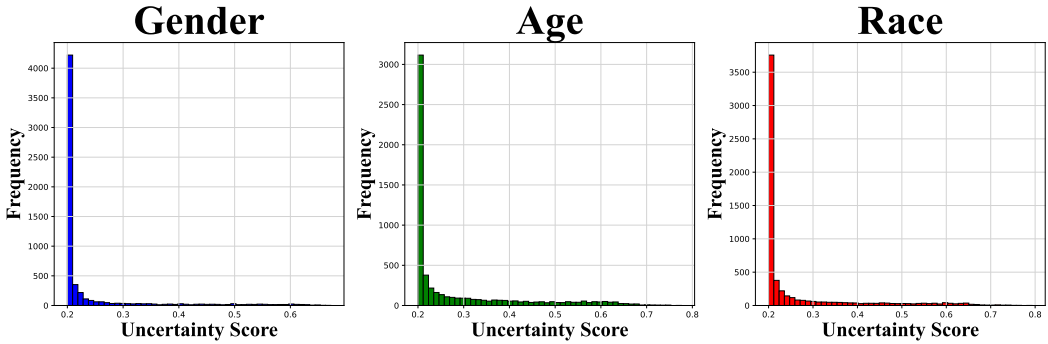


Figure A.8: Uncertainty Score histograms for gender, age and race for AttGAN [49] dataset.

Where  $D$  is the demographic variable,  $\mathcal{J}$  is the set of subgroups with each subgroup  $\mathcal{J}_j \in \mathcal{J}$ .  $M$  is the set of detection models and  $F$  is the set of fairness metrics.  $R_{m,f}$  is the rank of detection model  $m \in M$  for fairness metric  $f \in F$ .  $|F|$  is the total number of fairness metrics.  $T$  is the set of model types, and  $M_t$  is the set of detection models within model type  $t \in T$ .  $|M_t|$  is the total number of detection models within model type  $t$ .  $F_{EO}$  measures the disparity in TPR or FPR between each subgroup and the overall population.  $F_{OAE}$  measures the maximum ACC gap across all demographic groups.  $F_{DP}$  measures the maximum difference in prediction rates across all demographic groups. And  $F_{MEO}$  captures the largest disparity in prediction outcomes (either positive or negative) when comparing different demographic groups.  $\delta$  in  $F_{IND}$  is a predefined scale factor (0.06 in our experiments).  $f(X_j)$  represents the predicted logits of the model for input sample  $X_j$ .  $F_{IND}$  points that a model should be fair across individuals if similar individuals have similar predicted outcomes. Avg- $F_R$  is the average fairness rank of detection model  $m$ , Avg- $F_{MR}$  is the average fairness rank of a model type.

#### B.4 Full Subsets Evaluation Results

Detailed test results of each subset as shown from Table 16 to Table 35 are presented in this section. The findings align with the results reported in Fig. 4.

#### B.5 Details of Post-Processing

In Section 4 we have applied 6 post-processing methods to evaluate detectors' robustness. Fig. B.1 visualizes the image after being applied different post-processing methods. We describe each post-processing method as follows:

**JPEG Compression:** Image compression introduces compression artifacts and reduces the image quality, simulating real-world scenarios where images may be of lower quality or have compression artifacts. In Fig. 6 we apply image compression with quality 60 to each image in the test set.

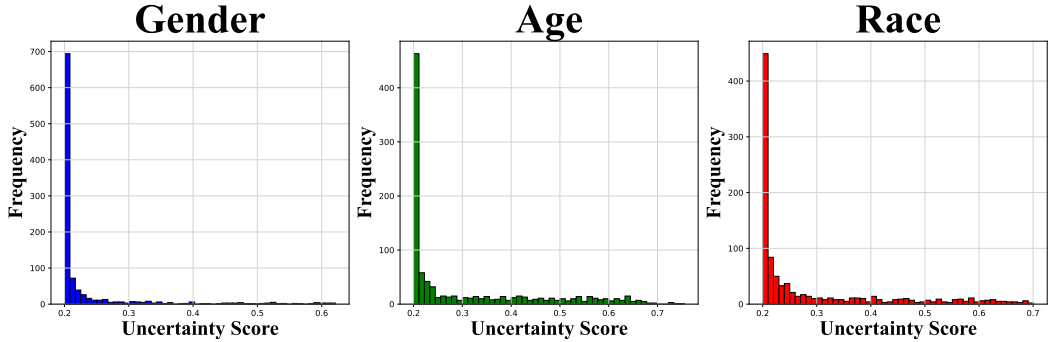


Figure A.9: *Uncertainty Score histograms for gender, age and race for MMDGAN [50] dataset.*

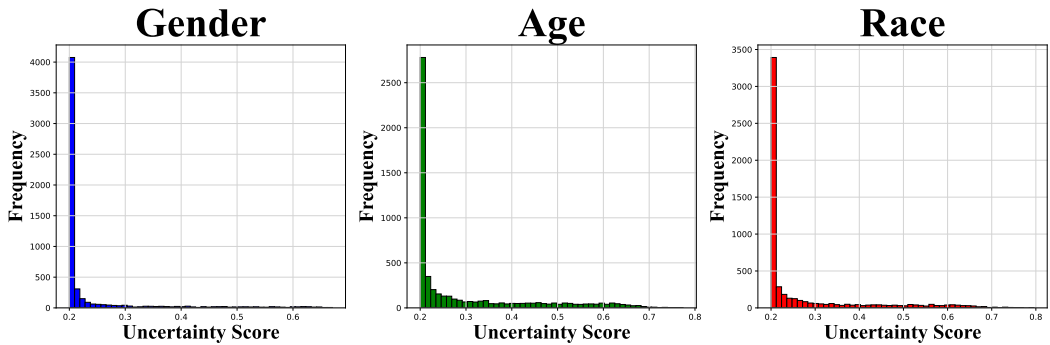


Figure A.10: *Uncertainty Score histograms for gender, age and race for StarGAN [49] dataset.*

**Gaussian Blur:** This post-processing reduces image detail and noise by smoothing it through averaging pixel values with a Gaussian kernel. In Fig. 6 we apply gaussian blur with kernel size 7 to each image in the test set.

**Hue Saturation Value:** Alters the hue, saturation, and value of the image within specified limits. This post-processing technique is used to simulate variations in color and lighting conditions. Adjusting the hue changes the overall color tone, saturation controls the intensity of colors, and value adjusts the brightness. The results in Fig. 6 are after we adjust hue, saturation, and value with shifting limits 30.

**Random Brightness and Contrast:** This post-processing method adjusts the brightness and contrast of the image within specified limits. By applying random brightness and contrast variations, it introduces changes in the illumination and contrast levels of the images. This evaluates detector’s robustness to different illumination conditions. The results in Fig. 6 are after we adjust brightness and contrast with shifting limits 0.2.

**Random Crop:** Resizes the image to a specified size and then randomly crops a portion of it to the target dimensions. This post-processing method is used to evaluate the detector’s robustness to variations in the spatial content of the image. The results in Fig. 6 are after we randomly crop the image with target dimension of  $244 \times 244$ .

**Rotation:** Rotates the image within a specified angle limit. This post-processing method is used to evaluate the detector’s robustness to changes in the orientation of objects within the image. The results in Fig. 6 are after we randomly rotate the image within a range of -45 to 45 degrees.

## B.6 Additional Fairness Robustness Evaluation Results

Fig. B.2 to Fig. B.6 demonstrate detectors’ robustness analysis in more detail as a function of different degrees of post-processing. Overall, ViT-B/16 [63] and UnivFD [67] show stronger robustness to various post-processing methods compared to other detection methods. Fairness-enhanced detectors do not have robustness against post-processing; this would be a direction for future studies to work on.

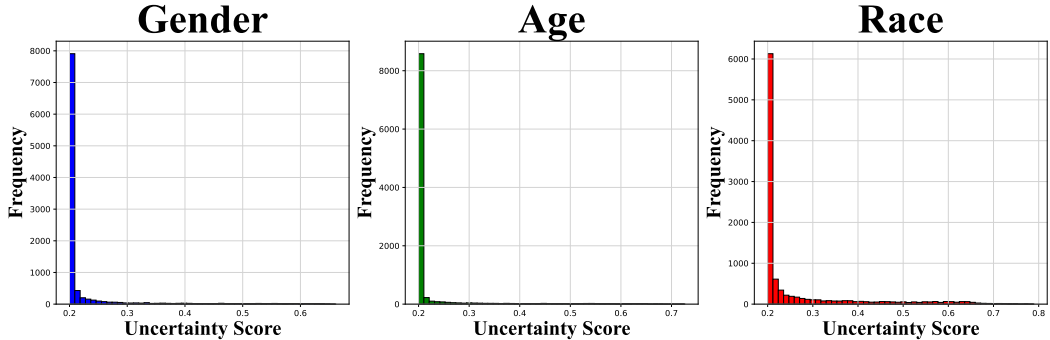


Figure A.11: *Uncertainty Score histograms for gender, age and race for StyleGAN [49] dataset.*

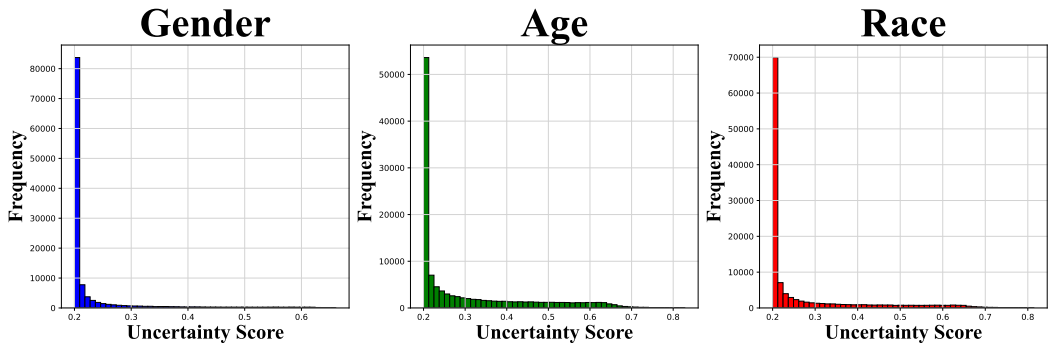


Figure A.12: *Uncertainty Score histograms for gender, age and race for StyleGAN2 [51] dataset.*

Figure B.2 presents a detailed robustness analysis in terms of utility and fairness under varying degrees of JPEG compression. The utility of all detectors decreases as image quality is reduced. Among the detectors, UnivFD [67] exhibits the highest utility robustness, while ViT-B/16 [63] demonstrates the strongest fairness robustness. When considering Gaussian blur, ViT-B/16 stands out as the most robust detector in terms of utility, whereas EfficientB4 [62] shows the greatest robustness in terms of fairness. Against Hue Saturation Value adjustments, DAW-FDD [20] shows the strongest utility robustness, while UnivFD excels in fairness robustness. ViT-B/16 demonstrates superior robustness in both utility and fairness when facing rotations. For brightness contrast variations, DAG-FDD [20] is the most robust detector in terms of utility, while UnivFD once again shows superior robustness in terms of fairness.

## B.7 Additional Fairness Generalization Evaluation Results

We conduct additional generalization experiments by using models trained on FF++ [2] to evaluate their generalization performance on our AI-Face test set. For these experiments, we utilize the trained weights and intra-domain performance metrics provided by [16]. Consequently, only the detectors with the pre-trained weights available from [16] are evaluated on our AI-Face test set. Results are shown in Table 6. We report the detailed performance on generation category subsets (*i.e.*, Deepfake Videos, GANs, and DMs) and the overall performance on the whole test set. We observe that detectors exhibit significant performance degradation, approaching coin-toss performance when trained on FF++ and tested on our AI-Face test set. This suggests that detectors trained solely on one deepfake video dataset is not sufficient for detecting face images generated by current more advanced generation models. This also highlights the significance of our AI-Face dataset, which is extensive, diverse and comprehensive in generation methods to develop and evaluate existing AI face detectors. The lowest performance is observed with GANs, likely due to the higher variety of generation methods within this category. Conversely, performance on the Deepfake Videos subset is relatively better. This could be because, despite being different datasets, the deepfake videos may share similar generation methods, resulting in less variation in the artifacts present in the generated images.

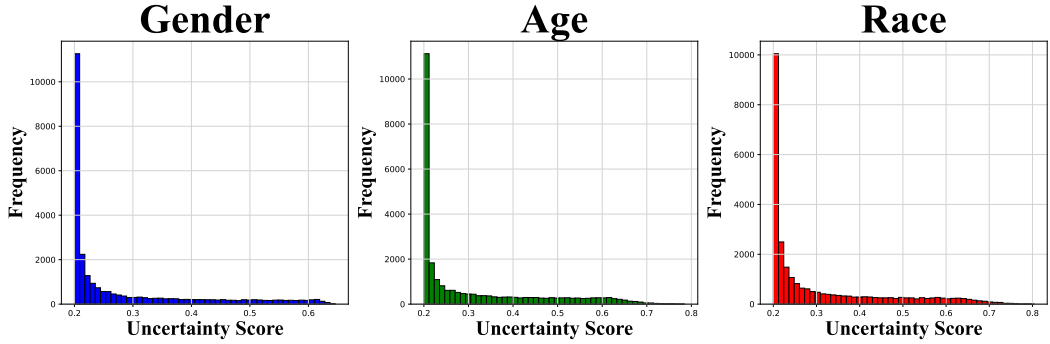


Figure A.13: *Uncertainty Score histograms for gender, age and race for StyleGAN3 [52] dataset.*

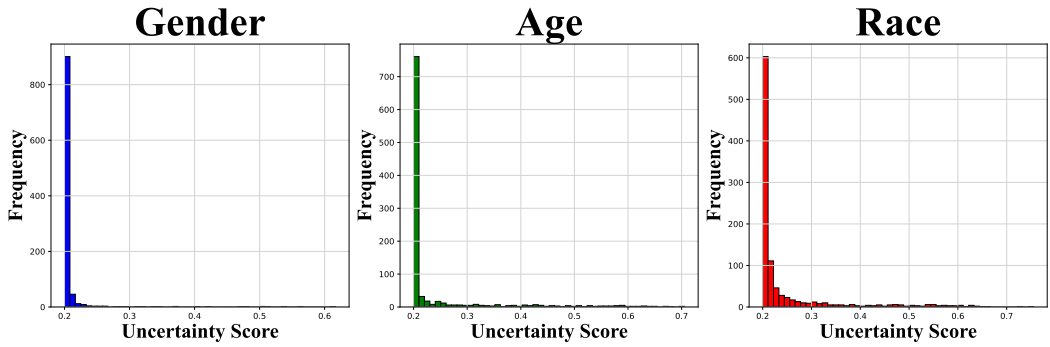


Figure A.14: *Uncertainty Score histograms for gender, age and race for MSG-StyleGAN [50] dataset.*

## B.8 Full Results of Effect of Increasing the Size of Train Set

In this section, we provide the full evaluation results tested under different sizes of train set, as shown from Table 37 to Table 40. Intersection  $F_{EO}$  and AUC align with the results in Fig. 7 of the submitted manuscript.

## B.9 Fairness and Utility Trade-off

Fig. B.7 presents the trade-offs between  $F_{DP}$  on age and AUC of three fairness-enhanced methods. This is to analyze how well these methods balance optimizing utility and ensuring fairness in decision-making. 1) PG-FDD [21] achieves the best utility-fairness trade-off overall. It improves fairness without compromising the precision of utility, maintaining high accuracy in detection. For instance, PG-FDD achieves a higher AUC than DAW-FDD and DAG-FDD while maintaining comparable fairness metrics. 2) DAW-FDD [20] is sensitive to the hyperparameter that balances utility-fairness. For example, when its fairness approaches to zero, its utility also drops to a coin-tossing performance. This sensitivity can hinder practical deployment, as extensive tuning is required to optimize performance. 3) To ensure broader applicability and reliability, future fairness approaches should aim to minimize sensitivity to hyperparameter settings.

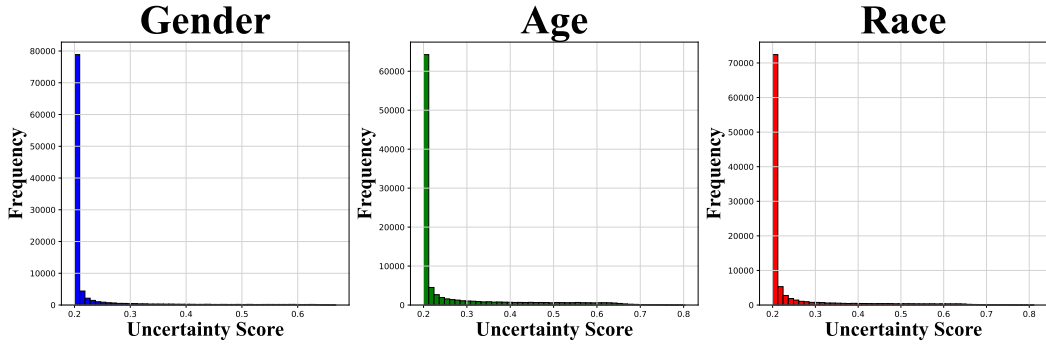


Figure A.15: *Uncertainty Score histograms for gender, age and race for ProGAN [53] dataset.*

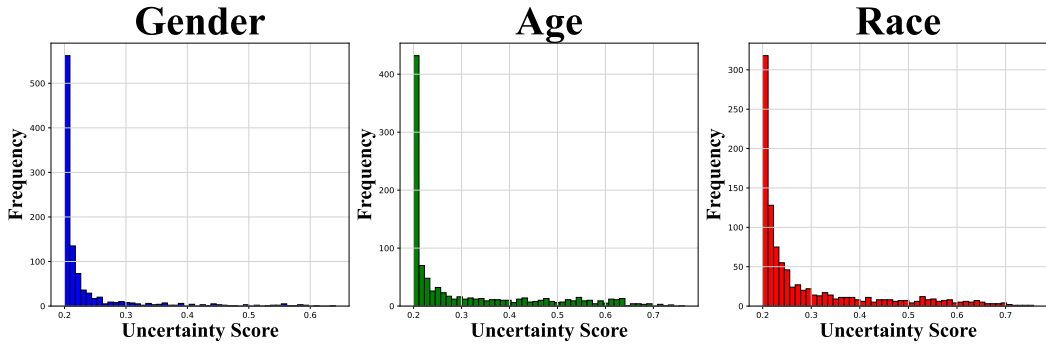


Figure A.16: *Uncertainty Score histograms for gender, age and race for STGAN [50] dataset.*

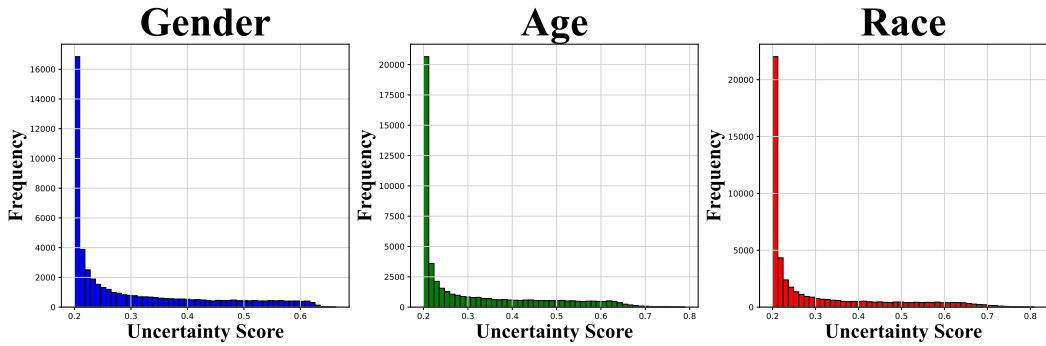


Figure A.17: *Uncertainty Score histograms for gender, age and race for VQGAN [54] dataset.*

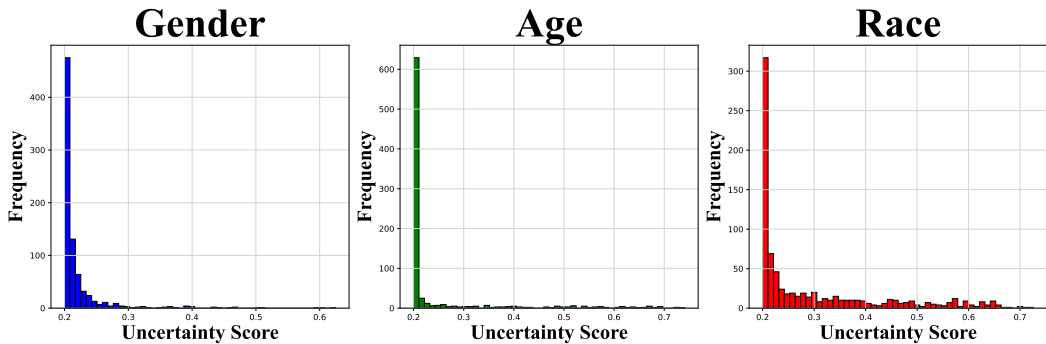


Figure A.18: *Uncertainty Score histograms for gender, age and race for DALLE2 [55], IF [55], Midjourney [55] dataset.*

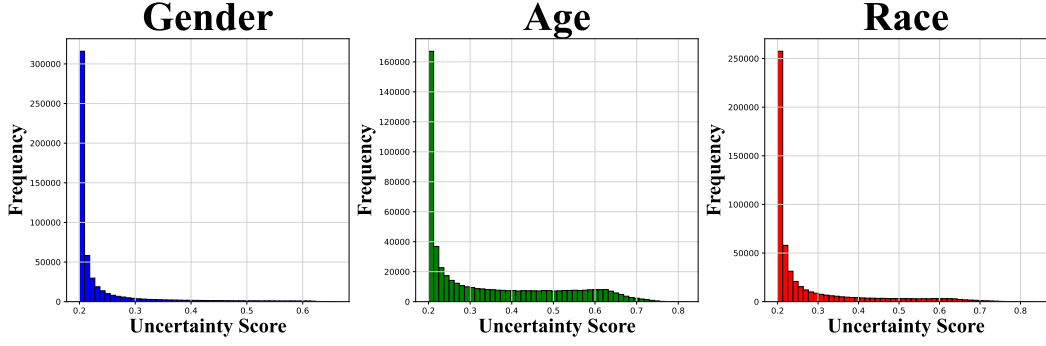


Figure A.19: *Uncertainty Score histograms for gender, age and race for DCFace [56] dataset.*

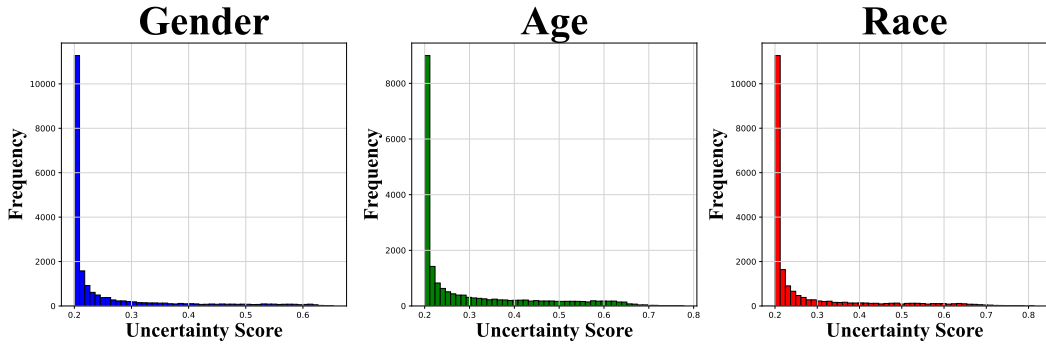


Figure A.20: *Uncertainty Score histograms for gender, age and race for Latent Diffusion [57] dataset.*

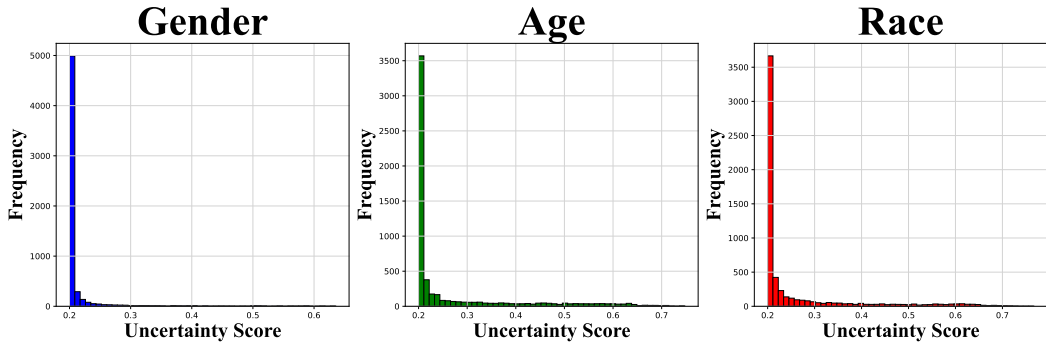


Figure A.21: *Uncertainty Score histograms for gender, age and race for Palette [58] dataset.*

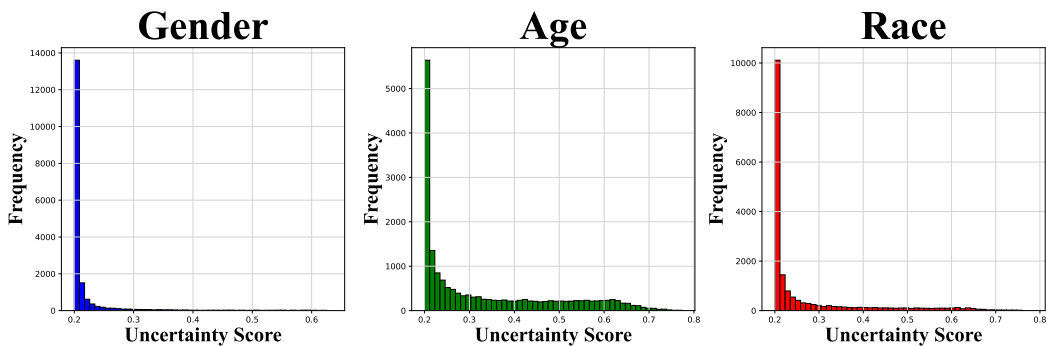


Figure A.22: *Uncertainty Score histograms for gender, age and race for SD v1.5 [59] dataset.*

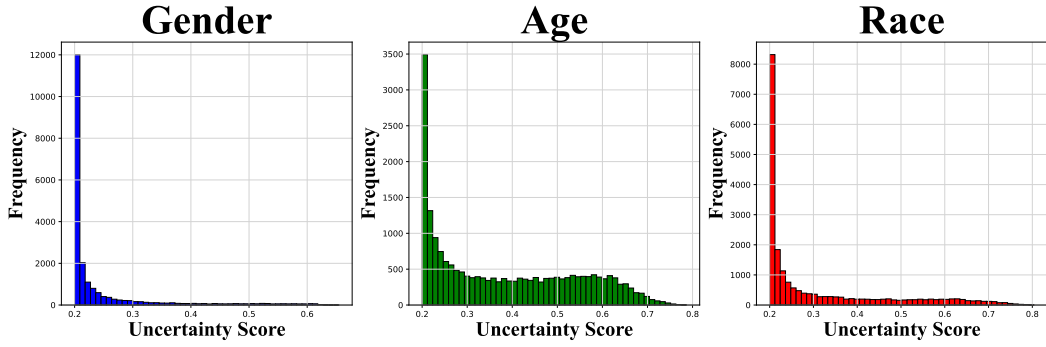


Figure A.23: *Uncertainty Score histograms for gender, age and race for SD Inpainting [59] dataset.*

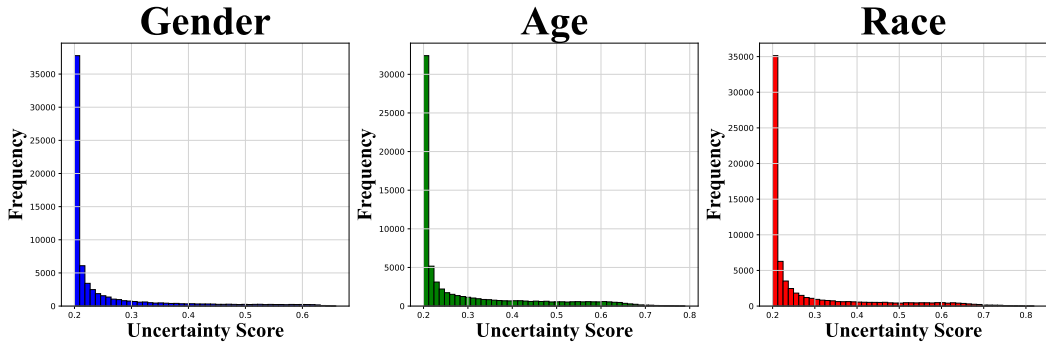


Figure A.24: *Uncertainty Score histograms for gender, age and race for FFHQ [6] dataset.*

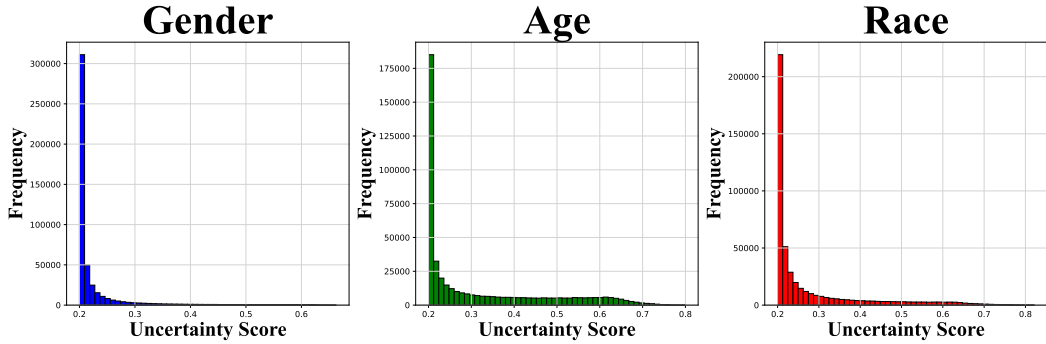


Figure A.25: *Uncertainty Score histograms for gender, age and race for CASIA-WebFace [37] dataset.*

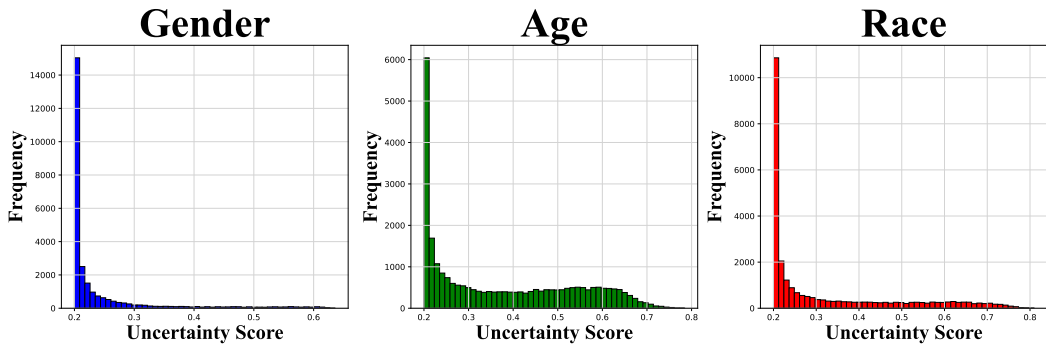


Figure A.26: *Uncertainty Score histograms for gender, age and race for IMDB-WIKI [38] dataset.*

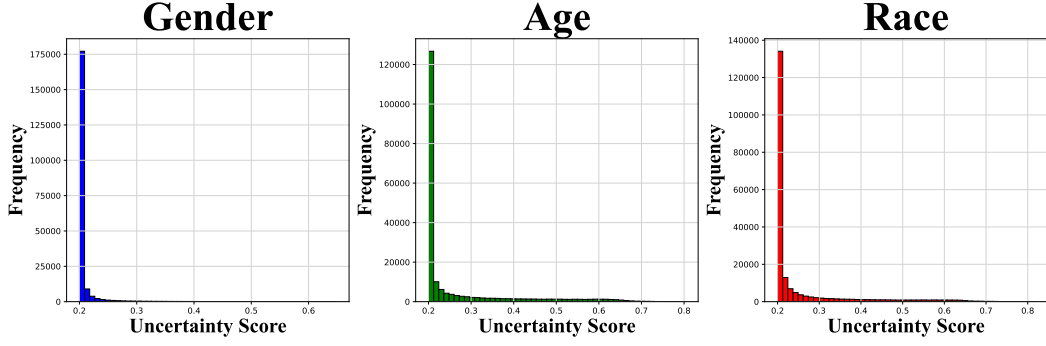


Figure A.27: *Uncertainty Score histograms for gender, age and race for CelebA [36] dataset.*

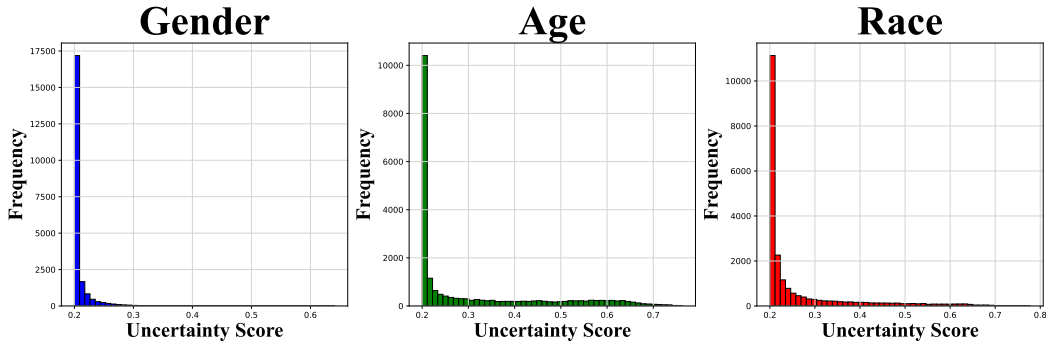


Figure A.28: *Uncertainty Score histograms for gender, age and race for A-FF++ [2] real dataset.*

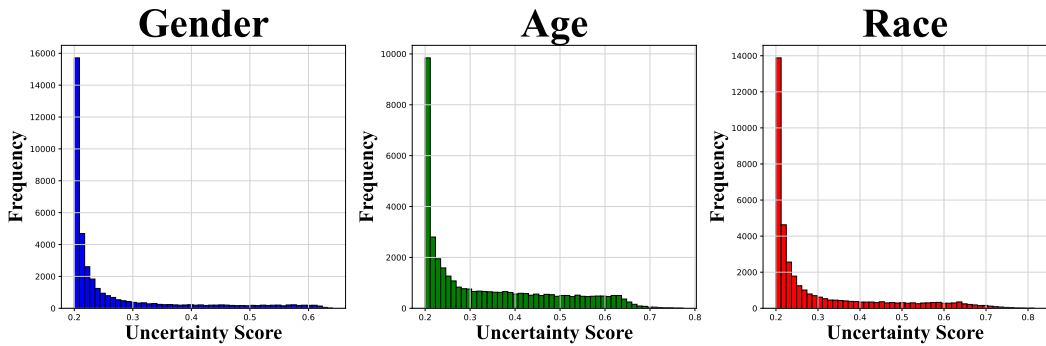


Figure A.29: *Uncertainty Score histograms for gender, age and race for A-DFDC [39] real dataset.*

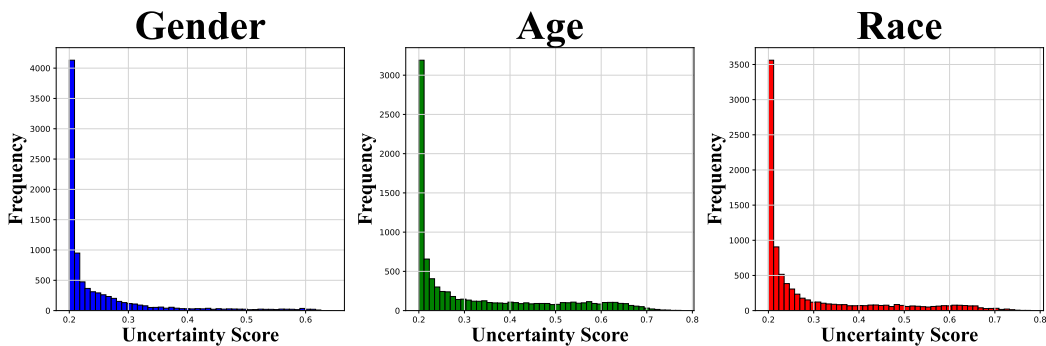


Figure A.30: *Uncertainty Score histograms for gender, age and race for A-DFD [40] real dataset.*

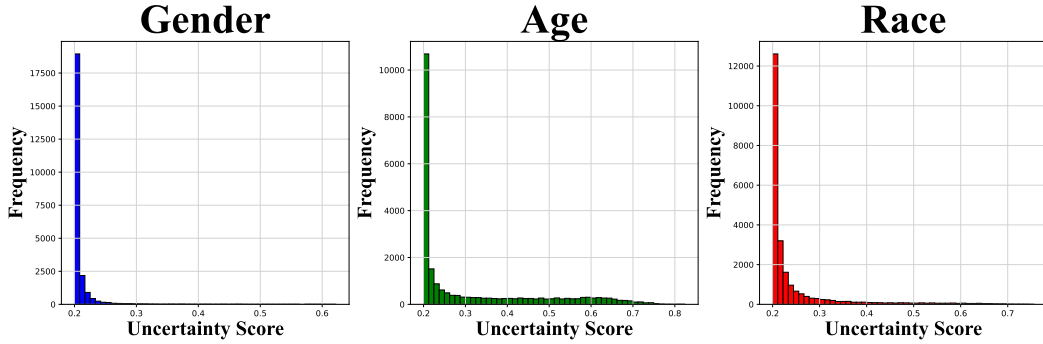


Figure A.31: *Uncertainty Score histograms for gender, age and race for A-Celeb-DF-v2 [41] real dataset.*

Model Type	Detector	Backbone	GitHub Link	VENUE
Naive	Xception [61]	Xception	<a href="https://github.com/ondyari/FaceForensics/blob/master">https://github.com/ondyari/FaceForensics/blob/master</a>	ICCV-2019
	EfficientB4 [62]	EfficientNet	<a href="https://github.com/lukemelas/EfficientNet-PyTorch">https://github.com/lukemelas/EfficientNet-PyTorch</a>	ICML-2019
	ViT-B/16 [63]	Transformer	<a href="https://github.com/lucidrains/vit-pytorch">https://github.com/lucidrains/vit-pytorch</a>	ICLR-2021
Spatial	UCF [16]	Xception	<a href="https://github.com/SCLBD/DeepfakeBench/tree/main">https://github.com/SCLBD/DeepfakeBench/tree/main</a>	ICCV-2023
	UnivFD [67]	CLIP VIT	<a href="https://github.com/Yuheng-Li/UniversalFakeDetect">https://github.com/Yuheng-Li/UniversalFakeDetect</a>	CVPR-2023
	CORE [68]	Xception	<a href="https://github.com/niyunsheng/CORE">https://github.com/niyunsheng/CORE</a>	CVPRW-2022
Frequency	F3Net [64]	Xception	<a href="https://github.com/yyk-wew/F3Net">https://github.com/yyk-wew/F3Net</a>	ECCV-2020
	SRM [66]	Xception	<a href="https://github.com/SCLBD/DeepfakeBench/tree/main">https://github.com/SCLBD/DeepfakeBench/tree/main</a>	CVPR-2021
	SPSL [65]	Xception	<a href="https://github.com/SCLBD/DeepfakeBench/tree/main">https://github.com/SCLBD/DeepfakeBench/tree/main</a>	CVPR-2021
Fairness-enhanced	DAW-FDD [20]	Xception	Unpublished code, reproduced by us	WACV-2024
	DAG-FDD [20]	Xception	Unpublished code, reproduced by us	WACV-2024
	PG-FDD [21]	Xception	<a href="https://github.com/Purdue-M2/Fairness-Generalization">https://github.com/Purdue-M2/Fairness-Generalization</a>	CVPR-2024

Table 15: *Summary of the implemented detectors in our fairness benchmark.*

Dataset	Attribute	Metric	Model Type											
			Naive			Frequency			Spatial			Fairness-enhanced		
			Xception [61]	EfficientB4 [62]	ViT-B/16 [63]	F3Net [64]	SPSL [65]	SRM [66]	UCF [16]	UnivFD [67]	CORE [68]	DAW-FDD [20]	DAG-FDD [20]	PG-FDD [21]
FF++	Gender	$F_{MEO}$	4.353	3.346	1.161	2.595	0.887	2.492	4.916	10.873	2.516	12.198	1.606	2.214
		$F_{DP}$	1.250	1.096	0.276	0.601	0.392	0.409	1.231	2.874	0.61	2.722	1.024	0.772
		$F_{OAE}$	0.177	0.132	0.396	0.426	0.231	0.228	0.489	0.015	0.196	0.977	0.941	0.095
		$F_{EO}$	4.749	4.293	1.335	2.728	1.012	2.839	5.117	12.323	3.221	12.993	2.969	2.362
FF++	Race	$F_{MEO}$	10.304	9.813	7.630	15.051	6.844	22.26	9.791	23.588	4.564	22.598	2.607	15.657
		$F_{DP}$	3.562	9.544	3.485	3.22	5.864	3.516	5.554	12.934	8.75	8.954	6.65	2.943
		$F_{OAE}$	4.465	7.396	6.232	4.045	2.541	5.227	4.388	6.889	3.522	7.382	1.939	3.764
		$F_{EO}$	17.066	27.404	12.835	20.586	11.277	36.221	17.288	70.499	11.944	48.644	6.882	18.386
FF++	Age	$F_{MEO}$	9.851	5.348	5.984	6.204	3.622	14.005	9.692	15.205	9.423	24.413	1.857	6.136
		$F_{DP}$	2.887	4.708	1.280	5.661	6.479	7.919	6.196	9.205	7.693	4.346	6.221	4.339
		$F_{OAE}$	1.038	5.813	6.417	2.049	0.856	1.581	2.606	8.927	1.138	4.263	1.472	2.112
		$F_{EO}$	18.191	11.876	8.199	13.665	5.636	20.696	17.291	29.607	14.781	47.613	6.419	12.446
FF++	Intersection	$F_{MEO}$	28.949	16.662	11.994	18.672	8.505	30.828	19.132	54.201	8.784	39.858	5.130	16.994
		$F_{DP}$	11.648	12.215	5.127	6.721	10.157	4.449	11.268	32.584	14.697	20.864	10.087	4.831
		$F_{OAE}$	8.442	10.876	10.295	7.210	4.868	8.742	5.638	15.415	8.209	10.843	3.322	4.491
		$F_{EO}$	70.162	68.005	32.625	48.53	25.922	78.296	40.971	169.535	33.428	131.755	19.399	38.887
FF++	-	ACC	92.280	89.282	86.051	94.832	93.676	92.587	94.982	83.652	95.183	91.420	93.254	96.237
		AUC	95.605	91.281	83.542	97.878	97.820	96.164	98.115	76.839	98.147	94.618	97.996	98.245
		AP	99.207	98.381	96.712	99.631	99.619	99.29	99.668	95.321	99.684	99.011	99.658	99.681
		EER	10.951	16.807	24.299	6.756	5.656	9.888	6.02	30.755	5.993	12.449	6.429	7.273

Table 16: *Detailed fairness and utility evaluation results on FF++.*

Dataset	Attribute	Metric	Model Type											
			Naive			Frequency			Spatial			Fairness-enhanced		
			Xception [61]	EfficientB4 [62]	ViT-B/16 [63]	F3Net [64]	SPSL [65]	SRM [66]	UCF [16]	UnivFD [67]	CORE [68]	DAW-FDD [20]	DAG-FDD [20]	PG-FDD [21]
DFDC	Gender	$F_{MEO}$	6.011	3.708	5.567	4.415	2.357	8.711	1.492	7.444	2.062	4.87	2.944	3.687
		$F_{DP}$	5.878	0.998	3.43	4.959	3.829	8.35	3.776	5.039	3.662	5.271	4.468	6.348
		$F_{OAE}$	2.97	2.744	1.88	2.645	2.537	2.438	1.427	0.075	2.178	3.012	2.233	0.869
		$F_{EO}$	6.222	5.564	7.742	5.609	3.833	10.841	2.517	12.51	3.784	4.898	3.95	4.968
DFDC	Race	$F_{MEO}$	8.525	6.846	24.319	7.667	9.726	9.139	11.603	22.342	10.74	15.529	11.403	5.992
		$F_{DP}$	21.619	11.534	20.596	25.03	24.594	21.463	25.9	24.317	26.634	23.997	25.534	24.613
		$F_{OAE}$	1.622	3.701	12.756	3.048	2.816	5.793	4.722	11.051	2.699	14.659	3.46	2.523
		$F_{EO}$	26.728	15.611	47.784	25.2	25.744	24.09	22.014	65.788	23.784	47.679	26.64	12.268
DFDC	Age	$F_{MEO}$	6.193	7.721	17.868	5.022	7.375	10.382	4.608	13.078	5.683	20.119	5.578	3.96
		$F_{DP}$	11.068	4.752	14.277	9.967	12.117	8.172	11.987	9.764	9.112	13.229	10.702	11.48
		$F_{OAE}$	2.817	5.951	4.984	3.918	2.585	6.092	2.513	7.523	3.869	12.581	2.498	1.653
		$F_{EO}$	14.397	16.233	26.396	14.327	13.88	16.625	12.03	22.816	11.274	31.018	8.736	6.954
DFDC	Intersection	$F_{MEO}$	14.479	15.029	35.979	14.067	24.924	14.117	16.119	38.533	17.421	20.447	18.268	10.973
		$F_{DP}$	28.877	17.816	30.153	32.117	31.493	27.666	31.604	28.815	33.791	27.812	30.224	31.389
		$F_{OAE}$	5.619	8.088	20.771	4.456	7.453	9.306	5.922	14.994	4.423	18.877	5.642	3.832
		$F_{EO}$	72.695	60.893	111.03	59.238	67.19	60.749	63.262	133.283	58.174	90.761	64.155	33.495
DFDC	-	ACC	81.223	71.939	71.044	87.658	87.482	83.536	89.155	64.164	88.75	81.452	88.867	92.905
		AUC	90.395	80.17	81.942	95.158	95.789	91.837	96.025	72.228	95.65	91.695	95.916	97.014
		AP	91.284	81.442	82.547	95.764	96.313	92.435	96.567	75.304	96.219	92.37	96.447	97.081
		EER	18.443	28.133	26.271	12.367	10.805	15.588	10.818	33.542	10.927	17.043	10.709	8.317

Table 17: *Detailed fairness and utility evaluation results on DFDC.*

Dataset	Attribute	Metric	Model Type											
			Naive			Frequency			Spatial			Fairness-enhanced		
			Xception [61]	EfficientB4 [62]	ViT-B/16 [63]	F3Net [64]	SPSL [65]	SRM [66]	UCF [16]	UnivFD [67]	CORE [68]	DAW-FDD [20]	DAG-FDD [20]	PG-FDD [21]
DFD	Gender	$F_{MEO}$	7.052	2.139	3.857	6.07	0.269	10.037	6.095	1.039	2.257	3.605	3.059	0.717
		$F_{DP}$	5.543	5.864	1.231	4.871	7.154	2.188	5.342	2.327	7.261	6.893	8.593	6.827
	Race	$F_{OAE}$	3.445	3.199	5.624	2.212	0.232	4.177	2.313	5.785	2.198	2.996	2.609	1.241
		$F_{EO}$	8.657	3.812	3.868	6.325	0.467	10.381	6.731	1.300	4.139	5.855	3.900	1.326
	Age	$F_{MEO}$	5.975	6.844	12.306	5.574	0.319	18.91	6.141	20.641	6.292	10.597	6.021	11.641
		$F_{DP}$	25.863	19.116	11.976	25.678	40.64	21.081	28.174	44.104	26.949	28.784	28.439	29.743
	Intersection	$F_{OAE}$	6.002	10.714	16.754	4.602	0.206	8.565	3.89	15.842	4.917	4.594	4.125	3.797
		$F_{EO}$	16.002	17.914	24.819	14.628	0.884	32.788	15.477	51.098	17.872	19.959	13.855	17.467
	-	$F_{MEO}$	14.485	13.629	2.744	9.24	0.9	9.38	10.383	6.69	10.768	10.107	10.942	5.6
		$F_{DP}$	34.386	18.578	10.063	32.355	20.119	18.826	33.553	4.892	34.865	32.253	34.503	27.165
	-	$F_{OAE}$	11.001	18.255	22.847	6.943	0.434	13.797	7.41	23.7	5.315	7.635	6.256	6.095
		$F_{EO}$	22.487	33.616	6.473	15.786	1.97	13.894	18.326	12.859	16.44	14.035	13.272	8.349

Table 18: Detailed fairness and utility evaluation results on DFD.

Dataset	Attribute	Metric	Model Type											
			Naive			Frequency			Spatial			Fairness-enhanced		
			Xception [61]	EfficientB4 [62]	ViT-B/16 [63]	F3Net [64]	SPSL [65]	SRM [66]	UCF [16]	UnivFD [67]	CORE [68]	DAW-FDD [20]	DAG-FDD [20]	PG-FDD [21]
Celeb-DF-v2	Gender	$F_{MEO}$	1.764	8.434	10.889	0.584	2.701	2.377	2.645	13.511	2.78	1.312	0.997	1.584
		$F_{DP}$	6.072	7.227	0.405	6.219	8.541	7.023	7	9.706	6.693	6.071	7.104	6.023
	Race	$F_{OAE}$	1.578	2.063	5.663	1.092	2.149	0.976	0.884	8.053	0.636	2.411	0.831	0.429
		$F_{EO}$	2.585	10.238	11.073	1.108	3.236	3.379	3.564	20.484	3.369	1.599	1.519	1.601
	Age	$F_{MEO}$	5.583	9.879	14.539	7.288	8.943	9.753	4.16	32.306	4.502	21.999	8.275	7.45
		$F_{DP}$	19.474	19.627	14.411	21.812	24.643	16.882	20.953	12.222	21.337	22.694	24.787	16.744
	Intersection	$F_{OAE}$	6.569	9.664	12.618	4.032	6.035	5.493	3.524	10.82	3.813	3.092	5.392	2.815
		$F_{EO}$	10.691	25.652	28.759	13.013	11.726	15.42	14.684	63.524	9.671	58.225	14.714	12.384
	-	$F_{MEO}$	7.172	7.331	15.248	6.974	1.948	8.784	3.873	29.904	3.539	5.903	2.508	5.968
		$F_{DP}$	33.004	25.16	6.737	33.891	33.072	33.644	32.236	18.794	32.986	24.932	34.577	32.264
	-	$F_{OAE}$	1.925	8.576	26.359	1.628	1.532	1.149	2.502	12.526	3.482	10.577	0.845	1.183
		$F_{EO}$	11.497	14.073	19.966	11.657	5.013	11.178	7.669	53.72	9.685	10.027	5.404	7.037

Table 19: Detailed fairness and utility evaluation results on Celeb-DF-v2.

Dataset	Attribute	Metric	Model Type											
			Naive			Frequency			Spatial			Fairness-enhanced		
			Xception [61]	EfficientB4 [62]	ViT-B/16 [63]	F3Net [64]	SPSL [65]	SRM [66]	UCF [16]	UnivFD [67]	CORE [68]	DAW-FDD [20]	DAG-FDD [20]	PG-FDD [21]
AttGAN	Gender	$F_{MEO}$	0.56	1.669	0.472	0.946	0.459	1.554	0.422	4.79	3.544	1.941	0.153	1.47
		$F_{DP}$	10.923	12.249	10.678	11.069	11.068	10.489	11.295	9.998	12.045	11.936	11.171	12.205
	Race	$F_{OAE}$	0.619	0.287	0.739	1.053	0.432	1.136	0.085	3.38	0.75	0.721	0.165	0.288
		$F_{EO}$	1.096	3.05	0.816	1.695	0.617	2.078	0.676	6.049	3.62	2.379	0.177	2.275
	Age	$F_{MEO}$	3.39	3.613	3.228	3.198	3.918	4.013	3.03	18.643	17.655	7.576	1.887	1.695
		$F_{DP}$	11.859	13.88	11.05	12.876	10.628	11.582	13.059	22.615	16.834	13.753	13.054	13.502
	Intersection	$F_{OAE}$	1.587	2.174	2.526	2.387	2.033	2.31	2.521	4.713	5.636	5.042	1.6	1.6
		$F_{EO}$	5.016	10.539	9.994	5.975	9.472	9.239	5.592	37.89	19.269	12.917	4.291	5.117
	-	$F_{MEO}$	3.086	4.899	7.144	1.194	3.704	3.096	2.469	15.211	5.996	2.855	2.206	5.493
		$F_{DP}$	22.439	21.386	18.175	23.439	22.14	22.789	24.491	20.473	21.175	22.14	24.789	21.193
	-	$F_{OAE}$	1.105	3.595	4.689	0.942	2.563	3.132	2.456	6.436	4.493	2.309	0.398	3.758
		$F_{EO}$	5.209	10.255	13.136	4.103	10.371	10.312	5.807	36.092	8.639	6.932	3.746	7.407

Table 20: Detailed fairness and utility evaluation results on AttGAN.

Dataset	Attribute	Metric	Model Type											
			Naive			Frequency			Spatial			Fairness-enhanced		
			Xception [61]	EfficientB4 [62]	ViT-B/16 [63]	F3Net [64]	SPSL [65]	SRM [66]	UCF [16]	UnivFD [67]	CORE [68]	DAW-FDD [20]	DAG-FDD [20]	PG-FDD [21]
MMDGAN	Gender	$F_{MEO}$	2.722	17.144	0.773	1.087	3.809	3.261	4.622	1.626	3.394	8.439	11.417	2.448
		$F_{DP}$	8.077	16.007	6.925	7.801	8.077	7.939	9.604	6.787	9.584	11.082	13.928	9.141
		$F_{OAE}$	2.335	7.348	1.084	1.271	3.398	3.26	2.797	0.63	0.512	4.275	4.994	1.133
		$F_{EO}$	4.772	18.286	0.773	2.028	6.9	6.352	5.63	3.071	4.481	9.447	12.493	2.448
	Race	$F_{MEO}$	10	73.95	8.974	16.667	14.286	8.333	8.333	33.333	16.667	28.571	28.571	2.21
		$F_{DP}$	33	55	32	33	38	33	33	33	33	43	43	33
		$F_{OAE}$	9.091	22	5.233	9.091	5	4.545	4.545	18.182	9.091	10	10	1.187
	Age	$F_{MEO}$	23.462	91.198	13.141	22.352	28.661	15.508	19.122	48.478	25.201	39.585	44.593	5.931
		$F_{DP}$	17.703	20.303	10.909	9.394	11.515	11.212	11.818	10.303	12.727	8.788	12.727	11.818
		$F_{EO}$	23.368	39.483	6.422	13.465	22.203	25.61	17.407	13.78	17.996	21.652	24.926	10.142
	Intersection	$F_{MEO}$	11.706	22.297	4.808	10.345	10.345	10.345	7.642	6.924	9.091	14.336	14.559	9.091
		$F_{DP}$	58.088	62.5	51.471	58.088	58.088	58.088	58.088	58.088	58.088	70.588	58.088	58.088
		$F_{EO}$	11.765	41.667	12.5	11.765	8.333	5.882	5.882	11.529	11.765	12.5	16.667	1.948
	-	$F_{MEO}$	51.536	230.67	59.507	44.743	59.982	39.11	42.671	103.142	55.926	161.146	85.72	14.412
		$F_{DP}$	97.525	90.099	95.792	98.02	97.03	98.02	97.772	93.812	96.535	94.307	96.287	99.01
		$F_{EO}$	99.393	97.839	99.299	99.687	99.508	99.392	99.781	97.987	98.521	99.515	99.808	99.98
	-	ACC	98.918	97.589	99.226	99.691	99.461	99.215	99.792	97.182	98.25	99.525	99.812	99.983
		AUC	99.94	99.797	99.56	99.933	99.826	99.832	99.97	99.724	99.079	99.809	99.929	99.986
		AP	2.646	7.407	3.704	1.587	2.646	2.646	2.116	6.349	4.233	1.587	1.587	0.529

Table 21: Detailed fairness and utility evaluation results on MMDGAN.

Dataset	Attribute	Metric	Model Type											
			Naive			Frequency			Spatial			Fairness-enhanced		
			Xception [61]	EfficientB4 [62]	ViT-B/16 [63]	F3Net [64]	SPSL [65]	SRM [66]	UCF [16]	UnivFD [67]	CORE [68]	DAW-FDD [20]	DAG-FDD [20]	PG-FDD [21]
StarGAN	Gender	$F_{MEO}$	0.281	2.181	0.472	0.33	0.388	0.552	0.044	2.075	1.737	0.344	0.627	0.33
		$F_{DP}$	4.379	5.639	3.887	4.547	4.555	4.744	4.461	5.32	5.209	4.678	4.954	4.65
		$F_{OAE}$	0.181	0.604	0.435	0.3	0.275	0.332	0.008	0.095	0.214	0.07	0.107	0.197
		$F_{EO}$	0.408	2.679	0.59	0.486	0.561	0.619	0.049	2.74	2.18	0.606	0.957	0.375
	Race	$F_{MEO}$	4	4.577	11.031	4	8	4	8	22.727	11.197	6.113	4	2.062
		$F_{DP}$	27.875	27.493	29.459	28.39	29.39	26.875	29.086	35.768	30.974	27.403	27.875	26.056
		$F_{EO}$	1.515	3.036	4.571	1.515	3.03	3.03	3.03	6.682	2.931	1.395	1.515	1.325
	Age	$F_{MEO}$	2.479	3.577	5.091	3.167	1.667	2.5	1.379	1.167	4.562	2.033	1.667	0.943
		$F_{DP}$	19.078	17.476	16.434	19.802	19.399	19.078	19.319	17.244	18.927	17.39	19.078	19.158
		$F_{EO}$	1.132	2.264	2.119	0.323	1.201	2.264	1.132	2.075	0.843	0.908	1.509	0.601
	Intersection	$F_{MEO}$	14.286	12.5	21.774	6.25	11.111	6.25	14.286	25	18.75	11.111	5.556	2.381
		$F_{DP}$	30.971	32.154	36.599	31.973	33.612	29.993	31.571	38.639	36.417	31.791	31.571	28.326
		$F_{EO}$	5.882	5.882	7.418	2.222	4.082	4.082	5.882	8.889	5.462	4.082	2.041	1.471
	-	ACC	99.326	98.289	96.216	99.015	99.274	99.378	99.43	94.66	96.319	98.237	99.482	99.533
		AUC	99.874	99.773	99.556	99.909	99.86	99.869	99.964	99.626	99.076	99.796	99.909	99.983
		AP	99.899	99.797	99.56	99.933	99.826	99.832	99.97	99.724	99.079	99.809	99.929	99.986
	-	EER	0.795	1.135	2.611	0.454	0.795	0.681	0.568	1.93	3.973	1.589	0.568	0.454

Table 22: Detailed fairness and utility evaluation results on StarGAN.

Dataset	Attribute	Metric	Model Type											
			Naive			Frequency			Spatial			Fairness-enhanced		
			Xception [61]	EfficientB4 [62]	ViT-B/16 [63]	F3Net [64]	SPSL [65]	SRM [66]	UCF [16]	UnivFD [67]	CORE [68]	DAW-FDD [20]	DAG-FDD [20]	PG-FDD [21]
StyleGAN	Gender	$F_{MEO}$	0.436	2.543	1.046	1.136	1.558	0.561	0.447	3.248	3.136	0.44	0.789	0.136
		$F_{DP}$	20.675	21.927	20.009	20.923	21.864	20.013	20.847	20.617	21.168	20.521	21.311	21.15
		$F_{OAE}$	0.17	0.208	0.551	0.344	0.496	0.205	1.003	1.003	0.029	0.404	0.027	
		$F_{EO}$	0.533	3.444	1.191	1.686	2.035	0.926	0.454	3.747	3.316	0.73	1.009	0.205
	Race	$F_{MEO}$	4.078	13.916	11.459	4.498	3.659	11.815	2.439	20.18	18.22	2.941	1.22	2.105
		$F_{DP}$	25.95	25.845	24.097	24.671	24.566	27.593	24.207	27.273	25.481	23.849	24.053	24.257
		$F_{EO}$	1.149	5.309	4.74	1.905	1.693	4.72	0.607	8.377	7.544	0.892	0.635	1.075
	Age	$F_{MEO}$	9.065	19.373	11.673	18.17	19.059	17.073	1.491	9.843	7.494	9.065	9.53	1.556
		$F_{DP}$	49.291	52.488	44.166	48.832	50.785	49.475	47.41	40.723	44.455	49.356	49.553	48.55
		$F_{EO}$	0.783	2.425	14.36	2.943	2.104	1.163	1.068	10.291	8.482	0.908	1.64	1.333
	Intersection	$F_{MEO}$	7.407	17.306	16.78	7.143	7.143	17.857	3.704	24.774	26.04	4.054	3.571	2.817
		$F_{DP}$	47.301	51.383	47.73	47.13	50.191	48.999	47.301	50.62	50.534	47.215	48.236	48.322
		$F_{EO}$	4.545	6.281	6.404	4.082	2.273	6.818	2.273	8.961	9.494	3.061	2.041	1.105
	-	ACC	98.975	97.819	96.347	98.476	99.08	97.976	99.527	94.77	96.399	99.054	99.448	99.685
		AUC	99.925	99.794	99.392	99.861	99.964	99.902	99.985	99.703	99.51	99.892	99.986	99.979
		AP	99.94	99.854	99.386	99.904	99.97	99.916	99.988	99.756	99.316	99.925	99.989	99.981
		EER	0.982	1.443	3.753	1.501	0.693	1.27	0.52	2.887	2.483	0.982	0.52	0.462

Table 23: Detailed fairness and utility evaluation results on StyleGAN.

Dataset	Attribute	Metric	Model Type											
			Naive			Frequency			Spatial			Fairness-enhanced		
			Xception [61]	EfficientB4 [62]	ViT-B/16 [63]	F3Net [64]	SPSL [65]	SRM [66]	UCF [16]	UnivFD [67]	CORE [68]	DAW-FDD [20]	DAG-FDD [20]	PG-FDD [21]
StyleGAN2	Gender	$F_{MEO}$	0.847	0.56	1.556	0.976	0.487	0.666	0.27	0.447	1.073	0.534	0.241	0.045
		$F_{DP}$	3.512	2.482	3.231	3.434	2.926	2.668	2.988	2.775	2.129	2.984	2.961	2.871
		$F_{OAE}$	0.077	0.341	0.624	0.246	0.342	0.636	0.092	0.117	0.698	0.31	0.092	0.022
		$F_{EO}$	1.538	0.594	1.7	1.338	0.686	1.192	0.317	0.482	1.113	0.56	0.263	0.047
	Race	$F_{MEO}$	1.037	5.147	6.385	1.057	1.401	6.072	1.244	15.519	16.197	2.565	0.926	0.517
		$F_{DP}$	33.803	35.296	33.103	34.638	35.076	36.619	35.925	38.228	38.381	34.674	35.711	35.522
		$F_{OAE}$	1.451	1.354	1.4	0.471	0.506	1.907	0.229	2.583	2.74	1.331	0.38	0.247
		$F_{EO}$	2.251	7.675	13.968	2.428	2.762	7.489	2.377	17.827	19.998	5.173	2.369	1.48
	Age	$F_{MEO}$	2.766	2.561	8.543	3.408	3.328	2.493	2.486	9.408	9.634	6.514	2.532	0.607
		$F_{DP}$	16.251	16.177	16.677	16.418	16.74	15.95	16.669	16.91	18.079	12.621	16.323	15.762
		$F_{OAE}$	1.016	0.375	2.35	1.05	1.265	2.008	0.647	1.74	2.042	5.433	0.97	0.528
		$F_{EO}$	5.353	2.926	13.051	5.249	4.883	6.547	3.779	12.811	10.052	11.092	3.689	1.966
	Intersection	$F_{MEO}$	2.436	5.448	9.55	2.127	2.384	7.475	1.468	18.286	20.753	3.132	1.511	0.695
		$F_{DP}$	37.77	39.222	35.56	38.81	38.411	39.991	39.446	42.732	42.186	38.965	39.128	38.732
		$F_{OAE}$	1.896	2.822	2.726	0.658	1.073	2.369	0.643	3.644	4.862	1.795	0.575	0.488
		$F_{EO}$	9.7	18.646	26.948	7.826	7.696	17.235	5.947	35.527	41.168	13.195	5.737	3.074
	-	ACC	97.46	98.044	95.299	98.472	98.799	98.351	99.311	94.745	96.23	97.207	99.32	99.479
		AUC	99.738	99.698	98.85	99.794	99.816	99.741	99.877	99.205	99.209	99.713	99.883	99.968
		AP	99.787	99.656	98.871	99.819	99.794	99.715	99.861	99.205	98.979	99.759	99.901	99.97
		EER	2.161	1.066	5.234	1.542	1.17	1.309	0.704	3.906	3.019	2.374	0.699	0.535

Table 24: Detailed fairness and utility evaluation results on StyleGAN2.

Dataset	Attribute	Metric	Model Type											
			Naive			Frequency			Spatial			Fairness-enhanced		
			Xception [61]	EfficientB4 [62]	ViT-B/16 [63]	F3Net [64]	SPSL [65]	SRM [66]	UCF [16]	UnivFD [67]	CORE [68]	DAW-FDD [20]	DAG-FDD [20]	PG-FDD [21]
StyleGAN3	Gender	$F_{MEO}$	0.645	1.688	1.345	0.399	0.177	0.132	0.339	1.194	1.626	1.868	0.378	0.23
		$F_{DP}$	5.585	6.032	4.495	5.195	5.327	5.274	5.532	5.417	5.837	6.14	5.536	5.482
		$F_{OAE}$	0.374	0.558	1.26	0.235	0.113	0.031	0.174	0.062	0.221	0.886	0.173	0.086
		$F_{EO}$	0.774	1.792	1.843	0.56	0.254	0.219	0.382	1.305	1.842	1.952	0.421	0.264
	Race	$F_{MEO}$	1.701	8.361	11.792	0.605	0.498	1.546	0.893	19.275	17.174	2.079	0.708	3.61
		$F_{DP}$	41.75	42.909	41.384	42.642	43.108	42.823	43.681	45.108	45.534	42.603	43.073	44.332
		$F_{OAE}$	0.259	1.66	2.29	0.514	0.47	0.436	0.612	2.527	2.103	0.757	0.335	0.761
		$F_{EO}$	4.543	13.614	18.916	1.177	1.092	2.955	1.47	21.59	24.212	4.237	2.164	4.885
	Age	$F_{MEO}$	1.403	2.138	10.825	1.727	0.743	0.459	2.1	11.432	14.27	3.777	1.792	0.892
		$F_{DP}$	14.913	14.783	17.612	14.285	14.734	14.734	14.04	17.735	19.446	15.206	13.967	15.198
		$F_{OAE}$	0.782	0.986	4.387	1.1	0.612	0.465	1.408	3.895	5.177	1.775	0.984	0.31
		$F_{EO}$	3.378	4.108	14.744	3.685	1.714	1.141	3.498	15.191	16.05	5.888	3.075	1.073
	Intersection	$F_{MEO}$	2.439	10.814	14.81	1.096	1.429	2.381	1.429	24.377	22.722	3.681	2.439	4.138
		$F_{DP}$	50.071	51.956	50.376	50.55	51.369	51.129	52.043	53.357	55.475	51.27	51.514	52.961
		$F_{OAE}$	0.893	2.808	3.841	0.644	1.013	0.526	1.124	6.702	5.604	2.306	2.143	1.429
		$F_{EO}$	11.913	30.289	40.686	3.519	4.723	6.395	5.967	44.341	52.555	14.502	7.765	12.542
	-	ACC	98.696	98.009	95.771	98.645	99.364	99.548	99.374	94.703	96.12	97.444	99.199	99.672
		AUC	99.86	99.613	99.263	99.863	99.923	99.906	99.941	99.04	98.621	99.749	99.929	99.996
		AP	99.906	99.568	99.302	99.906	99.951	99.9	99.961	99.172	98.577	99.814	99.956	99.996
		EER	1.373	1.733	4.142	1.351	0.675	0.445	0.72	4.66	5.088	2.139	0.653	0.36

Table 25: Detailed fairness and utility evaluation results on StyleGAN3.

Dataset	Attribute	Metric	Model Type											
			Naive			Frequency			Spatial			Fairness-enhanced		
			Xception [61]	EfficientB4 [62]	ViT-B/16 [63]	F3Net [64]	SPSL [65]	SRM [66]	UCF [16]	UnivFD [67]	CORE [68]	DAW-FDD [20]	DAG-FDD [20]	PG-FDD [21]
MSG StyleGAN	Gender	$F_{MEO}$	1.136	12.078	0.703	3.409	0.654	2.219	0.654	14.301	7.359	0.614	0.039	0
		$F_{DP}$	27.6	31.71	25.179	26.151	27.903	26.151	27.903	15.658	29.646	27.059	27.784	28.325
		$F_{OAE}$	0.725	3.146	3.146	2.174	0.422	1.33	0.422	8.063	1.321	0.66	0.541	0
		$F_{EO}$	1.136	13.323	0.703	3.409	0.654	2.872	0.654	15.978	7.359	0.668	0.039	0
	Race	$F_{MEO}$	0.709	12.5	18.762	9.091	0.515	17.473	0.515	18.182	13.217	2.577	12.5	0
		$F_{DP}$	49.876	46.294	36.493	50.174	49.279	32.91	49.279	41.228	43.333	48.682	48.682	49.577
		$F_{OAE}$	0.299	10.526	13.085	5.263	0.299	16.07	0.299	7.456	8.437	2.09	5.263	0
		$F_{EO}$	1.291	22.112	27.06	9.417	1.008	25.246	1.008	50.251	14.169	7.622	12.924	0
	Age	$F_{MEO}$	2.857	37.594	5.714	2.894	0.526	16.667	0.526	33.333	12.381	3.846	15.614	0
		$F_{DP}$	47.334	49.913	48.962	47.673	49.434	50.451	49.434	42.249	51.74	48.417	51.534	49.773
		$F_{OAE}$	2.439	6.652	1.993	2.691	0.339	4.2	0.339	4.807	4.407	3.03	2.352	0
		$F_{EO}$	3.439	51.965	7.906	4.007	1.019	19.632	1.019	37.676	17.663	9.151	27.929	0
	Intersection	$F_{MEO}$	1.493	20	41.892	11.111	0.667	25	0.667	50	50	2.667	20	0
		$F_{DP}$	55.853	54.067	57.778	55.853	55.407	33.631	55.407	68				

Dataset	Attribute	Metric	Model Type											
			Naive			Frequency			Spatial			Fairness-enhanced		
			Xception	EfficientB4	ViT-B/16	F3Net	SPSL	SRM	UCF	UnivFD	CORE	DAW-FDD	DAG-FDD	PG-FDD
ProGAN	Gender	$F_{MEO}$	0.381	1.296	1.134	0.428	0.315	0.403	0.243	0.834	2.333	0.236	0.242	0.138
		$F_{DP}$	16.706	17.133	15.201	16.709	16.918	16.671	17.043	15.652	16.838	16.708	17.082	16.882
	Race	$F_{OAE}$	0.341	0.006	1.793	0.39	0.305	0.187	0.131	1.442	0.227	0.236	0.081	0.19
		$F_{EO}$	0.504	1.501	1.137	0.610	0.613	0.437	0.257	0.947	2.389	0.304	0.271	0.167
	Age	$F_{MEO}$	3.598	5.357	9.424	2.721	3.565	4.177	2.743	18.043	20.491	3.027	3.149	0.822
		$F_{DP}$	35.504	30.506	25.824	35.179	36.143	35.551	35.743	22.053	18.852	35.97	35.661	34.624
	Intersection	$F_{OAE}$	1.285	5.514	10.036	1.232	0.609	1.279	0.693	15.502	17.141	0.48	0.926	0.844
		$F_{EO}$	5.759	9.542	14.448	4.235	4.912	5.619	3.788	22.113	25.053	4.519	4.381	1.968
	-	$F_{MEO}$	1.374	1.953	8.853	0.898	0.798	0.932	0.656	6.036	5.397	1.262	0.656	1.244
	-	$F_{DP}$	21.22	22.383	19.714	21.441	21.587	21.342	21.717	19.868	21.597	21.319	21.817	21.601
	-	$F_{OAE}$	0.897	0.912	5.411	0.808	0.583	0.726	0.503	4.49	2.83	1.067	0.367	0.702
	-	$F_{EO}$	2.875	3.954	11.106	2.453	2.53	2.744	1.763	10.015	6.825	3.491	1.646	1.582
	-	$F_{MEO}$	4.284	6.829	10.793	6.557	6.581	8.513	6.604	20.936	24.845	6.406	6.581	0.935
	-	$F_{DP}$	50.437	47.389	40.919	50.462	51.762	51.533	52.347	38.606	36.209	51.858	51.988	50.523
	-	$F_{OAE}$	1.882	5.836	11.532	2.432	1.162	1.529	0.818	16.738	19.088	0.956	0.993	0.961
	-	$F_{EO}$	13.14	22.712	31.013	13.286	13.577	16.796	11.759	42.997	52.525	13.479	12.476	3.729
	-	ACC	99.357	98.286	96.458	99.344	99.558	99.384	99.639	95.045	96.418	99.243	99.688	99.68
	-	AUC	99.968	99.899	99.84	99.938	99.961	99.948	99.977	99.895	99.105	99.954	99.984	99.996
	-	AP	99.976	99.928	99.861	99.959	99.974	99.959	99.984	99.927	98.838	99.966	99.988	99.997
	-	EER	0.535	0.916	1.838	0.547	0.44	0.595	0.363	0.69	3.094	0.696	0.345	0.321

Table 27: Detailed fairness and utility evaluation results on ProGAN.

Dataset	Attribute	Metric	Model Type											
			Naive			Frequency			Spatial			Fairness-enhanced		
			Xception	EfficientB4	ViT-B/16	F3Net	SPSL	SRM	UCF	UnivFD	CORE	DAW-FDD	DAG-FDD	PG-FDD
STGAN	Gender	$F_{MEO}$	17.404	18.772	4.36	13.333	12.912	5.087	6.737	12.632	7.965	12.596	14.737	5.333
		$F_{DP}$	16.581	15	5.161	12.984	13.419	7.823	11.774	0.097	14.984	12.935	15.645	11.194
	Race	$F_{OAE}$	7.968	10.419	2.452	8.532	7.387	4.661	2.452	12.774	0.048	5.903	6.323	2.581
		$F_{EO}$	17.404	21.708	5.238	17.171	15.412	9.087	7.812	19.085	15.123	13.934	15.812	5.333
	Age	$F_{MEO}$	13.299	20	4.167	11.765	17.647	4.412	17.647	50	40	26.961	10	5.882
		$F_{DP}$	25	32.197	18.561	20.613	19.048	19.697	22.811	13.258	29.337	13.62	18.215	20.613
	Intersection	$F_{OAE}$	8.97	4.5	2.464	8	12	3.297	12	36.742	10.023	19.833	7.955	4
		$F_{EO}$	18.036	47.951	6.249	27.305	24.367	17.005	33.472	83.525	53.832	35.574	17.67	8.072
	-	$F_{MEO}$	18.277	28.125	22.581	20	23.333	8.696	20	22.5	14.146	19.916	20.784	10
	-	$F_{DP}$	10.656	11.688	10.343	14.52	19.438	10.82	16.159	10.134	8.765	13.574	14.844	12.881
	-	$F_{OAE}$	10.99	20	11.475	13.115	11.475	5.455	11.475	14.637	8.67	12.404	9.115	4.918
	-	$F_{EO}$	26.439	43.956	36.21	42.739	41.293	15.487	29.446	43.298	35.301	48.478	32.922	13.125
	-	$F_{MEO}$	28.571	30.612	16.667	16.327	23.077	7.812	25	66.667	66.667	38.462	24.49	7.692
	-	$F_{DP}$	40.833	45	39.167	35.177	32.78	35	36.947	33.333	47.677	23.82	33.038	35
	-	$F_{OAE}$	16.667	22.222	7.143	10.619	15.789	7.08	16.667	48.333	20.833	26.316	16.667	5.263
	-	$F_{EO}$	73.153	131.743	58.478	75.809	70.579	43.757	85.001	236.087	150.768	101.162	90.191	22.28
	-	ACC	93.521	88.451	94.93	95.775	97.465	94.93	69.577	93.521	90.423	93.239	98.873	
	-	AUC	99.573	96.465	98.534	99.541	99.547	97.807	99.538	85.921	97.335	99.194	99.522	99.908
	-	AP	99.639	95.872	98.139	99.59	99.607	97.132	99.579	82.016	96.354	99.242	99.554	99.922
	-	EER	4.217	7.831	3.614	3.614	3.614	3.614	3.614	19.277	6.024	3.614	3.614	3.614

Table 28: Detailed fairness and utility evaluation results on STGAN.

Dataset	Attribute	Metric	Model Type											
			Naive			Frequency			Spatial			Fairness-enhanced		
			Xception	EfficientB4	ViT-B/16	F3Net	SPSL	SRM	UCF	UnivFD	CORE	DAW-FDD	DAG-FDD	PG-FDD
VQGAN	Gender	$F_{MEO}$	0.359	1.689	0.682	0.732	0.368	0.47	0.241	1.789	1.021	0.642	0.338	0.207
		$F_{DP}$	12.221	13.117	11.324	12.105	12.491	12.466	12.581	9.224	12.203	12.216	12.609	12.755
	Race	$F_{OAE}$	0.231	0.067	1.264	0.49	0.377	0.454	0.187	0.12	0.625	0.482	0.243	0.069
		$F_{EO}$	0.371	2.198	0.722	0.829	0.719	0.876	0.367	2.226	1.274	0.853	0.513	0.386
	Age	$F_{MEO}$	1.267	8.893	10.064	2.257	3.158	2.321	3.273	20.147	20.549	4.11	3.183	1.429
		$F_{DP}$	59.881	60.677	57.134	60.756	60.89	60.225	61.269	54.127	62.9	60.342	61.099	61.113
	Intersection	$F_{OAE}$	0.692	1.985	3.926	0.611	0.47	0.855	0.58	9.087	2.245	0.726	0.518	0.283
		$F_{EO}$	3.139	13.952	15.64	3.751	4.581	4.174	4.947	34.162	25.23	6.323	4.388	2.143
	-	$F_{MEO}$	1.104	1.105	9.03	1.813	1.533	1.533	0.648	5.925	8.977	1.61	0.703	0.897
	-	$F_{DP}$	29.715	29.264	30.54	29.734	30.239	30.338	30.415	22.037	31.068	30.059	30.343	30.537
	-	$F_{OAE}$	0.956	0.953	2.392	0.984	0.785	0.866	0.339	4.197	3.12	0.992	0.444	0.461
	-	$F_{EO}$	2.363	4.055	11.65	3.145	2.892	3.001	1.344	18.036	10.529	3.499	1.421	1.653
	-	$F_{MEO}$	3.846	13.893	12.515	3.44	3.504	3.112	3.671	23.965	25.638	4.721	3.525	2
	-	$F_{DP}$	67.678	69.217	64.056	68.414	68.785	67.971	69.072	60.076	71.221	68.725	69.149	69.359
	-	$F_{OAE}$	1.703	3.567	5.313	0.889	1.029	1.408	0.787	10.854	3.869	2.36	1.186	0.976
	-	$F_{EO}$	9.427	27.715	31.838	9.934	10.748	11.46	11.34	66.065	46.268	16.097	10.787	5.751
	-	ACC	99.092	97.936	96.313	99.102	99.344	99.387						

Dataset	Attribute	Metric	Model Type											
			Naïve			Frequency			Spatial			Fairness-enhanced		
			Xception [61]	EfficientB4 [62]	ViT-B/16 [63]	F3Net [64]	SPSL [65]	SRM [66]	UCF [16]	UnivFD [67]	CORE [68]	DAW-FDD [20]	DAG-FDD [20]	PG-FDD [21]
Commercial Tools	Gender	$F_{MEO}$	7.689	8.221	4.167	4.432	2.879	0.435	3.258	8.864	2.708	2.348	4.432	2.083
		$F_{DP}$	18.977	22.798	18.901	18.527	16.616	16.540	18.714	20.701	16.540	16.990	17.440	17.177
		$F_{OAE}$	5.961	1.613	3.337	3.337	2.326	1.350	2.250	5.137	3.524	2.700	4.424	2.887
		$F_{EO}$	10.397	14.471	5.714	4.867	3.459	0.435	4.950	10.411	4.791	2.929	7.140	2.664
	Race	$F_{MEO}$	33.333	14.286	33.333	28.571	33.333	28.571	28.571	28.571	33.333	33.333	33.333	33.333
		$F_{DP}$	69.398	61.706	71.572	69.398	65.050	73.746	69.398	65.050	73.746	73.746	71.572	74.089
		$F_{OAE}$	21.053	7.018	10.526	10.526	15.789	4.348	8.696	13.043	10.526	15.789	15.789	5.263
		$F_{EO}$	77.098	29.869	62.147	52.682	73.558	36.044	48.191	50.286	63.706	70.345	70.475	57.018
	Age	$F_{MEO}$	28.571	28.571	14.286	28.571	6.711	12.500	14.286	14.286	14.286	14.286	14.286	5.833
		$F_{DP}$	49.346	58.824	52.778	50.817	47.876	52.288	51.797	49.346	52.288	51.307	50.327	52.288
		$F_{OAE}$	9.225	10.205	8.170	8.170	6.566	11.111	8.170	6.566	9.641	7.680	7.680	8.660
		$F_{EO}$	37.679	36.583	21.513	43.361	20.392	13.639	27.762	28.094	22.990	22.156	22.837	8.656
	Intersection	$F_{MEO}$	50.000	25.000	50.000	33.333	50.000	33.333	33.333	33.333	50.000	50.000	50.000	50.000
		$F_{DP}$	65.714	62.637	68.889	68.000	68.000	72.000	68.000	65.714	72.000	72.000	72.000	74.444
		$F_{OAE}$	22.222	8.547	11.111	11.111	19.048	5.128	9.524	20.000	11.111	16.667	16.667	7.692
		$F_{EO}$	131.495	67.938	105.685	81.793	129.065	59.940	76.252	91.701	105.535	114.665	126.561	109.221
	-	ACC	93.976	95.582	95.582	95.582	92.771	97.590	95.984	92.369	96.787	95.181	95.181	96.386
		AUC	95.778	99.541	99.005	96.349	94.798	95.716	95.681	96.808	97.371	97.141	94.812	93.365
		AP	96.193	99.751	99.401	96.966	95.607	96.184	93.761	98.000	98.153	97.779	94.066	90.493
		EER	7.692	3.297	5.495	6.593	8.791	6.593	6.593	9.890	6.593	6.593	6.593	7.692

Table 30: *Detailed fairness and utility evaluation results on Commercial Tools (DALLE2, IF & MidJourney).*

Dataset	Attribute	Metric	Model Type											
			Naïve			Frequency			Spatial			Fairness-enhanced		
			Xception [61]	EfficientB4 [62]	ViT-B/16 [63]	F3Net [64]	SPSL [65]	SRM [66]	UCF [16]	UnivFD [67]	CORE [68]	DAW-FDD [20]	DAG-FDD [20]	PG-FDD [21]
DCFace	Gender	$F_{MEO}$	0.525	0.87	1.201	0.637	0.196	0.338	0.052	0.596	1.77	0.368	0.066	0.04
		$F_{DP}$	5.465	4.56	5.28	5.534	5.342	5.371	5.274	4.012	4.012	5.351	5.265	5.213
		$F_{OAE}$	0.191	0.412	0.311	0.214	0.062	0.163	0.015	0.191	1.155	0.161	0.048	0.018
		$F_{EO}$	0.549	0.873	1.393	0.704	0.231	0.343	0.066	0.944	1.86	0.415	0.085	0.076
	Race	$F_{MEO}$	0.667	5.55	8.151	0.608	0.737	0.591	0.663	16.794	18.582	0.78	0.669	0.938
		$F_{DP}$	18.219	18.877	20.375	18.181	18.285	18.201	18.441	26.177	25.501	18.289	18.292	18.522
		$F_{OAE}$	0.535	2.088	3.419	0.384	0.294	0.359	0.431	5.528	6.893	0.322	0.304	0.392
		$F_{EO}$	2.333	10.815	14.05	1.889	1.94	1.649	2.154	29.148	23.112	1.838	1.661	1.454
	Age	$F_{MEO}$	1.448	2.989	9.273	1.071	0.567	1.055	0.425	6.914	7.59	1.253	0.706	0.594
		$F_{DP}$	12.708	13.621	9.357	12.926	13.119	12.754	13.08	10.929	8.445	12.763	13.314	12.741
		$F_{OAE}$	0.918	1.218	4.94	0.772	0.501	0.831	0.358	6.765	4.839	0.973	0.4	0.388
		$F_{EO}$	2.782	6.577	12.53	2.419	1.552	2.202	1.108	15.928	8.071	2.468	1.232	0.924
	Intersection	$F_{MEO}$	1.327	7.377	9.272	1.463	0.892	0.923	0.866	19.337	22.619	0.886	0.868	1.29
		$F_{DP}$	21.136	20.833	22.531	21.04	20.964	20.909	21.006	27.504	28.454	21.116	20.984	21.006
		$F_{OAE}$	0.764	3.089	4.017	0.649	0.362	0.518	0.498	6.588	8.981	0.548	0.391	0.568
		$F_{EO}$	5.666	22.247	27.649	6.712	4.452	4.176	4.367	58.647	45.831	5.043	3.709	2.873
	-	ACC	99.361	96.935	96.038	99.314	99.542	99.395	99.627	92.834	96.443	99.329	99.654	99.727
		AUC	99.961	99.513	99.718	99.938	99.934	99.956	99.965	97.415	99.129	99.956	99.965	99.994
		AP	99.972	99.602	99.776	99.955	99.947	99.963	99.97	97.347	98.913	99.969	99.977	99.995
		EER	0.422	3.07	2.649	0.414	0.414	0.612	0.363	7.661	3.26	0.515	0.368	0.322

Table 31: *Detailed fairness and utility evaluation results on DCFace.*

Dataset	Attribute	Metric	Model Type											
			Naïve			Frequency			Spatial			Fairness-enhanced		
			Xception [61]	EfficientB4 [62]	ViT-B/16 [63]	F3Net [64]	SPSL [65]	SRM [66]	UCF [16]	UnivFD [67]	CORE [68]	DAW-FDD [20]	DAG-FDD [20]	PG-FDD [21]
Latent Diffusion	Gender	$F_{MEO}$	0.711	1.315	6.822	0.587	0.269	0.404	0.343	0.523	1.341	0.709	0.343	0.005
		$F_{DP}$	6.704	7.776	1.172	6.844	7.154	7.227	7.274	6.063	7.26	6.444	7.367	7.15
		$F_{OAE}$	0.339	0.192	3.448	0.376	0.232	0.315	0.206	0.052	0.059	0.069	0.113	0.02
		$F_{EO}$	0.723	1.748	8.477	0.706	0.467	0.658	0.411	0.993	1.39	1.186	0.464	0.005
	Race	$F_{MEO}$	1.377	7.837	10.67	1.602	0.319	0.559	1.116	19.547	20.291	0.763	0.633	0.503
		$F_{DP}$	39.89	41.058	30.225	39.89	40.64	40.819	40.462	39.759	42.918	40.116	40.95	40.593
		$F_{OAE}$	1.202	1.262	9.842	0.921	0.206	0.387	0.658	4.85	2.278	0.691	0.299	0.31
		$F_{EO}$	2.443	10.604	26.477	3.081	0.884	1.541	2.659	30.757	21.909	2.097	1.363	0.765
	Age	$F_{MEO}$	2.771	2.325	12.515	1.798	0.9	0.803	0.762	3.544	4.117	1.896	1.571	1.604
		$F_{DP}$	20.503	20.83	20.755	20.183	20.119	19.742	19.955	15.919	20.598	20.183	20.062	20.823
		$F_{OAE}$	0.913	0.495	5.504	0.508	0.434	0.505	0.275	2.119	0.437	1.088	0.319	0.518
		$F_{EO}$	4.881	4.303	35.584	3.991	1.97	1.782	1.411	11.437	6.184	4.923	1.425	2.165
	Intersection	$F_{MEO}$	3.571	10.805	13.52	3.846	1.786	1.7						

Dataset	Attribute	Metric	Model Type											
			Naive			Frequency			Spatial			Fairness-enhanced		
			Xception [61]	EfficientB4 [62]	ViT-B/16 [63]	F3Net [64]	SPSL [65]	SRM [66]	UCF [16]	UnivFD [67]	CORE [68]	DAW-FDD [20]	DAG-FDD [20]	PG-FDD [21]
Palette	Gender	$F_{MEO}$	1.164	0.544	1.2	1.164	1.121	2.159	1.611	9.265	0.757	1.348	0.503	0.727
		$F_{DP}$	13.196	13.889	12.155	13.052	13.571	13.763	13.705	2.952	13.466	12.548	13.542	13.928
	Race	$F_{OAE}$	1.164	0.278	2.166	1.02	0.848	1.308	1.077	9.412	0.95	0.803	0.55	0.147
		$F_{EO}$	1.999	0.866	1.844	1.45	1.814	3.043	2.412	10.763	1.438	1.536	0.884	0.791
	Age	$F_{MEO}$	3.659	5.947	11.668	3.333	6.098	7.317	6.098	20.528	20.242	5.108	2.83	7.317
		$F_{DP}$	5.979	6.385	4.834	7.61	5.135	4.144	5.922	16.802	8.742	5.776	7.261	5.922
	Intersection	$F_{OAE}$	1.965	4.123	8.436	2.97	2.963	2.046	2.329	6.372	13.877	2.402	2.062	3.319
		$F_{EO}$	8.157	11.825	18.769	7.416	9.477	14.029	10.363	43.621	26.601	12.368	6.161	10.827
	-	$F_{MEO}$	4.688	3.002	7.966	3.756	4.042	3.765	4.425	12.333	8.923	4.995	4.042	1.948
		$F_{DP}$	19.14	19.394	18.86	20.025	18.688	19.789	20.438	14.893	21.909	20.674	20.674	17.134
	-	$F_{OAE}$	3.534	1.426	4.149	2.78	3.775	3.392	2.765	10.627	4.861	2.715	2.271	0.865
		$F_{EO}$	11.998	6.893	14.031	9.808	11.945	12.703	12.283	38.971	10.877	11.605	9.98	3.288
	-	$F_{MEO}$	9.375	8.995	20.066	5.556	12.5	12.5	12.5	58	22.231	12.5	4.412	9.375
		$F_{DP}$	37.067	39.108	27.455	36.047	37.067	37.352	38.372	23.106	27.997	36.047	39.393	35.026
	-	$F_{OAE}$	5.769	5.454	18.902	4.808	4.808	4.808	4.808	22.672	17.864	4.137	3.54	4.082
		$F_{EO}$	24.367	23.905	43.338	18.623	24.071	33.455	25.185	150.941	53.279	30.359	16.799	27.109
	-	ACC	98.547	97.465	94.189	98.671	98.578	98.423	98.702	73.447	94.405	97.682	98.887	99.073
		AUC	99.736	99.581	99.501	99.756	99.644	99.387	99.856	80.642	97.922	99.704	99.781	99.923
	-	AP	99.423	98.911	99.063	99.497	99.079	98.07	99.725	67.995	95.558	99.432	99.657	99.867
		EER	1.525	1.672	2.951	1.279	1.426	1.574	1.328	26.365	6.05	2.361	1.279	1.082

Table 33: Detailed fairness and utility evaluation results on Palette.

Dataset	Attribute	Metric	Model Type											
			Naive			Frequency			Spatial			Fairness-enhanced		
			Xception [61]	EfficientB4 [62]	ViT-B/16 [63]	F3Net [64]	SPSL [65]	SRM [66]	UCF [16]	UnivFD [67]	CORE [68]	DAW-FDD [20]	DAG-FDD [20]	PG-FDD [21]
SD1.5	Gender	$F_{MEO}$	0.509	3.139	0.317	1.139	1.186	0.248	1.674	2.635	0.891	0.457	1.275	0.345
		$F_{DP}$	22.081	19.548	20.978	22.834	22.776	22.724	22.857	11.878	20.185	20.993	23.084	22.934
	Race	$F_{OAE}$	0.495	1.293	1.576	0.178	0.153	0.021	0.332	4.404	2.235	1.599	0.07	0.119
		$F_{EO}$	0.613	3.185	0.554	1.705	1.56	0.359	1.886	3.738	1.065	0.625	1.661	0.399
	Age	$F_{MEO}$	1.968	7.1	8.289	2.12	1.5	1.342	1.950	19.503	18.674	2.837	1.469	1.323
		$F_{DP}$	15.903	16.759	15.365	15.889	15.045	14.817	15.624	11.712	14.571	14.654	15.689	14.94
	Intersection	$F_{OAE}$	0.943	2.918	4.108	1.294	0.879	0.297	1.454	10.28	9.562	1.645	1.347	0.901
		$F_{EO}$	4.614	15.815	13.016	4.227	2.198	2.227	3.486	40.819	27.388	6.944	3.342	3.124
	-	$F_{MEO}$	2.87	3.457	5.482	1.658	3.43	1.295	3.244	5.749	11.164	4.406	2.534	1.061
		$F_{DP}$	31.026	28.27	31.043	30.768	32.076	31.734	31.627	16.203	30.92	31.262	31.78	32.059
	-	$F_{OAE}$	2.054	2.83	1.832	1.244	2.275	0.828	2.1	11.13	2.965	2.806	1.818	0.942
		$F_{EO}$	6.24	9.127	9.167	3.913	6.148	2.276	5.276	12.176	15.841	7.182	5.215	2.787
	-	$F_{MEO}$	3.333	11.68	11.018	3.333	6.667	2.439	6.206	24.497	23.778	3.283	6.206	1.695
		$F_{DP}$	34.936	32.557	32.823	35.564	34.066	33.963	34.985	24.536	30.941	32.333	35.227	34.35
	-	$F_{OAE}$	1.928	5.084	4.661	1.915	3.382	1.667	2.27	14.398	11.932	3.428	2.27	1.208
		$F_{EO}$	10.679	35.812	28.777	12.75	18.354	10.377	15.07	88.474	69.692	15.9	13.668	8.346
	-	ACC	97.272	95.847	95.862	97.833	97.848	99.045	98.151	73.219	94.983	95.696	98.424	99.47
		AUC	99.792	98.953	99.499	99.803	99.826	99.766	99.877	86.563	97.922	99.63	99.893	99.963
	-	AP	99.832	98.661	99.538	99.828	99.862	99.716	99.914	85.449	97.861	99.675	99.928	99.969
		EER	1.887	4.073	2.947	1.755	1.523	0.993	1.192	21.159	6.424	2.682	0.861	0.53

Table 34: Detailed fairness and utility evaluation results on SD v1.5.

Dataset	Attribute	Metric	Model Type											
			Naive			Frequency			Spatial			Fairness-enhanced		
			Xception [61]	EfficientB4 [62]	ViT-B/16 [63]	F3Net [64]	SPSL [65]	SRM [66]	UCF [16]	UnivFD [67]	CORE [68]	DAW-FDD [20]	DAG-FDD [20]	PG-FDD [21]
SD Inpainting	Gender	$F_{MEO}$	2.241	6.934	2.814	2.686	1.636	2.432	1.652	4.449	1.288	2.495	1.455	0.849
		$F_{DP}$	20.739	14.685	21.614	23.834	21.747	23.587	23.36	12.632	19.574	19.711	22.764	22.798
	Race	$F_{OAE}$	2.701	7.184	0.172	1.041	2.434	1.154	0.901	6.926	1.511	3.887	1.367	0.746
		$F_{EO}$	2.704	6.971	3.64	3.722	3.096	2.449	2.302	5.737	2.278	2.932	1.837	1.048
	Age	$F_{MEO}$	2.353	8.159	13.709	4.767	2.884	3.957	4.424	15.135	23.357	4.628	4.424	1.599
		$F_{DP}$	11.33	9.279	10.32	11.773	10.267	12.654	11.567	6.414	10.94	12.332	13.285	12.717
	Intersection	$F_{OAE}$	2.569	6.514	5.566	1.598	2.857	1.908	2.863	7.86	9.299	2.983	2.904	1.378
		$F_{EO}$	6.652	21.735	26.462	7.096	7.51	8.601	8.098	34.693	34.503	9.538	11.207	3.61
	-	$F_{MEO}$	6.106	10.945	8.907	8.131	6.14	6.319	6.518	5.833	5.738	6.494	6.329	1.77
		$F_{DP}$	34.829	24.512	35.588	35.072	36.422	36.373	35.589	22.872	33.578	35.295	35.397	36.172
	-	$F_{OAE}$	5.83	11.618	4.664	3.031	4.865	2.925	3.538	10.413	2.475	6.172	3.678	1.276
		$F_{EO}$	11.823	19.295	20.31	11.192	12.313	8.877	10.26	16.169	10.115	11.654	10.325	4.012
	-	$F_{MEO}$	6.237	19.863	19.037	8.725	5.369							

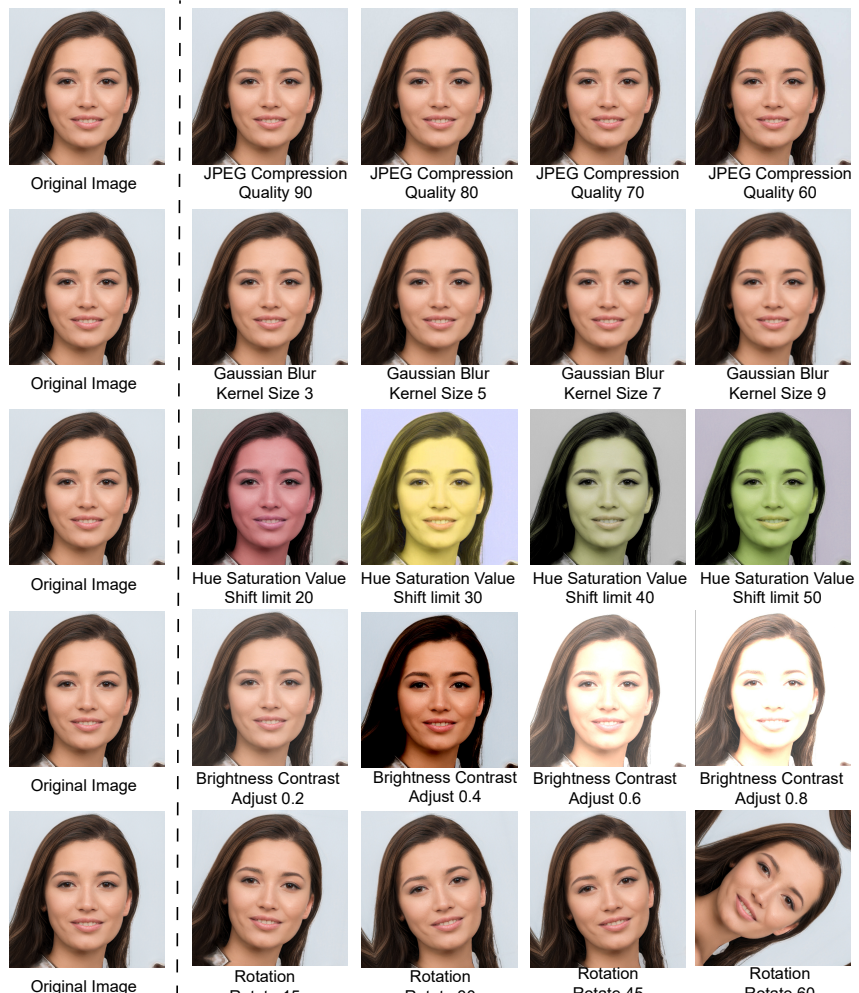


Figure B.1: Visualization of the image after different post-processing.

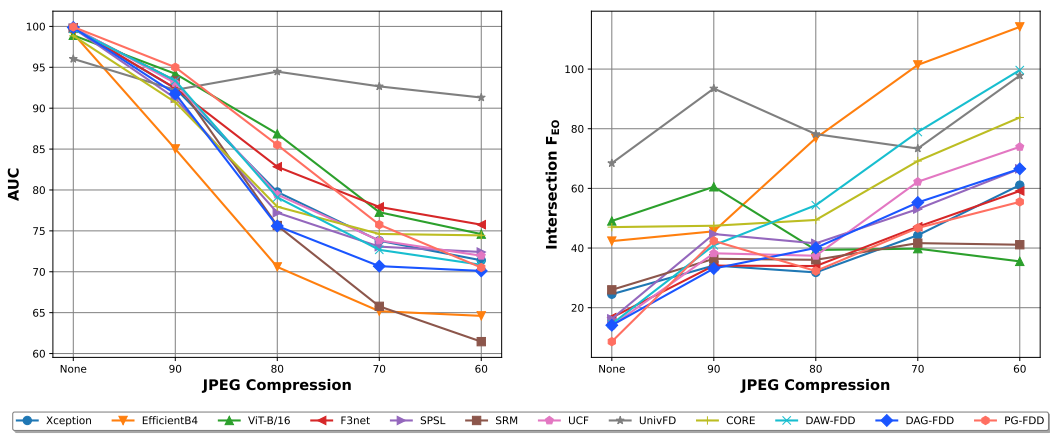


Figure B.2: Robustness analysis in terms of utility and fairness under varying degrees of JPEG compression.

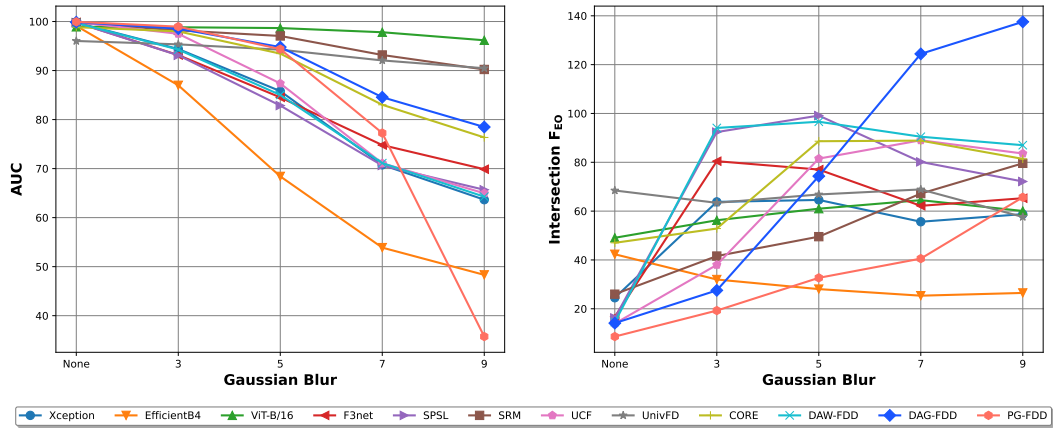


Figure B.3: Robustness analysis in terms of utility and fairness under varying kernel sizes of Gaussian Blur.

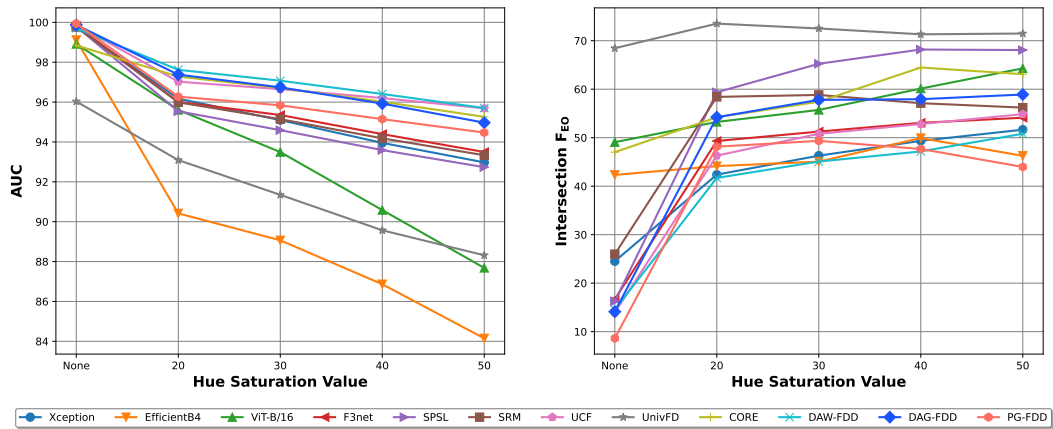


Figure B.4: Robustness analysis in terms of utility and fairness under varying degrees of Hue Saturation Value.

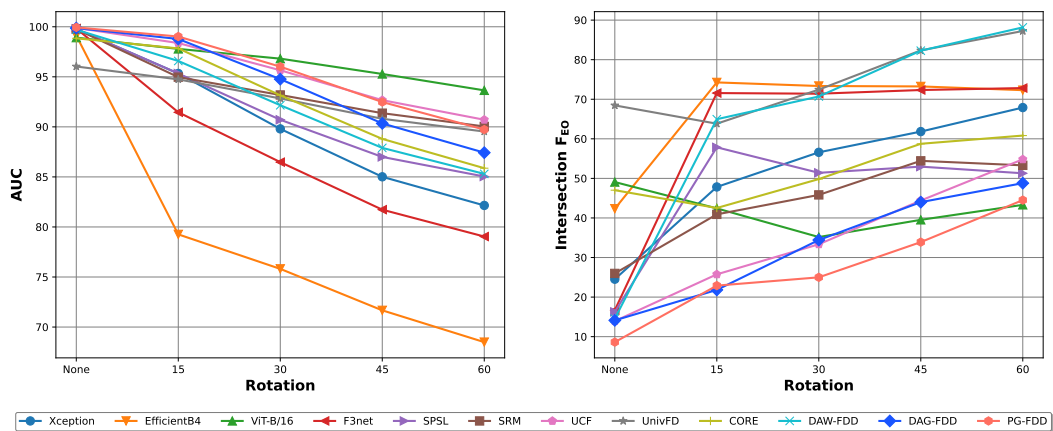


Figure B.5: Robustness analysis in terms of utility and fairness under varying degrees of Rotations.

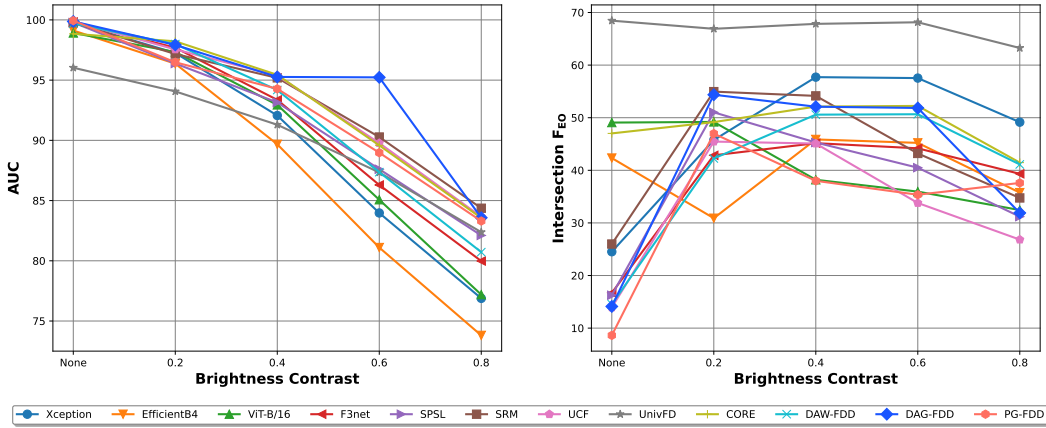


Figure B.6: Robustness analysis in terms of utility and fairness under varying degrees of Brightness Contrast.

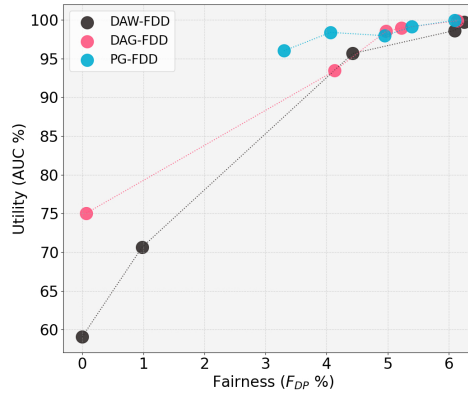


Figure B.7: The utility-fairness trade-off of Fairness-enhanced methods.

Dataset Size	Attribute	Metric	Model Type											
			Naive			Frequency			Spatial			Fairness-enhanced		
			Xception [61]	EfficientB4 [62]	ViT-B/16 [63]	F3Net [64]	SPSL [65]	SRM [66]	UCF [16]	UnivFD [67]	CORE [68]	DAW-FDD [20]	DAG-FDD [20]	PG-FDD [21]
20%	Gender	$F_{MEO}$	1.725	0.366	0.863	1.523	0.916	1.818	0.652	0.369	2.196	1.657	1.549	1.428
		$F_{DP}$	1.944	2.239	2.618	2.083	2.305	1.586	2.811	2.317	1.543	1.823	2.269	2.106
	Race	$F_{OAE}$	1.076	0.419	0.906	1.057	0.775	0.800	0.617	0.620	1.076	0.950	1.145	0.904
		$F_{EO}$	2.030	0.386	1.635	1.945	1.280	2.081	0.768	0.629	2.214	1.738	2.244	1.742
20%	Race	$F_{MEO}$	14.155	11.039	10.108	13.887	12.235	15.231	11.756	14.625	16.804	16.116	12.021	12.645
		$F_{DP}$	23.488	20.018	22.360	23.285	22.782	22.998	22.994	22.628	25.752	23.457	23.093	22.572
	Age	$F_{OAE}$	5.266	5.286	5.057	5.416	4.807	5.425	5.063	6.459	5.913	5.009	4.877	4.676
		$F_{EO}$	24.015	19.947	25.662	25.293	22.940	23.207	24.837	28.765	29.623	22.162	22.625	21.318
20%	Intersection	$F_{MEO}$	6.766	5.613	3.335	7.254	5.765	6.506	8.761	5.411	7.208	5.948	5.672	5.769
		$F_{DP}$	5.086	5.581	6.666	5.089	5.561	4.659	6.170	6.073	4.556	5.080	5.291	5.337
	Intersection	$F_{OAE}$	3.784	3.177	4.958	3.745	3.493	3.435	4.491	4.692	4.209	4.183	3.159	3.242
		$F_{EO}$	9.533	9.157	12.476	9.632	9.222	9.203	11.928	14.228	10.548	9.699	8.470	8.339
-	Intersection	$F_{MEO}$	17.912	12.056	14.781	17.613	14.966	19.221	14.360	17.533	20.977	19.466	15.288	15.734
		$F_{DP}$	25.299	22.237	23.053	25.005	23.895	25.807	23.863	23.563	27.720	25.542	24.273	24.374
	-	$F_{OAE}$	8.001	9.313	8.647	7.898	7.506	6.137	8.856	11.806	8.713	5.859	7.538	5.378
		$F_{EO}$	54.208	45.790	54.752	56.299	50.295	52.526	55.119	66.894	63.986	44.272	49.137	45.127
	-	ACC	95.175	94.292	93.972	94.913	95.084	95.534	95.249	90.810	94.835	94.996	95.243	95.602
	-	AUC	98.620	99.055	98.765	98.284	98.851	98.026	98.728	96.404	98.237	98.403	98.731	98.533
	-	AP	98.805	99.325	99.132	98.441	99.083	98.353	98.931	97.227	98.410	98.578	98.980	98.695
	-	EER	5.563	5.208	6.267	6.142	5.292	5.489	4.933	10.001	6.169	5.696	5.424	5.148

Table 37: Detailed fairness and utility evaluation results on 20% training subset.

Dataset Size	Attribute	Metric	Model Type													
			Naive				Frequency				Spatial			Fairness-enhanced		
			Xception [61]	EfficientB4 [62]	ViT-B/16 [63]	F3Net [64]	SPSL [65]	SRM [66]	UCF [16]	UnivFD [67]	CORE [68]	DAW-FDD [20]	DAG-FDD [20]	PG-FDD [21]		
40%	Gender	$F_{MEO}$	1.771	2.562	1.588	1.383	1.277	0.567	1.191	0.752	1.465	1.034	1.303	1.41		
		$F_{DP}$	1.801	3.841	1.948	2.33	2.088	1.955	2.715	2.756	2.113	2.362	2.128	2.998		
	Race	$F_{OAE}$	0.908	0.439	0.881	1.117	0.661	0.078	1.281	0.625	0.971	0.811	0.793	1.193		
		$F_{EO}$	1.799	3.236	1.809	2.034	1.415	1.095	2.286	1.023	1.796	1.474	1.51	2.263		
	Age	$F_{MEO}$	14.7	12.688	9.731	14.333	10.203	7.959	14.511	14.169	14.04	11.7	12.504	7.79		
		$F_{DP}$	23.675	21.948	22.57	23.424	22.165	21.403	25.546	23.264	22.811	21.994	22.856	21.024		
	Intersection	$F_{OAE}$	5.079	6.318	4.774	4.986	4.49	3.571	5.708	6.282	5.222	3.819	4.448	4.043		
		$F_{EO}$	23.443	17.727	22.852	22.917	20.787	17.734	30.682	30.21	22.288	17.342	20.633	18.703		
	-	$F_{MEO}$	7.594	3.343	4.055	6.859	5.051	4.126	6.145	5.676	6.85	5.874	6.46	3.48		
		$F_{DP}$	4.951	6.723	5.222	5.421	5.485	4.937	5.55	6.471	5.272	5.672	5.447	6.276		
	-	$F_{OAE}$	3.873	1.951	2.928	3.709	3.057	2.589	3.747	4.713	3.447	3.655	3.689	3.158		
		$F_{EO}$	9.596	9.58	8.258	8.736	8.461	8.457	9.256	14.995	8.374	9.236	9.119	8.222		
	-	ACC	95.796	94.03	94.822	95.844	95.794	95.393	94.754	90.711	95.984	95.975	96.257	95.337		
		AUC	98.696	98.932	99.024	98.851	99.064	98.722	98.306	96.371	98.824	98.974	98.949	99.092		
	-	AP	98.778	99.269	99.31	98.959	99.236	98.968	98.588	97.224	98.984	99.139	99.035	99.318		
		EER	5.027	5.442	5.474	5.002	4.574	4.77	6.037	10.044	5.009	4.567	4.285	4.729		

Table 38: Detailed fairness and utility evaluation results on 40% training subset.

Dataset Size	Attribute	Metric	Model Type													
			Naive				Frequency				Spatial			Fairness-enhanced		
			Xception [61]	EfficientB4 [62]	ViT-B/16 [63]	F3Net [64]	SPSL [65]	SRM [66]	UCF [16]	UnivFD [67]	CORE [68]	DAW-FDD [20]	DAG-FDD [20]	PG-FDD [21]		
60%	Gender	$F_{MEO}$	0.801	0.489	2.239	1.576	1.787	1.179	0.745	0.539	0.907	1.512	1.527	0.408		
		$F_{DP}$	2.899	2.747	4.223	1.996	1.638	3.062	2.596	2.509	2.291	3.01	1.88	2.857		
	Race	$F_{OAE}$	0.692	0.109	0.935	0.908	0.802	0.361	0.783	0.634	0.697	1.296	0.716	0.27		
		$F_{EO}$	1.136	0.677	3.474	1.757	2.002	1.22	1.328	0.586	1.153	2.435	1.594	0.547		
	Age	$F_{MEO}$	8.652	16.885	6.328	13.433	16.19	6.243	9.96	14.482	14.243	9.849	14.223	5.96		
		$F_{DP}$	21.794	26.205	14.609	23.519	21.498	18.874	20.947	23.469	24.031	20.453	23.547	15.86		
	Intersection	$F_{OAE}$	3.781	6.63	5.65	4.671	5.716	4.346	4.133	6.328	4.569	3.77	5.247	3.746		
		$F_{EO}$	18.942	23.67	21.707	22.128	23.478	12.107	15.885	29.99	22.562	14.96	22.213	14.735		
	-	$F_{MEO}$	5.047	5.153	5.719	6.155	4.154	3.81	4.71	5.243	5.789	5.512	3.699	3.553		
		$F_{DP}$	6.012	4.411	7.664	5.157	5.456	6.02	6.042	6.245	5.444	7.926	5.023	6.488		
	-	$F_{OAE}$	2.916	2.496	4.283	3.316	3.897	2.374	2.752	4.555	3.422	3.886	2.858	2.244		
		$F_{EO}$	7.607	10.635	13.662	8.084	9.08	7.503	6.872	14.282	8.089	8.321	6.951	8.124		
	-	$F_{MEO}$	10.466	25.134	7.982	16.425	17.532	10.693	12.44	17.613	16.374	12.417	17.272	9.574		
		$F_{DP}$	22.891	27.88	18.106	25.118	24.338	20.236	22.678	23.819	25.063	22.277	25.459	18.176		
	-	$F_{OAE}$	5.884	11.229	7.443	5.547	6.822	7.714	4.749	11.612	5.287	5.726	5.873	5.899		
		$F_{EO}$	39.873	51.509	46.548	46.511	52.673	28.055	35.888	66.884	45.261	30.682	47.626	31.167		
	-	ACC	96.505	93.931	93.612	96.221	95.676	96.951	96.567	90.882	96.009	95.025	96.332	96.488		
		AUC	98.97	98.828	98.536	99.075	99.102	99.236	99.026	96.461	99.189	99.003	99.354	99.401		
	-	AP	98.987	99.195	98.953	99.17	99.234	99.415	99.012	97.279	99.351	99.285	99.503	99.461		
		EER	3.829	6.004	6.668	4.322	4.314	3.248	3.592	9.875	4.351	5.072	3.882	3.583		

Table 39: Detailed fairness and utility evaluation results on 60% training subset.

Dataset Size	Attribute	Metric	Model Type													
			Naive				Frequency				Spatial			Fairness-enhanced		
			Xception [61]	EfficientB4 [62]	ViT-B/16 [63]	F3Net [64]	SPSL [65]	SRM [66]	UCF [16]	UnivFD [67]	CORE [68]	DAW-FDD [20]	DAG-FDD [20]	PG-FDD [21]		
80%	Gender	$F_{MEO}$	1.753	0.256	1.697	0.976	1.199	0.166	1.235	0.447	1.428	0.398	0.526	0.339		
		$F_{DP}$	1.925	2.648	1.891	2.861	3.002	2.642	3.511	2.461	1.881	2.762	2.695	2.643		
	Race	$F_{OAE}$	0.943	0.002	0.988	0.280	0.474	0.316	0.737	0.596	0.665	0.214	0.408	0.172		
		$F_{EO}$	1.893	0.364	1.910	1.214	1.489	0.218	1.237	0.467	1.495	0.522	0.788	0.384		
	Age	$F_{MEO}$	11.908	11.806	9.589	4.724	3.751	8.864	2.988	14.911	13.396	3.892	5.036	2.891		
		$F_{DP}$	22.332	21.476	19.620	18.520	17.354	18.431	16.783	23.411	22.809	16.666	18.631	17.598		
	Intersection	$F_{OAE}$	4.298	6.127	4.724	3.890	3.573	4.030	2.667	6.322	4.970	3.282	4.350	2.731		
		$F_{EO}$	18.793	19.118	20.637	10.997	9.458	14.889	10.966	29.610	22.226	9.621	13.148	8.090		
	-	$F_{MEO}$	5.554	4.823	4.219	2.168	3.355	2.588	1.699	5.731	6.528	2.822	1.498	1.076		
		$F_{DP}$	5.307	5.675	5.586	6.111	6.492	6.159	6.884	6.433	4.840	6.781	5.943	5.842		
	-	$F_{OAE}$	3.001	2.397	3.365	1.221	1.905	1.389	0.832	4.916	3.150	2.718	1.133	0.744		
		$F_{EO}$	7.274	8.476	8.710	4.026	8.252	5.533	5.139	15.746	8.380	7.114	4.174	2.835		
	-	$F_{MEO}$	14.979	17.336	11.294	6.650	6.863	9.372	5.369	18.159	16.769	5.729	8.210	5.443		
		$F_{DP}$	24.220	21.943	21.145	21.258	20.254	20.920	19.077	24.033	24.954	18.015	20.556	19.798		
	-	$F_{OAE}$	5.025	10.608	7.908	6.697	5.709	6.343	5.118	11.541	5.558	5.760	7.955	4.583		
		$F_{EO}$	40.744	44.028	45.684	27.249	22.360	32.012	24.504	66.750	46.492	21.906	29.401	17.687		
	-	ACC	96.629	94.917	94.904	95.309	96.461	96.548	97.736	90.898	95.586	95.808	97.317	98.277		
		AUC	9													

## C Datasheet for AI-Face

In this section, we present a DataSheet [87] for AI-Face.

### C.1 Motivation For Dataset Creation

- **Why is the dataset created?** For researchers to evaluate the fairness of AI face detection models or to train fairer models. Please see Section 2 ‘Background and Motivation’ in the submitted manuscript.
- **Has the dataset been used already?** Yes. Our fairness benchmark is based on this dataset.
- **What (other) tasks could the dataset be used for?** Could be used as training data for generative methods attribution task.
- **Who funded dataset creation?** This work is supported by the U.S. National Science Foundation (NSF) under grant IIS-2348419 and the National Artificial Intelligence Research Resource (NAIRR) Pilot and TACC Lonestar6. Please see Acknowledgment 5.

### C.2 Data Composition

- **What are the instances?** The instances that we consider in this work are real face images and AI-generated face images from public datasets.
- **How many instances are there?** We include more than 2 million face images from public datasets. Please see Table 13 for details.
- **What data does each instance consist of?** Each instance consists of an image.
- **Is there a label or target associated with each instance?** Each image is associated with uncertainty score for gender prediction, uncertainty score for age prediction, uncertainty score for race prediction, gender annotation, age annotation, race annotation, and target label (fake or real).
- **Is any information missing from individual instances?** No.
- **Are relationships between individual instances made explicit?** Not applicable – we do not study the relationship between each image.
- **Does the dataset contain all possible instances or is it a sample?** Contains all instances our curation pipeline collected. Since the current dataset does not cover all available images online, there is a high probability more instances can be collected in the future.
- **Are there recommended data splits (e.g., training, development/validation, testing)?** For detector development and training, the dataset can be split as 6:2:2.
- **Are there any errors, sources of noise, or redundancies in the dataset? If so, please provide a description.** Yes. Despite our extensive efforts to reduce demographic label noise, including human corrections based on uncertainty scores, there may still be mislabeled instances. Given the dataset’s size of over 2 million images, it is impractical for humans to manually check and correct each image individually.
- **Is the dataset self-contained, or does it link to or otherwise rely on external resources (e.g., websites, tweets, other datasets)?** The dataset is self-contained.

### C.3 Collection Process

- **What mechanisms or procedures were used to collect the data?** We build our AI-Face dataset by collecting and integrating public AI-generated face images sourced from academic publications, GitHub repositories, and commercial tools. Please see ‘Data Collection’ in Section 3.2
- **How was the data associated with each instance acquired? Was the data directly observable (e.g., raw text, movie ratings), reported by subjects (e.g., survey responses), or indirectly inferred/derived from other data?** The data can be acquired after our verification of user submitted and signed EULA.
- **If the dataset is a sample from a larger set, what was the sampling strategy (e.g., deterministic, probabilistic with specific sampling probabilities)?** Not applicable. We did not sample data from a larger set. But we use RetinaFace [60] for detecting and cropping faces to ensure each image only contains one face.
- **Over what timeframe was the data collected? Does this timeframe match the creation timeframe of the data associated with the instances (e.g., recent crawl of old news articles)? If not, please describe the timeframe in which the data associated with the**

**instances was created.** The data was collected from February 2024 to April 2024, even though the data were originally released before this time. Please refer to the cited papers in Table 13 for specific original data released time.

#### C.4 Data Processing

- **Was any preprocessing/cleaning/labeling of the data done (e.g., discretization or bucketing, tokenization, part-of-speech tagging, SIFT feature extraction, removal of instances, processing of missing values)?** Yes. We discussed in ‘Demographically Annotation Generation’ in Section 3.2.
- **Was the ‘raw’ data saved in addition to the preprocessed/cleaned/labeled data (e.g., to support unanticipated future uses)? If so, please provide a link or other access point to the ‘raw’ data.** The ‘raw’ data can be acquired through the original data publisher. Please see the cited papers in Table 13.
- **Is the software used to preprocess/clean/label the instances available? If so, please provide a link or other access point.** Yes. We use RetinaFace [60] for detecting and cropping faces to ensure each image only contains one face. Demographic annotations are given by our annotator, see ‘Annotator Development’ in Section 3.1. Our annotator code is available on Our GitHub repository.
- **Does this dataset collection/processing procedure achieve the motivation for creating the dataset stated in the first section of this datasheet? If not, what are the limitations?** Yes. The dataset does allow for the study of our goal, as it covers comprehensive generation methods, demographic annotations for evaluating current detectors and training fairer detectors.

#### C.5 Dataset Distribution

- **How will the dataset be distributed?** We distribute all the data as well as CSV files that formatted all annotations of images under the CC BY-NC-ND 4.0 license and strictly for research purposes.
- **When will the dataset be released/first distributed? What license (if any) is it distributed under?** The data has been released, under the permissible CC BY-NC-ND 4.0 license for research-based use only. Users can access our dataset by submitting an EULA. Dataset license and EULA is on our GitHub <https://github.com/Purdue-M2/AI-Face-FairnessBench>.
- **Are there any copyrights on the data?** We believe our use is ‘fair use’ since all data in our dataset is collected from public datasets.
- **Are there any fees or access restrictions?** No.

#### C.6 Dataset Maintenance

- **Who is supporting/hosting/maintaining the dataset?** The first author of this paper.
- **Will the dataset be updated? If so, how often and by whom?** We do not plan to update it at this time.
- **Is there a repository to link to any/all papers/systems that use this dataset?** Not right now, but we encourage anyone who uses the dataset to cite our paper so it can be easily found. Our fairness benchmark uses this dataset, the code of fairness benchmark is on our GitHub <https://github.com/Purdue-M2/AI-Face-FairnessBench>.
- **If others want to extend/augment/build on this dataset, is there a mechanism for them to do so?** Not at this time.

#### C.7 Legal and Ethical Considerations

- **Were any ethical review processes conducted (e.g., by an institutional review board)?** No official processes were done since all data in our dataset were collected from the existing public datasets.
- **Does the dataset contain data that might be considered confidential?** No. We only use data from public datasets.

- **Does the dataset contain data that, if viewed directly, might be offensive, insulting, threatening, or might otherwise cause anxiety? If so, please describe why** No. It is a face image dataset, we have not seen any instance of offensive or abusive content.
- **Does the dataset relate to people?** Yes. It is a face image dataset containing real face images and AI-generated face images.
- **Does the dataset identify any subpopulations (e.g., by age, gender)?** Yes, through demographic annotations.
- **Is it possible to identify individuals (i.e., one or more natural persons), either directly or indirectly (i.e., in combination with other data) from the dataset?** Yes. It is a face image dataset. The age, gender, and race can be identified through the face image, also through the demographic annotation we provide. All of the images that we use are from publicly available data.

#### C.8 Author Statement and Confirmation of Data License

The authors of this work declare that the dataset described and provided has been collected, processed, and made available with full adherence to all applicable ethical guidelines and regulations. We accept full responsibility for any violations of rights or ethical guidelines that may arise from the use of this dataset. We also confirm that the dataset is released under the CC BY-NC-ND 4.0 license, permitting sharing and downloading of the work in any medium, provided the original author is credited, and it is used non-commercially with no derivative works created.